7943

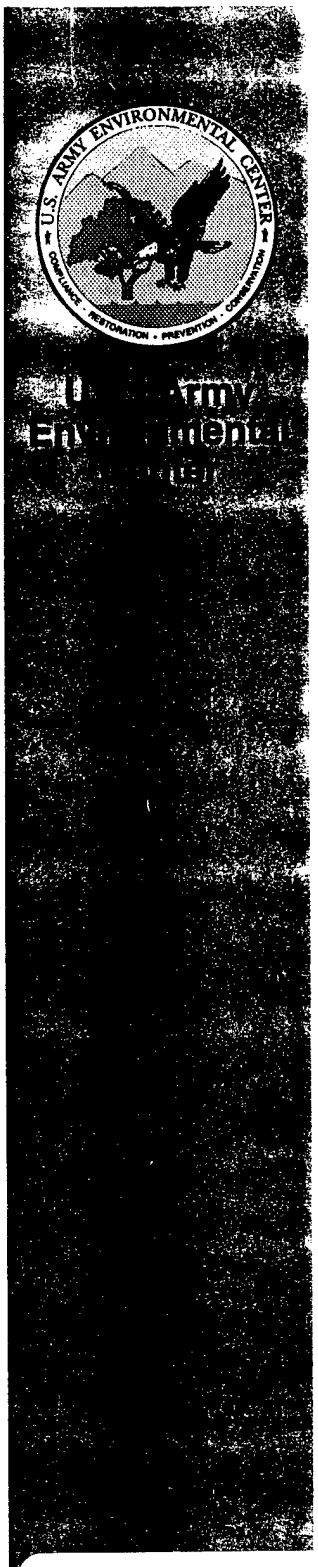

Report No. SFIM-AEC-ET-CR-97010

DEMONSTRATION AND EVALUATION OF AN AUTONOMOUS, MULTIPLE-SENSOR SYSTEM FOR CHARACTERIZING BURIED UNEXPLODED ORDNANCE

U.S. Army Environmental Center

Naval Explosive Ordnance Disposal Technology Division

U.S.A.F. Wright Laboratory

January 1997

19970327 057

Distribution Unlimited; Approved for Public Release

DTIC QUALITY INSPECTED 1

AEC Form 45. 1 Feb 93 replaces THAMA Form 45 which is obsolete.

DISCLAIMER NOTICE

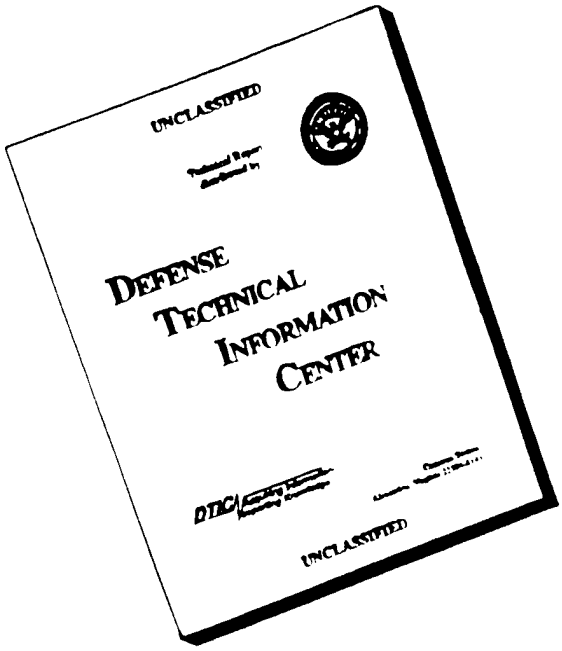

THIS DOCUMENT IS BEST QUALITY AVAILABLE. THE COPY FURNISHED TO DTIC CONTAINED A SIGNIFICANT NUMBER OF PAGES WHICH DO NOT REPRODUCE LEGIBLY.

REPORT DOCUMENTATION PAGE

Form Approved
OMB No. 0704-0188

1. AGENCY USE ONLY (Leave blank)	2. REPORT DATE	3. REPORT TYPE AND DATES COVERED
	28 Jan 97	Final Report; April 1995 - Nov. 1995

4. TITLE AND SUBTITLE
Demonstration and Evaluation of an Autonomous, Multiple-Sensor System for Characterizing Buried Unexploded Ordnance.

5. FUNDING NUMBERS

6. AUTHOR(S)

7. PERFORMING ORGANIZATION NAME(S) AND ADDRESS(ES)
i.) Naval EOD Technology Division, 2008 Stump Neck Road, Indian Head, MD 20640-5070 Code 50B22
Gerard Snyder (301) 743-6855x260
ii.) See 11.
iii.) See 11.

8. PERFORMING ORGANIZATION REPORT NUMBER
SFIM-AEC-ET-CR-97010

9. SPONSORING/MONITORING AGENCY NAME(S) AND ADDRESS(ES)
Environmental Security Technology Certification Program
c/o Booz-Allen and Hamilton
1725 Jefferson Davis Highway, Suite 1100
Arlington, VA 22202
Dr. Jeffrey Marqusee (703) 614-3090

10. SPONSORING/MONITORING AGENCY REPORT NUMBER

11. SUPPLEMENTARY NOTES
Army Environmental Center
SFIM-AEC-ETP (K. Rigano)
APG, MD 21010-5401

USAF Wright Laboratory, 139 Barnes Drive,
Tyndall AFB, FL 32403-5323
(A. Nease)

12a. DISTRIBUTION/AVAILABILITY STATEMENT
Unlimited Distribution

12b. DISTRIBUTION CODE

13. ABSTRACT (Maximum 200 words)

Unexploded Ordnance (UXO), consisting of bombs, projectiles, mortars, small arms, and submunitions, is the legacy of military troop training and weapon system testing. Department of Defense Force reductions over the past decades have resulted in real property being identified for alternate uses. Moreover, the cost to remediate these properties were estimated to be more than $48 billion. Through a series of commercial technology demonstrations at Jefferson Proving Ground (JPG), Indiana, the Government concluded that current technology does not provide effective and economical methods for UXO characterization and remediation. The results of the JPG demonstrations also indicated that using multiple sensors to characterize buried UXO may yield greater detection capability and reduced false alarms. This report provides an assessment of the Subsurface Ordnance Characterization System (SOCS) during tests performed at JPG and Tyndall Air Force Base (AFB). SOCS is a testbed system that is used to evaluate various sensors, combinations of sensors, autonomous control and navigation equipment, operating parameters, and data analysis techniques. Specific tests were performed using an array of magnetometers and ground penetrating radar to assess the feasibility of an autonomous, multiple-sensor system for characterizing buried UXO.

14. SUBJECT TERMS	15. NUMBER OF PAGES
i.) unexploded ordnance; ii.) subsurface ordnance characterization system; iii.) ground penetrating radar; iv.) magnetometers	134
	16. PRICE CODE

17. SECURITY CLASSIFICATION OF REPORT	18. SECURITY CLASSIFICATION OF THIS PAGE	19. SECURITY CLASSIFICATION OF ABSTRACT	20. LIMITATION OF ABSTRACT
Unclassified	Unclassified	Unclassified	UL

Table of Contents

Appendices

Tables

Figures

DEMONSTRATION AND EVALUATION OF AN AUTONOMOUS, MULTIPLE-SENSOR SYSTEM FOR CHARACTERIZING BURIED UNEXPLODED ORDNANCE

U.S. Army Environmental Center
Naval Explosive Ordnance Disposal Technology Division
U.S.A.F. Wright Laboratory

January 1997

1. Introduction

1.1 Background Information

The General Accounting Office (GAO) and Department of Defense (DoD) recently issued a report stating that more than 7 million acres throughout the United States contain unexploded ordnance (UXO).[1] This UXO, consisting of bombs, projectiles, mortars, small arms, and submunitions, is the legacy of military troop training and weapons system testing. DoD Force reductions over the past few decades have resulted in real property being identified for alternate uses. Moreover, the cost to remediate this property could exceed $48 billion. Current technology is inadequate to meet the Government's needs for UXO characterization and remediation, and has become the number one environmental priority within the Army and DoD.[2,3]

To address these needs, the U. S. Army Environmental Center (USAEC) and Naval Explosive Ordnance Disposal Technology Division (NAVEODTECHDIV) established a joint program to demonstrate and evaluate more effective, reliable, safe, and economical methods for UXO characterization and remediation. The scope of this program includes a comprehensive, systems engineering approach to enhancing, demonstrating, and evaluating Government and commercial systems for use at active and formerly used defense sites. As part of this comprehensive approach, USAEC and NAVEODTECHDIV formed an Integrated Product Team (IPT) with the U.S.A.F. Wright Laboratory (USAF/WL) to demonstrate and evaluate the capabilities of an autonomous, multiple-sensor system for characterizing buried UXO. This system was designated as the Subsurface Ordnance Characterization System (SOCS).

1.2 Official DoD Requirement Statement

At the time that this project was initiated, no formal DoD requirement existed for UXO clearance systems other than those identified by an Operational Requirements Document for active duty military personnel such as explosive ordnance disposal (EOD) technicians or combat engineers. While each of these military specialty groups dispose of UXO (including land mines), neither has the mission for remediating UXO at formerly used defense (FUD) sites or installations subjected to base realignment and closure (BRAC). The primary mission of the EOD technician is to render safe ordnance that has failed to detonate either by design or malfunction, and impedes continued military operations and training or poses an immediate hazard to human health. This mission is normally limited to a small area and a single or small number of UXO. The combat engineers support tactical military missions such as land mine clearance and breaching where time-on-site is a primary concern and 100 percent clearance is not required.

These two military missions differ greatly from DoD efforts to characterize and remediate FUD and BRAC sites. Work at these sites are mostly performed by private companies that are awarded Government contracts based on cost, past performance, experience, and proposed methods and systems. Nearly all of the employed technology for UXO clearance is either commercial equipment or systems developed jointly between the Government and private industry.

In 1993, Congress mandated that a program be established to demonstrate, characterize, and evaluate the capabilities and limitations of current and emerging technology for UXO clearance. Based on the results of Phase I completed in October 1994, no technology demonstrated the ability to achieve a high level of detection with an acceptable number of false alarms.[4] Moreover, none of the more than 30 systems were capable of discriminating between UXO and debris. During 1995, the program was expanded to include a second phase of controlled tests at Jefferson Proving Ground (JPG) and a series of demonstrations at five, geophysically diverse, "Live Sites" located at military installations throughout the United States. While there was an incremental increase in detection, none of the systems demonstrated a significant ability to discriminate or classify.[5,6] In summary, current technology would not meet the Army and DoD needs for effective, economical, and safe UXO characterization and remediation.

1.3 Objectives of the Demonstration

The information obtained during the JPG and Live Site demonstrations was used to establish several goals for the SOCS project. These goals included the demonstration and evaluation of key system capabilities:

- Remote or autonomous collection of sensor data.
- Simultaneous collection of data from multiple sensors.
- Precise location of sensor data using a global positioning system (GPS).
- Target discrimination and classification algorithms for magnetometers and ground penetrating radar.

Specifically, the objectives of the SOCS Environmental Security Technology Certification Program (ESTCP) demonstration were to:

- Determine the feasibility of using an autonomous vehicle to tow an array of sensors.
- Assess whether a compliment of a differential global positioning system (DGPS) and an inertial navigation system (INS) can provide the precise position information required for remote sensing.
- Determine the feasibility of collecting data from total-field magnetometers and ground penetrating radar (GPR) when operating simultaneously from a single platform.
- Evaluate the application of synthetic aperture radar (SAR) techniques for processing GPR data.
- Study the effectiveness of complex natural resonance (CNR) analysis techniques to classify UXO.
- Assess the capabilities and limitations of recently enhanced detection and discrimination techniques to interpret total-field magnetometer data.

1.4 Regulatory Issues

At the time this report was written, no specific federal or DoD regulations or policy existed for developing or procuring UXO clearance systems for use at BRAC and FUD sites. Pending policies such as the Military Munitions Rule (developed by the Environmental Protection Agency) and the DoD Munitions Range Rule are expected to provide guidance for the assessment, characterization, remediation, handling, transport, and disposition of UXO at inactive, closed, and closing military sites. Currently, DoD 6055.9-STD ("DoD Ammunition and Explosive Safety Standards") establishes policy and procedures regarding real property containing ammunition and explosives. The policy established, and pending, in each of these documents requires accurate information related to the scope of the UXO problem, procedures, safety, documentation, etc., which is directly dependent on the capabilities and limitations of available technology.

1.5 Previous Testing

SOCS is a system that evolved from several UXO clearance technology projects. These projects included the development, test and evaluation of: (1) active and passive sensors, (2) target discrimination and classification methods, (3) sensor platforms, (4) robotic vehicles, (5) navigation, communication and positioning equipment, and (6) data archiving and presentation techniques. Field tests were also performed at various sites to study the effects of operating procedures and environmental conditions on system performance. The following provides a brief description of projects that lead to the integration of SOCS:

- Towed Array of Magnetometers: From 1986 through 1993, USAEC, NAVEODTECHDIV, U.S. Army Corps of Engineers, and the Naval Research Laboratory developed and conducted several field tests of the Surface Towed Ordnance Locator System (STOLS). Early in the project, the focus was on the developing algorithms for locating and classifying ferromagnetic ordnance.[7] These algorithms were refined throughout the project to provide the capability to estimate the size, depth, and orientation of magnetic anomalies using an array of magnetometers. The resultant software was integrated with the system shown in Figure 1, and field tests were performed at the NAVEODTECHDIV magnetic test range, Aberdeen Proving Ground, and Marine Corps Air-Ground Combat Center. The information collected during the STOLS field tests demonstrated that a towed array of magnetometers is feasible, and provides a significant improvement over the most common methods for UXO detection -- hand held gradiometers and manual marking methods (commonly referred to as "mag and flag").[8] The towed array allows for survey rates up to 20 times that of the "mag and flag" method, provides a permanent site characterization record, and utilizes automated data

Figure 1. Surface Towed Ordnance Locator System (STOLS)

analysis techniques that provides increased detection and reduced false alarms. The following are lessons learned from the STOLS program that were directly applied to the integration of SOCS:

(a) The STOLS was incapable of distinguishing between ordnance targets and ferrous debris, including ferrous non-ordnance objects and compacted mineral deposits.

(b) The current noise levels of the STOLS were too high to detect the desired ordnance (60 mm, 105 mm, and 155 mm shells) to the desired probability of detections and false alarm rates at the maximum expected penetration depths (2 feet, 8.5 feet, and 12.5 feet, respectively).

(c) To achieve the desired performance at the maximum expected penetration depths (155 mm shell at 12.5 feet), the noise level of the processed output should be 0.3 gamma, which is equivalent to a noise reduction of 37 dB.

(d) Approximately 90 to 98 percent of the STOLS noise was due to irregular sensor motion in the earth's magnetic field while being towed over the ground. This motion-induced noise is Gaussian in nature.

(e) The direction of towing introduced a positive or negative shift of 5 gamma dependent on the orientation of the sensors and tow vehicle relative to the earth's magnetic field.

(f) The data compression algorithm did not have sufficient dynamic range to handle noisy sensors. It may have also distorted very strong magnetic signals, which would impair the STOLS ability to characterize the UXO.

(g) The differential GPS (DGPS) navigation system had absolute position accuracy to within 1 m 95 percent of the time. The original microwave navigation system had an absolute positioning accuracy to within 1.7 m 95 percent of the time.

The following recommendations were made to improve the performance of the current STOLS or future systems:

(a) To reduce the motion induced noise from the magnetometers, three axis accelerometers should be mounted on each sensor in the array and processed with some form of an adaptive noise cancellation technique.

(b) Techniques to remove the large scale fluctuation in the magnetometers (engine induced, tow direction, background clutter, etc.) should be investigated to further reduce the noise. Some of the techniques could include adaptive mean removal filters, adaptive median filters, two dimensional filters, etc.

(c) More robust data compression techniques with greater dynamic ranges should be investigated, or the full digitized information should be recorded and stored in uncompressed form.

(d) UXO size and depth primarily determine the strength of the magnetic signature; design goals for future systems should be stated in terms of specific UXO types and maximum penetration depths of interest.

(e) Estimation of the size and depth of the ordnance requires accurate calibration of the magnetometer sensor array; techniques for checking the calibration of the magnetometers in the field should be developed.

- Autonomous Vehicle Control: Under contract to USAEC and NAVEODTECHDIV, Ohio State University and Battelle completed a system design and trade study that identified requirements for successful navigation of air, man-portable and ground vehicle systems for performing UXO site investigations.[9] The report established design and operating parameters for an autonomous tow vehicle and integrated data acquisition system. In 1993, USAF/WL developed the capability to perform autonomous surveying using technology originally developed for the Air Force rapid runway repair mission. This technology integrated a commercial all-terrain vehicle with: (1) off-line path planning software, (2) automated path execution command and control actuators, (3) route tracking navigation and communications, (4) integrated collision avoidance; (5) multi-source data acquisition, and (6) data reduction and presentation equipment. The results of this project demonstrated that the capability exists to tow an array of sensors, follow a predetermined path, achieve nearly 100 percent coverage of an unobstructed area, and store data from multiple sources.[10] Figure 2 shows the Navigation Test Vehicle that was used for initial testing.

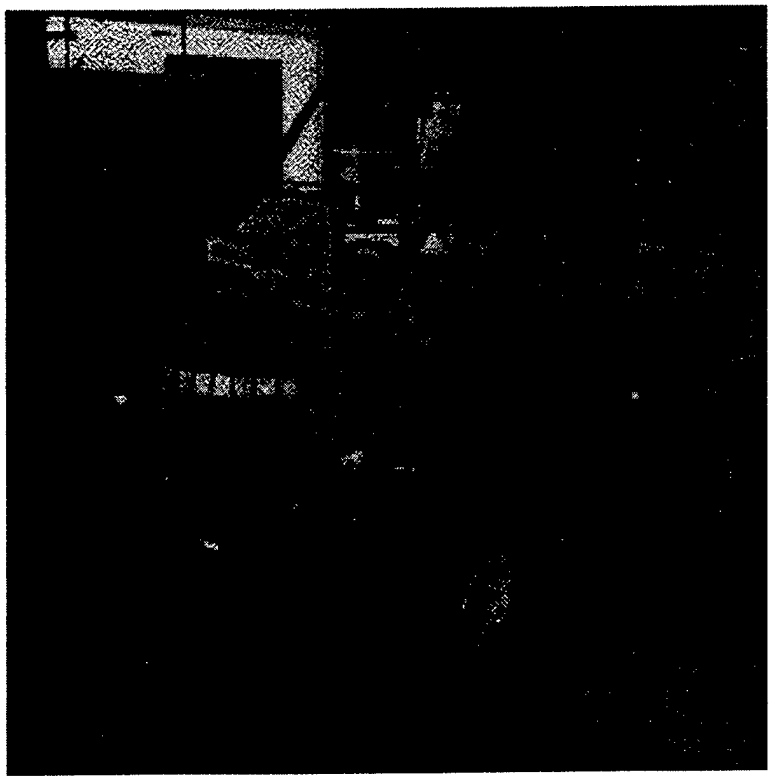

Figure 2. Navigation Test Vehicle

- Sensor Development, Test and Evaluation: USAEC and NAVEODTECHDIV, established three IPTs [radar, magnetometry and pulsed electromagnetic induction (PEMI)] to investigate the most appropriate sensors for the initial configuration of SOCS.

  The radar IPT focused on determining the feasibility of GPR for detecting and identifying buried UXO. This IPT was lead by Battelle and included Ohio State University ElectroScience Laboratory. During a two-year effort, Battelle and Ohio State University investigated different antenna designs and configurations, radar controllers, synthetic aperture radar processing techniques, and complex natural resonance techniques for target classification. Field tests were also performed in Columbus, Ohio and at JPG to evaluate brass board designs. Figure 3 shows one of the brass board systems being tested at the JPG controlled test site. The results of these investigations established the design criteria and performance goals of the SOCS radar subsystem.[11,12]

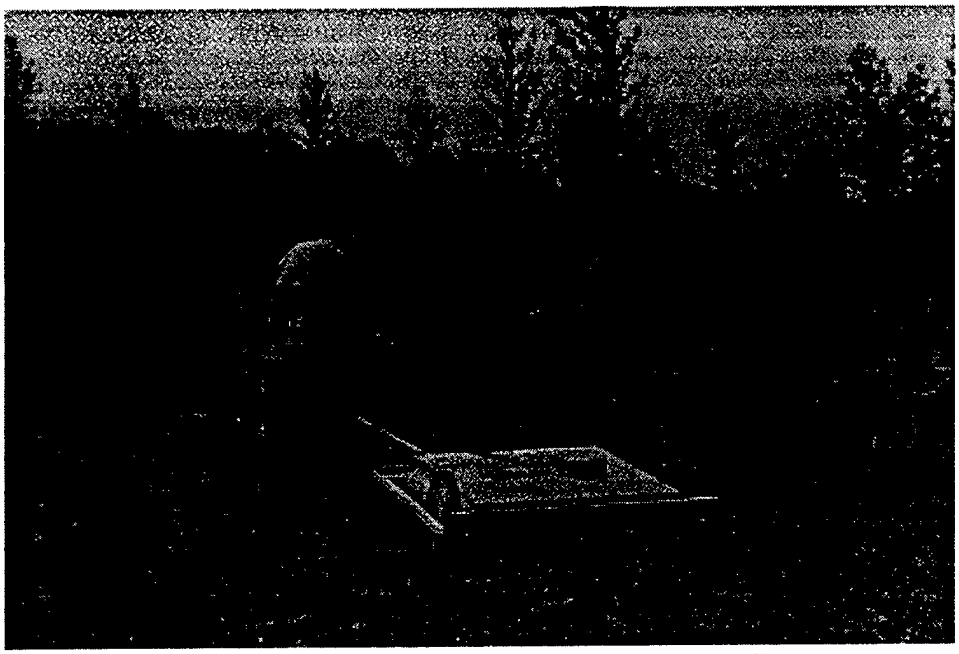

Figure 3. Brass Board Ground Penetrating Radar System

The magnetometry IPT was a cooperative effort between NAVEODTECHDIV and Areté Engineering Technologies Corporation. Much of the work performed was based on the lessons learned from the STOLS project and other projects that utilized magnetometers. AETC was awarded a contract to investigate detection and discrimination techniques for total field magnetometers and multi-axis gradiometers. The end product of this contract was a prototype automatic processor that is used to analyze data from an array of Geometrics model G-822A cesium vapor magnetometers. The automatic processor compiles and maps data from various total field magnetometers, preprocesses data to determine the influences of noise, performs threshold detection analyses, estimates target characteristics such as mass and depth, and provides graphic and tabular presentation of the results. Figure 4 shows an example of the graphic data presentation capability; indicating the strength and polarity of magnetic disturbances in the soil. The prototype automatic processor is written in American National Standards Institute (ANSI) C to ensure compatibility with SOCS and other magnetometer systems. A detailed description of the automatic processor and the methods used to analyze magnetometer data is provided in USAEC report no. SFIM-AEC-ET-CR-95093.[13]

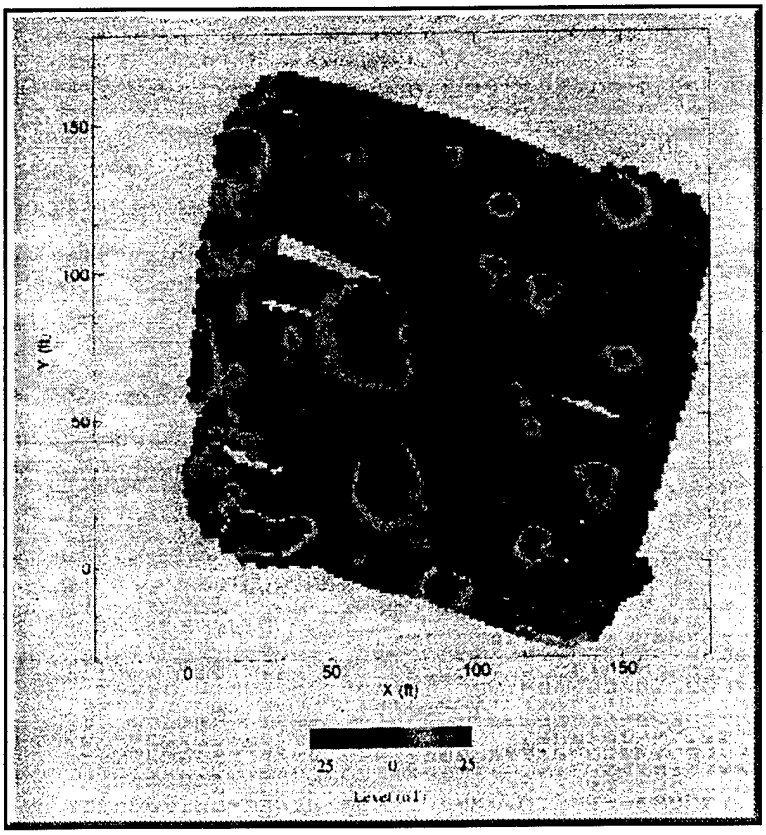

Figure 4. Magnetometer Data

The PEMI IPT was lead by Alliant Techsystems, Inc., and included the University of Washington's Applied Physics Laboratory. The objectives of the PEMI project were to investigate the feasibility of using an electromagnetic induction technique to detect and characterize buried metallic objects. To accomplish this objective, four principal tasks were performed: (1) Develop models to represent the response of UXO to a PEMI sensor; (2) Employ the models as a design aid in the development of proof-of-concept hardware for demonstrating PEMI; (3) Perform preliminary PEMI tests on UXO to calibrate models and validate performance; (4) Perform blind demonstration of the proof-of-concept PEMI sensor at the NAVEODTECHDIV magnetometer test range. The results of the project were very promising; showing that the PEMI method can be used to characterize UXO and the computer models developed accurately describe simple shapes and at least three different classes of projectiles.[14] The prototype system, Figure 5, was also able to resolve and identify targets that were buried less than 1.0 meter apart. The results of the PEMI project have also shown that a field-ready, man-portable or vehicle-based system could be fabricated using commercial-off-the-shelf equipment and integrating enhanced versions of the data modeling software. Due to resource and time limitations, the technology developed under the PEMI project was not integrated into the SOCS configuration that was demonstrated as part of the ESTCP effort. However, the information presented in the referenced report provides valuable information for evaluating the capabilities and limitations of future SOCS configurations.

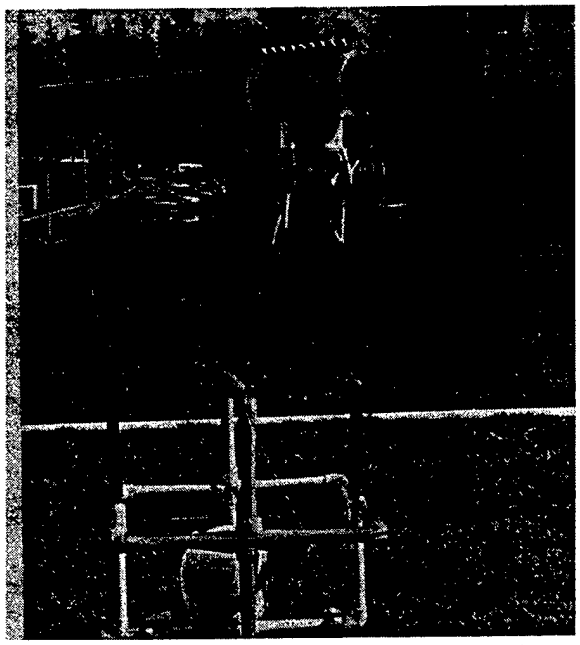

Figure 5. Pulsed Electromagnetic Induction - Prototype Configuration

2. Technology Description

2.1 Description

SOCS, Figure 6, is a testbed system which features a completely open hardware and software architecture. The system is designed to provide scientists and engineers with the ability to characterize and evaluate emerging technologies and methods for detecting, identifying, and classifying buried UXO. This will be accomplished during limited site investigations, and as a cooperative effort between the Government and private industry. Results of the limited site investigations provide the Government with two immediate benefits. First, empirical data collected provides a realistic assessment of technology capabilities and limitations when operated at a particular site. Second, SOCS provides actual UXO information to the managing facility or agency; validating the scope of the UXO problem.

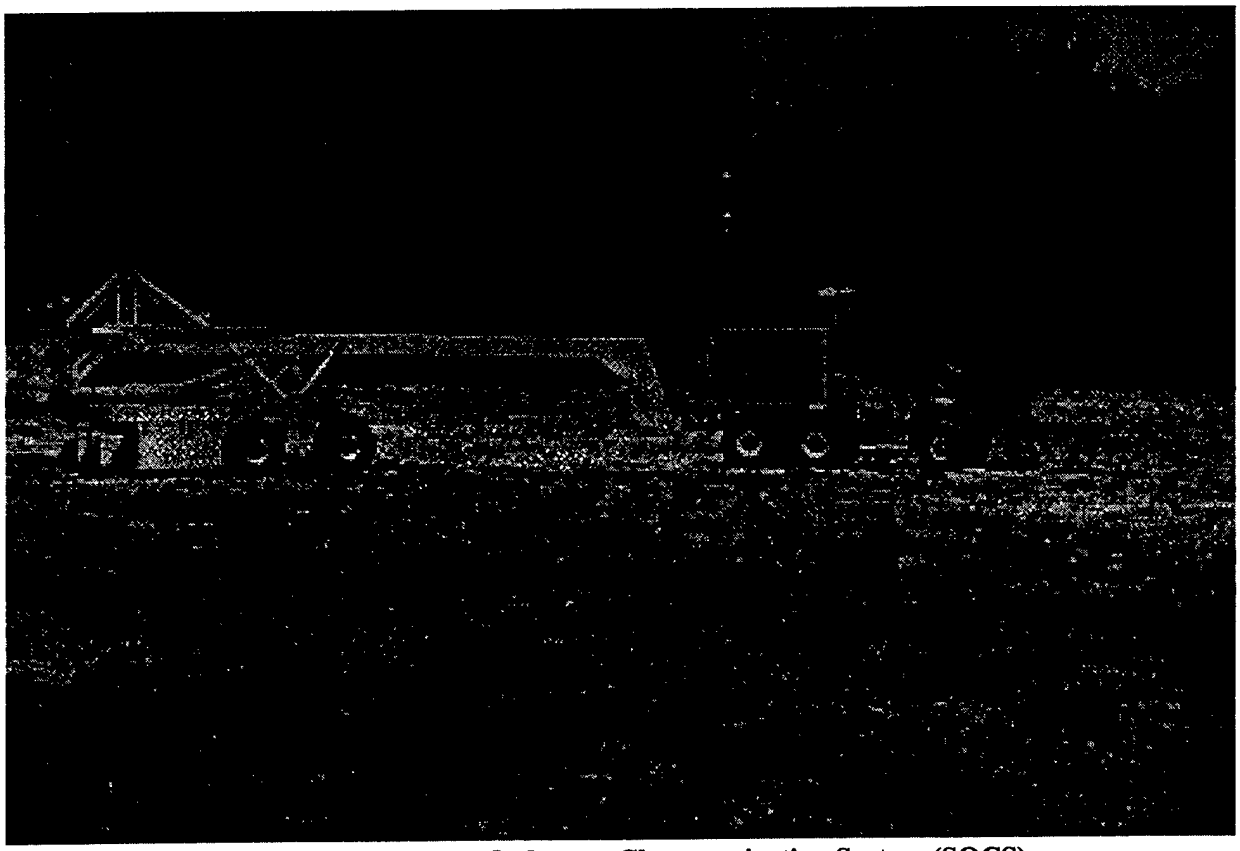

Figure 6. Subsurface Ordnance Characterization System (SOCS)

As stated earlier, SOCS is a testbed system that can be configured as necessary to meet the needs of the user. Based on the objectives of the ESTCP demonstration and the testing described in Section 1.5, USAEC, NAVEODTECHDIV and USAF/WL established a baseline configuration for SOCS. The baseline system configuration is comprised of five major subsystems:

(1) Autonomous Tow Vehicle And Mobile Command Station

(2) Multiple-sensor Platform

(3) Sensor Suite

(4) Simultaneous Data Collection And Processing System (SIDCAPS)

(5) Data Reduction and Post Processing Algorithms

Autonomous Tow Vehicle (ATV)

The ATV, Figure 7, is a modified commercial all terrain vehicle (John Deere Gator) that is integrated with precise navigation, vehicle control, communications, and data acquisition subsystems. The Gator was selected as the SOCS tow vehicle for several reasons. First, the Gator design provided the basic towing capability (4-wheel drive) and cargo capacity (800 lb) necessary for the SOCS mission. Second, the Gator design allowed for easy integration of actuators to control vehicle steering, throttle, brake and transmission. Some concerns existed about the hazards associated with driving a vehicle over shallow buried UXO. The Gator, with its 6 x 4 wheel drive configuration, exerts minimal pressure (7.1 psi when fully loaded) on the ground. This is far less than the approximately 65 psi load exerted by a 200 lb person walking in the area. Finally, the cost of the vehicle and required modifications were a fraction of that required to design, develop and fabricate a SOCS-specific vehicle. Modification of the Gator centered around minimizing noise induced to the sensor suite; primarily the magnetometers. The frame and cargo box were replaced with American Society for Testing and Materials (ASTM) 316L stainless steel - a high strength material with a low magnetic signature.

Figure 7. Autonomous Tow Vehicle

The ATV can be operated manually, by tele-operation using onboard cameras, or autonomously using a preprogrammed path, precise navigation and path execution software and controls. Manual and tele-operation modes are typically used for system preparation and transport; the autonomous mode for site characterization. In the autonomous mode, site information, such as terrain, boundaries and obstacles, are input to the path planner as an area map. The path planner automatically determines the most effective and efficient route to ensure maximum area coverage. The actual speed, direction, and location of the ATV is constantly reported by the navigation system -- a complement of INS and DGPS. The INS is based on the modular azimuth position system (MAPS). MAPS consists of ring laser gyros and three accelerometers to determine relative position, angular orientation and velocity at a rate of 20 Hz. The DGPS utilizes two earth-based antennas and a constellation of earth-orbiting satellites to determine absolute position on the earth at a rate of 1 Hz. One antenna is mounted at a known, fixed position and the other is mounted on the SOCS ATV. Information from the INS and DGPS is transmitted via radio signals to the path executioner, which compares the preprogrammed route against the actual, determines the necessary corrections, and sends the appropriate commands to adjust speed and direction.

SOCS operations are performed on-site within the mobile command station (MCS). The MCS is a commercial trailer that has been modified to allow integration of support equipment such as the GPS base station, video downlink for tele-operation, user interface for remote vehicle control, and radio frequency (RF) downlink for system position tracking and diagnostics. As an on-site work facility, the MCS also provides AC power to operate support equipment such as computers for downloading, storing, and post-processing data collected during SOCS operations. The MCS is also used to transport spare parts and tools for performing system maintenance and limited repairs.

Multiple-Sensor Platform (MSP)

As stated earlier, SOCS is a testbed system for demonstrating and evaluating new and emerging technologies, including various sensors. The SOCS MSP, Figure 8, is designed to permit mounting a variety of both active and passive sensors. The structural members are fabricated from materials that have low magnetic signatures (i.e., ASTM 316 stainless steel and 6061-T6 aluminum), and are connected together using nonconductive isolators to minimize secondary magnetic fields created by eddy

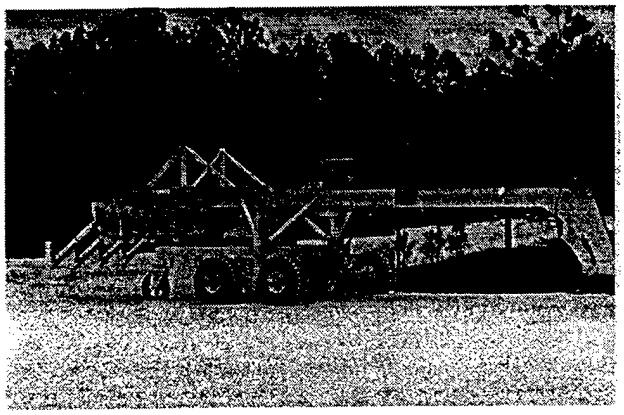

Figure 8. SOCS Multiple Sensor Platform

currents. The undercarriage and suspension are designed to minimize motion and vibration of the sensors during operation. Previous field tests conducted with STOLS[7] and the brass board GPR system[11] showed that motion and vibration are principal sources of noise that adversely affect sensor's ability to detect buried UXO. The undercarriage also allows the GPR antenna to stay nearly parallel with the soil surface when towed over uneven and rugged terrain. The magnetometer mounts are designed to allow the various orientations and positions including: (1) horizontal spacing between the sensors, (2) distance above the ground, and (3) orientation to the earth's surface. The GPR and magnetometer mounts are also positioned to minimize the influence of the simultaneously operating sensors, vehicle power sources, and other electronic noise sources. The MSP is connected to the ATV with a three-degree-of-freedom hitch. The hitch measures the roll, pitch and yaw of the MSP relative to the ATV. This information is stored with navigation data, which allows the user to accurately determine the orientation and motion of the sensors during SOCS operations.

Sensor Suite

SOCS is currently configured with two different sensors: an array of cesium vapor, total field magnetometers, and a single-antenna GPR. The magnetometers are commercial products manufactured by Geometrics. Four, model G-822A magnetometers are integrated into the SOCS MSP at .333 m horizontal spacing. This array spacing was selected based on previous tests conducted with STOLS that showed that the .333 m distance was necessary to detect small ordnance such as 60 mm mortars. The G-822A, magnetometer, Figure 9, operates at a range from 20,000 nT to 100,000 nT and provides a maximum sensitivity of .0005 nT/$\sqrt{}$Hz RMS. The sensitivity can be varied from .0005 nT at a sample rate of 1 Hz to .04 nT at 10 Hz. The G-822A model is designed for airborne, marine and vehicle applications; therefore, it is durable and weather proof. It also provides consistent performance when operated under extreme environmental conditions. For the ESTCP tests, all magnetometers were set at a height of .46 m above the ground.

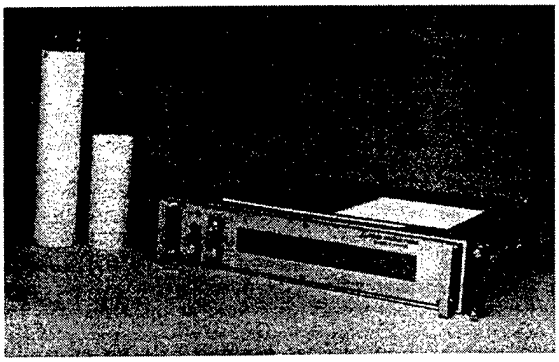

Figure 9. Geometrics G822-A Magnetometer

During SOCS operation, the four-sensor array is towed over an area and measures the earth's total magnetic field. This includes any perturbations due to local anomalies (i.e., ferrous objects, mineral concentrations, etc.) and changes in the earth's magnetic field due to solar and astronomical influences. A reference magnetometer is placed in an area free of local anomalies to measure diurnal changes to the earth's magnetic field. This provides the user with the ability to eliminate the effects of global magnetic changes during SOCS data reduction and analyses.

The SOCS GPR consists of two major subsystems: radar unit and antenna (see Figure 10). The commercial radar (Lintek, Inc.) is a step-chirp-time-domain system that operates at frequencies ranging from 50 - 500 MHz, and provides the user with the ability to increase the gain as a function of depth, commonly referred to as gain-slope. The ultra-wide band feature provides

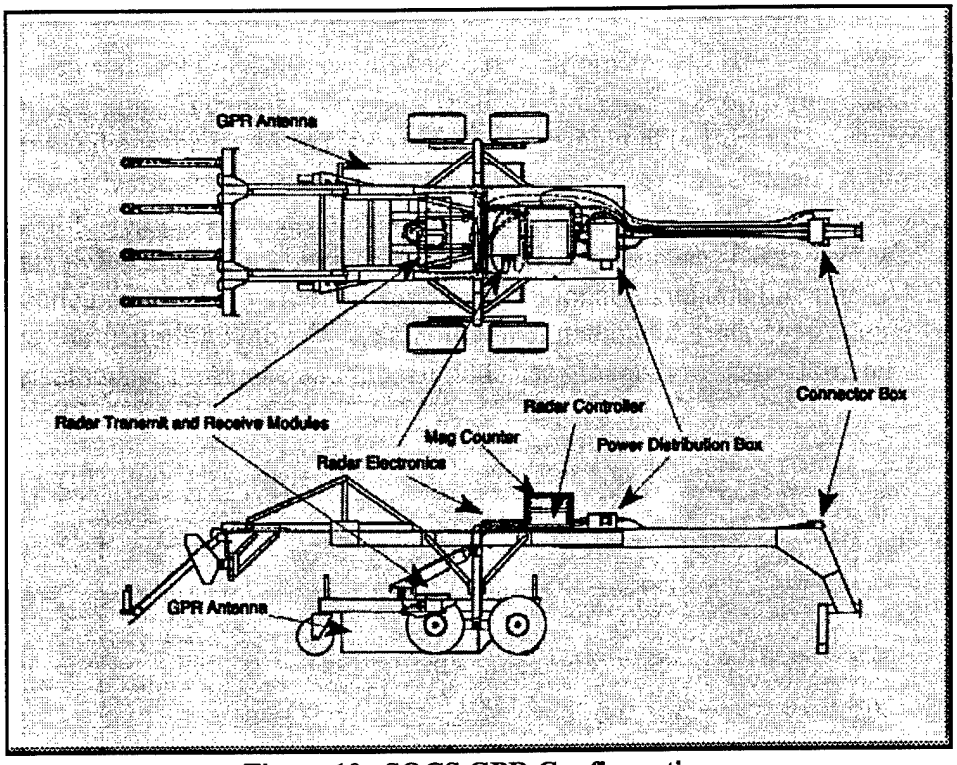

Figure 10. SOCS GPR Configuration

SOCS with the ability to detect small items near the surface and larger items buried more deeply. The step-chirp system minimizes interference from other RF sources such as television by "stepping" around those frequencies. Gain-slope, the ability to attenuate the constant power gain of the radar as a function of time, is critical to effective use of GPR in varying soil conditions.[12] The radar is controlled using an IBM compatible, Pentium-based personal computer (PC) operating under Windows NT. The PC has 32 Mbytes of random access memory and two SCSI hard drives that provide 2 Gbytes of non-volatile storage. The computer is inexpensive and provides high data throughput and an Industry Standard Architecture (ISA) 16-bit direct access memory board (DMA). All radar controller code was written in American National Standards Institute (ANSI) C. The function of the code is to control and receive raw data from the GPR and to transmit data sets to the SIDCAPS (described in Section 2.1).

The GPR antenna is a crossed-dipole configuration, Figure 11, that was fabricated by Ohio State University to meet the unique requirements for detecting buried UXO. The unique design resulted from testing referenced in Section 1.5, which showed that existing crossed-dipole antenna were not acceptable due to excessive ringing. The antenna ringing would interact with clutter and debris and inhibit the detection of UXO. The cross-dipole antenna is 5.0 ft x 5.0 ft x 1.5 ft and weighs approximately 285 lbs. It consists of a molded fiberglass cavity, lid, and deflector, which provided a stiff and rugged housing. Within the housing, antenna elements are formed from a single 3.0 ft x 3.0 ft sheet of printed circuit board material and copper that is cut away from the non-conducting areas. The antenna elements are covered with 2.0 in of polypropylene and 14.0 in of RF absorbing material. The RF absorbing material is used to suppress reflections from the antenna tips and from the shielded lid. The polypropylene layer reduces the influence of the RF absorbing material on the antenna impedance. Reference 12 provides a detailed description of the design, fabrication and operation of the antenna and GPR system.

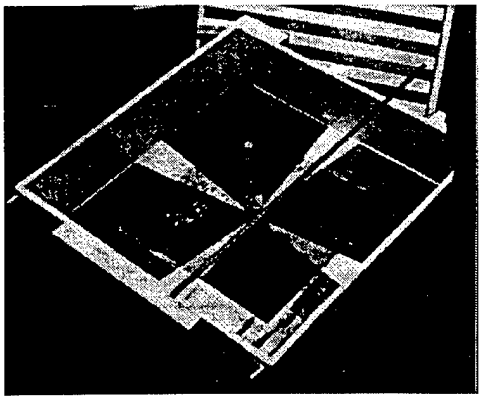

Figure 11. SOCS Crossed Bowtie GPR Antenna

Simultaneous Data Collection and Processing System (SIDCAPS)

The success of an open architecture, testbed system such as SOCS is highly dependent on the ability to collect data from many different sources and record this data in a standard format. SOCS accomplishes this using SIDCAPS. SIDCAPS is a VMEbus that conforms to ANSI/IEEE STD-1014-1987 and is mounted on the SOCS ATV. Use of this industry standard provides SOCS with the capability to easily integrate commercial devices (e.g., digital signal processors, mass storage, video, communications, motion control, etc.) necessary to interface emerging technologies with SOCS. Individual interface boards within SIDCAPS operate the ATV, track vehicle location and position using information from the GPS and INS, collect data from the magnetometers and GPR, and record MSP orientation information provided by the three-degree-of-freedom hitch. All data is stored on a removable hard disk that is transferred to a PC or computer work station for reduction and processing. Each data set is formatted in accordance with an Information Data Exchange Format (IDEF) established by NAVEODTECHDIV and USAF/WL.[15] The IDEF provides guidance for transferring data such as component identifiers, date, time, operating instructions and parameters, and hardware and software profiles among the SOCS subsystems. Data is transmitted from each of the subsystems to SIDCAPS using both Fiber Distributed Data Interface (FDDI) and ethernet links. Figures 12 and 13 show the data exchange links to SIDCAPS.[16,17]

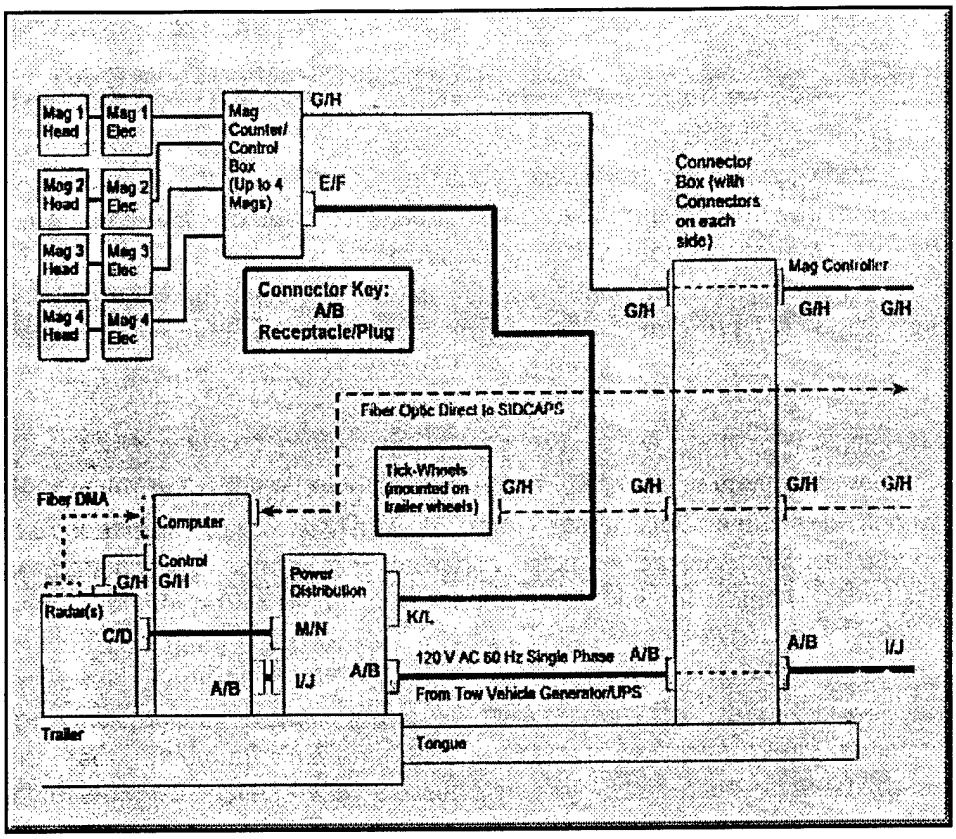

Figure 12. SOCS Sensor Interfaces

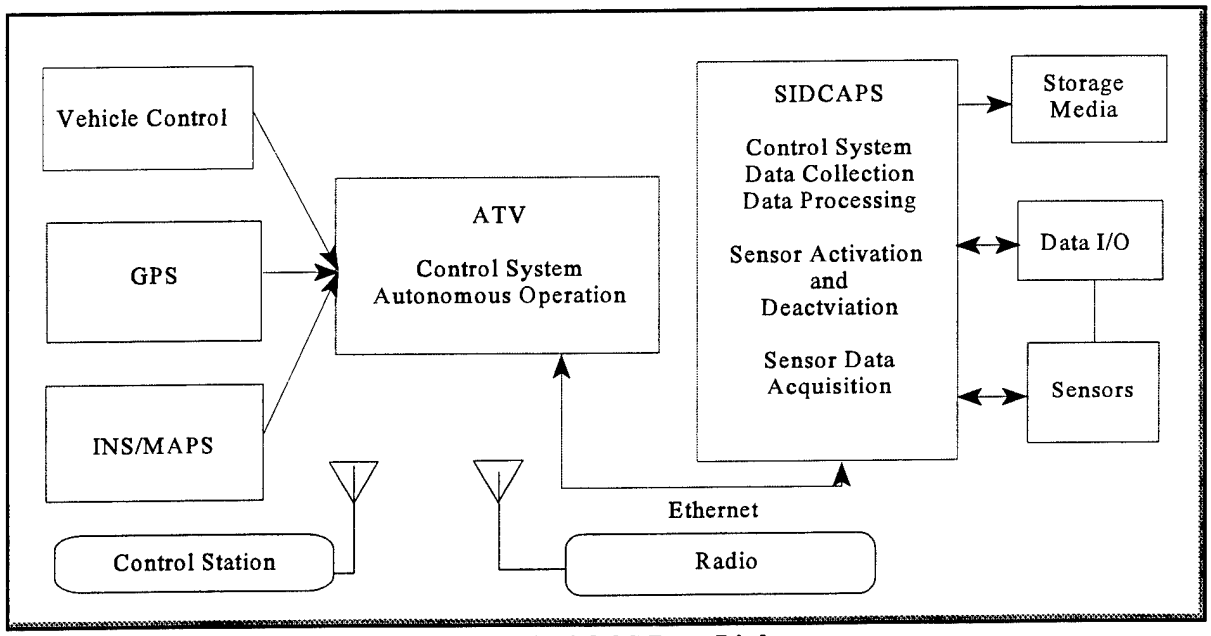

Figure 13. SOCS Data Links

Data Reduction and Post Processing Algorithms

The sensor data stored by SIDCAPS is transferred to a remote computer and processed off-line using methods unique to each sensor.

The GPR data collected by SOCS is analyzed using SAR and CNR techniques to provide the maximum ability to detect, minimize false alarms and provide a target classification capability. The SAR processor developed by Battelle reduces GPR false alarms caused by surface roughness or inhomogeneous soil. SAR processing is performed on discrete volumes of data referred to as voxels; each containing waveforms that include antenna ringing and reflections from buried objects and the surface. After preprocessing the GPR data to remove the effects of antenna ringing and the surface reflection, the waveforms can be displayed as a function of time - Figure 14. Since each voxel corresponds to a geographic position and MSP orientation that was recorded by the SOCS navigation system and three-degree-of-freedom hitch, a SAR image, Figure 15, can be constructed. This is accomplished by summing the waveform data from different SOCS positions into a coherent data set corresponding to each voxel of soil. The information resulting from the SAR image provides an accurate estimate of a target location and depth.

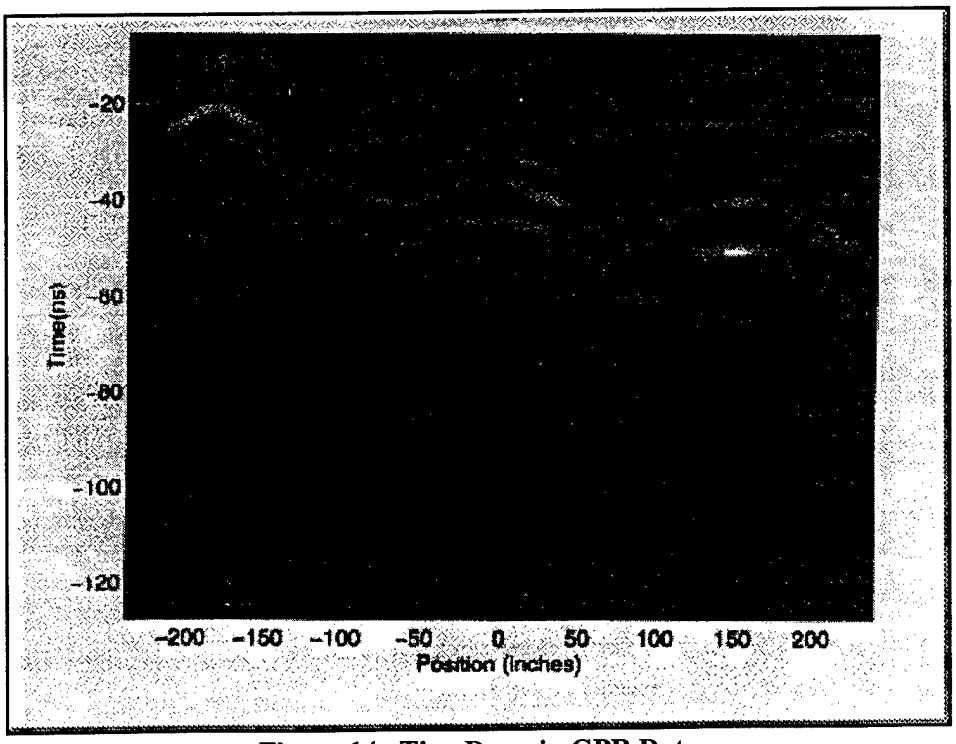

Figure 14. TimeDomain GPR Data

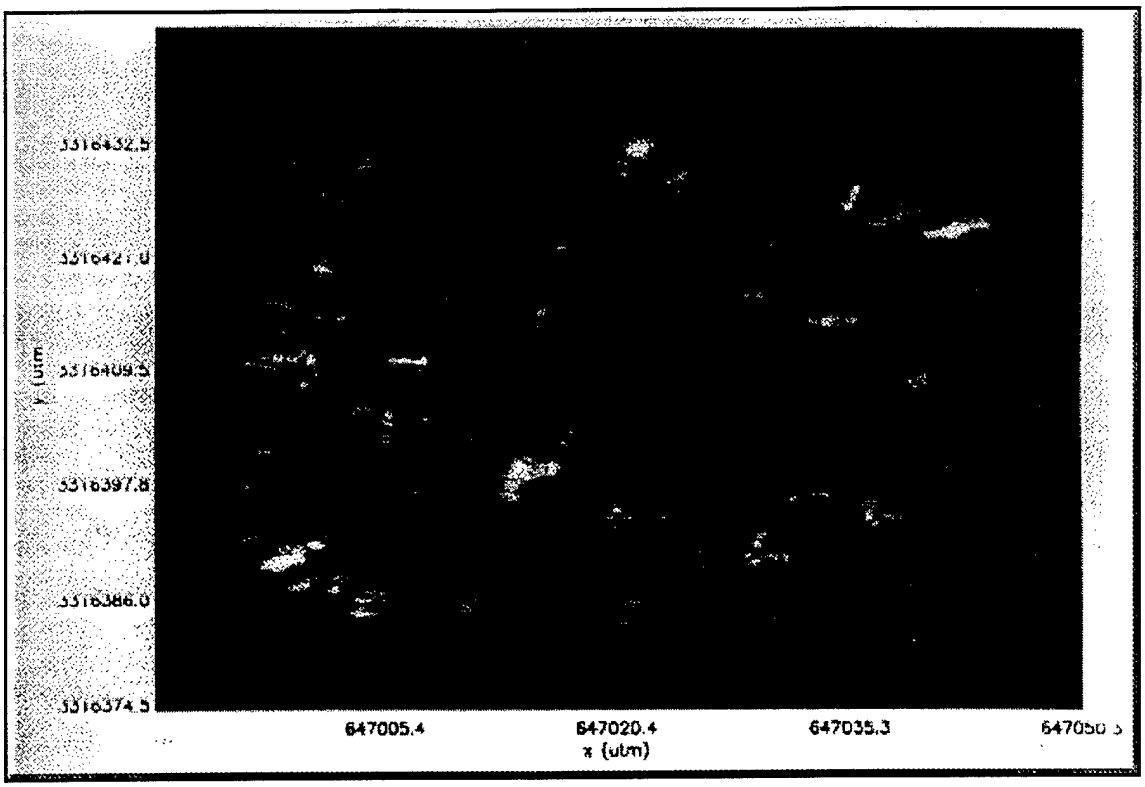

Figure 15. Synthetic Aperture Radar Image

The CNR technique uses GPR data to identify and classify detected targets and reduce false alarms caused by naturally occurring objects such as tree roots, rocks, etc. The principal behind the CNR technique is that nearly all UXO are conductive cylinders, and each resonates uniquely when excited by electromagnetic energy from a source such as GPR. A similar occurrence is evident with a tuning fork. When energy is introduced to the tuning fork by a force, it resonates at a certain frequency that is characteristic to its shape, size and composition. This phenomena was characterized during previous testing at the Ohio State University, referenced in Section 1.5. The results of this testing showed that the resonance behavior of UXO can be used to determine its length and shape. Moreover, an exact formula exists to determine the CNR of UXO when buried in different soils. A detailed description of the SAR and CNR processing methods are provided in Reference 12.

Data from the magnetometer array are mapped and analyzed using an automated processor that evaluates the characteristics of dipole signatures to determine the location, depth, and mass of ferrous objects. The automated processor compiles the data obtained from SOCS, and estimates the noise levels of the operating magnetometers, identifies any irregular data caused by a faulty sensor or excessive system noise, subtracts that earth's natural magnetic field (recorded by the reference magnetometer), and relates the magnetometer data to a physical position on the earth (stored in the SOCS navigation files). Time, from the very precise GPS clock, is the common parameter that synchronizes the navigation, three-degree-of-freedom hitch magnetometer array and reference magnetometer files

The position "tagged" magnetometer data is analyzed, and all magnetic field readings exceeding a level, specified by the user, are identified. This threshold level is typically a function of the total measured noise. A second series of algorithms uses a dipole model to determine the parameters (depth, location and size) of the identified magnetic anomaly. The algorithms also calculate a confidence level for detection probability. Finally, the automated processor provides a tabular report of the detected targets, and plots a map as shown in Figure 16. Note that the anomalies identified on the map exhibit typical dipole magnetic signatures of ferrous objects. A detailed description of the automated processor and methods used for analyzing total-field magnetometer is provided in Reference 7.

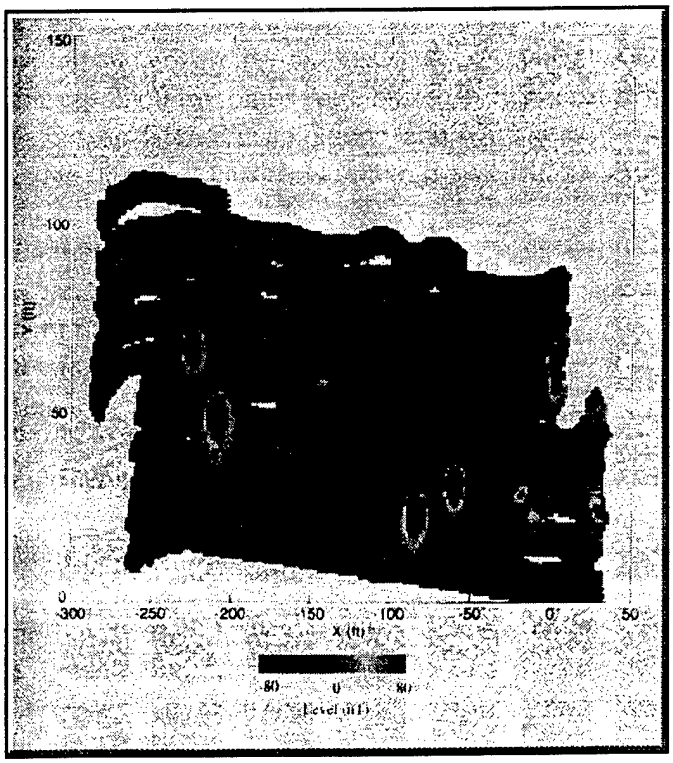

Figure 16. SOCS Magnetometer Data

2.2 Strengths, Advantages and Weaknesses

The strengths and advantages that SOCS has over other systems are many. First, the open architecture allows the user to configure the system to achieve optimum performance when operating in different environments. This includes varying the types and combinations of sensors, the orientation and position of those sensors, and the manner in which they are implemented. The flexible configuration can also be easily upgraded to integrate new sensors and evaluate their capabilities and limitations. The sensors currently used by SOCS are state-of-the-art equipment that provide complimentary information to improve UXO detection, identification, classification, and localization, while minimizing the number of reported false alarms.

SOCS has the capability to characterize areas containing UXO and create an archival record in the form of target maps and reports. The autonomous feature allows this to be accomplished without exposing a human operator to unnecessary hazards. This also reduces labor costs associated with manually traversing an area using hand-held devices and physically marking areas suspected of containing UXO.

SOCS also provides the Government with a tool to perform scientific studies, support technology enhancements, and provide information to the Government regarding future investments in research and development. SOCS can be used to employ new sensors, evaluate data analysis and fusion techniques, evaluate remote vehicle control technologies, and investigate various operating methodologies.

Like other land-based systems, SOCS has several limitations. SOCS is limited to operating in open areas that permit vehicle movement. Swamps, forests, mountains, and bodies of water prevent the system from traversing those areas and collecting sensor data.

2.3 Factors Influencing Cost and Performance

There is a common set of factors that affect the cost and performance of nearly all UXO characterization systems, including SOCS:

- Terrain, soil characteristics, vegetation coverage and other obstacles.
- UXO types, density and level of debris and clutter.
- Presence of cultural and environmental resources.
- Availability of local support services and experienced personnel.

Metrics for each of these factors are not well defined and are usually unique to each system. Additionally, the effects and influence of each factor varies based on the technology being implemented. For example, the performance of a system using an infrared sensor would be degraded by vegetation, while a magnetometer-based system would not be significantly affected. The environment that would permit optimum performance of SOCS would be one that consists of: (1) level or gently rolling terrain that is unobstructed, (2) soil that is homogenous, has low conductivity (less than 50 mmhos/m) and low permittivity/dielectric constant - the ability of a material to resist the formation of an electric field within it[18], (3) a UXO profile that includes large, ferrous UXO buried below 1 meter and small and medium size UXO buried less than 1 meter, and (4) minimal clutter and debris that would act as noise sources to the sensors. The SOCS IPT realizes that a site with these characteristic is rare; however, the ability to quantitatively predict the effects of each factor is a primary objective of the SOCS project.

3. Site/Facility Description

3.1 Background

Two sites were used during the SOCS ESTCP project: Tyndall Air Force Base (AFB), Florida and JPG. The test site at Tyndall AFB was in close proximity to USAF/WL, and provided a low-cost, convenient place to perform subsystem integration, calibration, and system operation tests. The JPG test site was part of the 120-acre controlled test site created as part of a comprehensive technology demonstration and evaluation program that is managed by USAEC.[4] The SOCS ESTCP demonstration was conducted at the southern test area (see page 28).

3.2 Site/Facility Description

The test area at Tyndall AFB, Figure 17, is approximately 1.5 acres and is comprised of homogeneous sand that is mostly clear of debris and clutter. The SOCS IPT did identify several metal fragments located in the test area, but no size or density data was collected or recorded. No vegetation or obstacles existed on the test area to impede vehicle movement. Seventeen inert ordnance targets, two 55-gallon storage drums, three steel pipes, and nine steel, calibration plates were buried at the site at precise locations. Figure 18 shows the profile of the targets located at the Tyndall AFB test site. This test area provided the SOCS IPT with near optimum conditions to operate and evaluate SOCS and each of the individual subsystems.

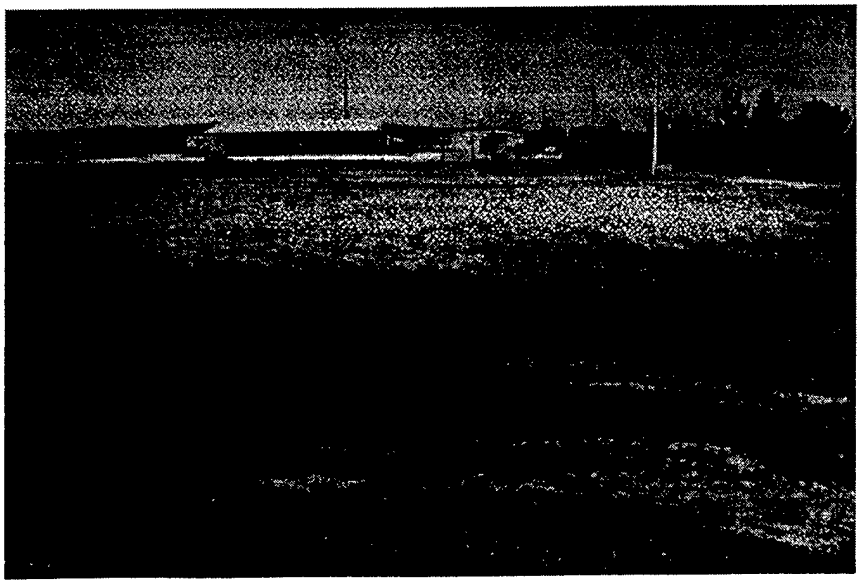

Figure 17. Tyndall AFB Test Site

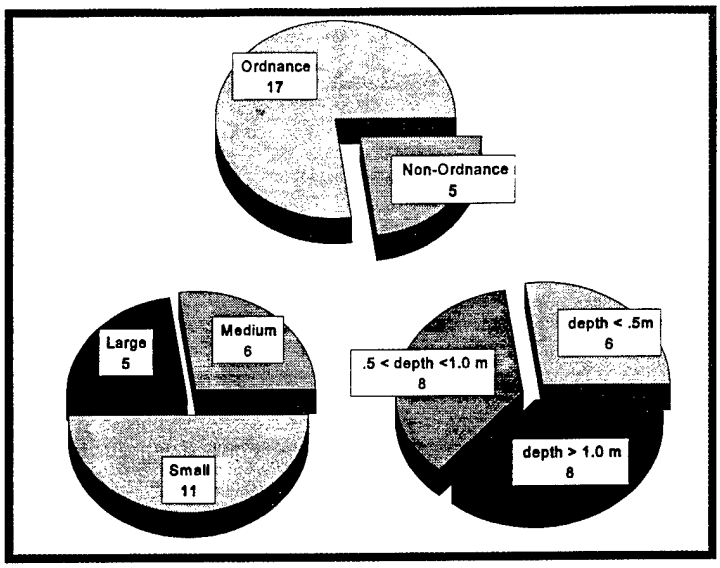

Figure 18. Baseline Target Population - Tyndall AFB

The JPG test site, Figure 19, is much different than the Tyndall AFB site. Located in southern Indiana, the test site was previously used as an artillery impact range and contains clutter and debris such as ordnance fragments, target remnants, and pieces of abandoned equipment. The soil is mostly clay and has very high permittivity (dielectric constant = 30 at a depth of .5 m). The terrain is gently rolling and covered with trees. Inert ordnance targets ranging in size from small grenades and mines to 2000 lb-bombs were buried at depths and orientations typically found at active military ranges, BRAC installations and FUD sites.[19] The following is a list of inert ordnance emplaced at the JPG test site and the range at which they were buried below the surface:

- 250 - 2,000 lb bombs: 0.15 to 5.37 m
- 76 mm - 8 in projectiles: 0.22 to 4.17 m
- 2.75 in and 5 in rocket warheads: 0.15 to 0.47 m
- 60 mm, 81 mm and 4.2 in mortars: 0.01 to 0.87 m
- M42 submunitions: surface to 0.87 m
- VS-50 and TS-50 low-metal, anti-personnel land mines: surface to 0.04 m
- 20 mm and 30 mm aircraft cannon rounds: 0.05 to 1.83 m

USAEC and NAVEODTECHDIV also emplaced false alarm sources that were also commonly found at UXO sites. This included objects such as ordnance fragments, electrical conduit and building materials ("false positives"). "False negatives" were also created by digging holes, disturbing the soil and replacing it. Section 5 provides definitions for these terms and performance metrics. Figure 20 illustrates the profile of targets located in JPG Mission NS3 (also to be discussed in Section 5).

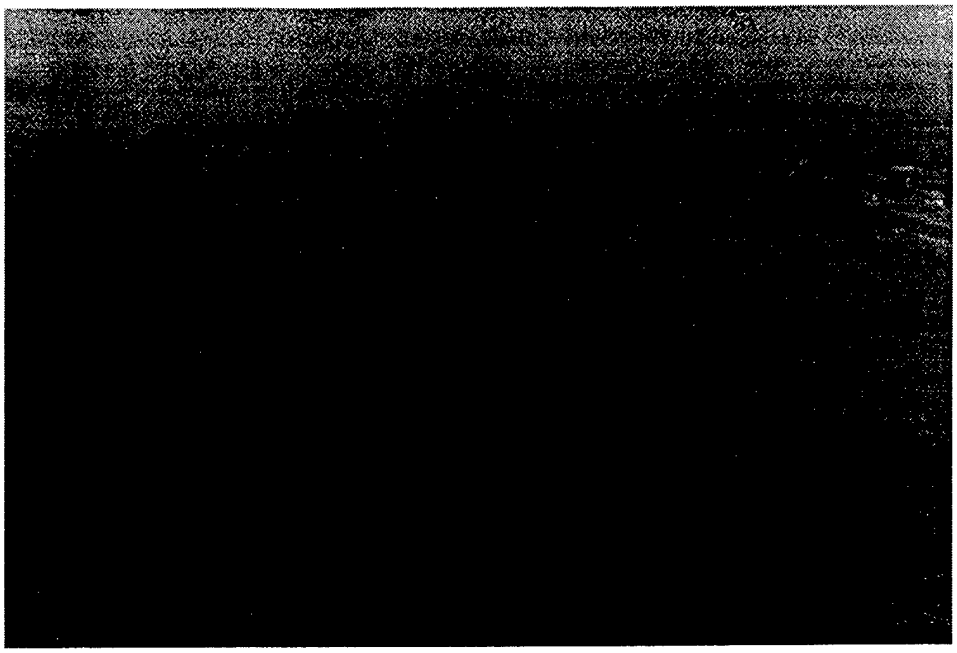

Figure 19. Test Site at JPG

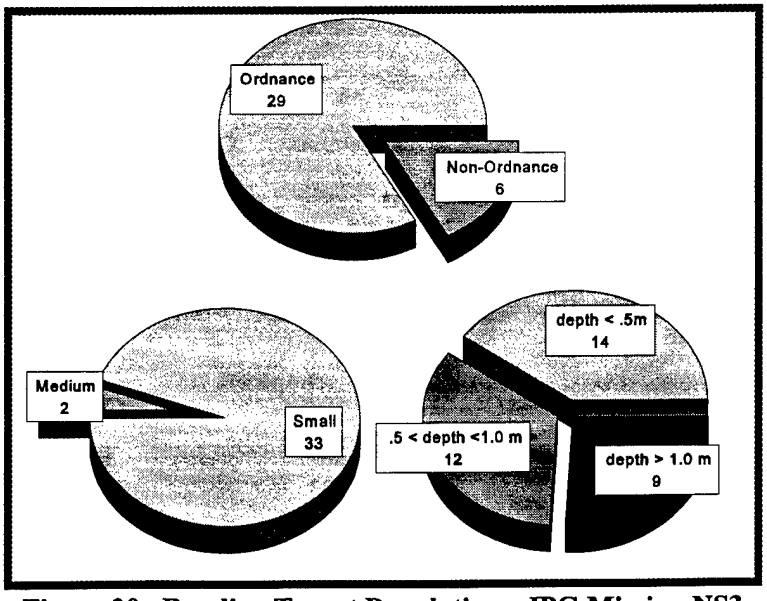

Figure 20. Baseline Target Population - JPG Mission NS3

4. Demonstration Approach

4.1 Performance Objectives

As stated in Section 1.3, the objectives of the SOCS ESTCP demonstration were to demonstrate and evaluate the capabilities and limitations of the system. To accomplish this, specific performance metrics, listed in Table 1, were established for each subsystem. Field tests were conducted at each test site and data was collected to assess each of these metrics.

Table 1. SOCS Subsystem Performance Metrics

Autonomous Tow Vehicle	Ability to program the system with a predetermined route.
	Precision of the system to autonomously traverse the preprogrammed route and avoid identified obstacles.
Multiple-Sensor Platform	Ease of sensor mounting and integration.
	Capability to traverse varying terrain.
Sensor Suite	Feasibility of operating a magnetometer array and GPR simultaneously on the platform.
	Durability of each sensor when operated under field conditions.
	Ability of each sensor to detect subsurface anomalies.
Simultaneous Data Collection and Processing System	Capability to control and record data from multiple sensors, vehicle navigation and control equipment, and the three-degree-of-freedom hitch.
Data Reduction and Post Processing Algorithms	Accuracy to identify, characterize and localize UXO detected with each sensor.
	Ability to present the information collected.

4.2 Physical Setup and Operation

There are four major tasks that are necessary to setup and operate SOCS. First, the SOCS operating team performs an initial investigation of the site. This includes: (1) defining the site boundary and mapping landmarks and geodetic benchmarks, (2) locating and recording the position of obstacles that would impede the SOCS ATV, (3) identifying access roads to the site, (4) performing a historical record search and compiling data related to the types and quantities of ordnance used at the site, and (5) characterizing the soil geophysical properties. The time, materials and labor hours required to perform each of these tasks varies significantly with each site.

Task two includes transporting SOCS and necessary supplies to the site, and assembling the major subsystems. Each of the major subsystems (ATV/MCS, sensor suite and MSP) are shipped individually using a semi-trailer truck. Upon arrival at the test site, the SOCS subsystems are assembled to reflect the configuration determined, based on information collected during task one, to be optimum for the site. Magnetometers and GPR are attached to the MSP and their position and orientation are set. The MSP is linked to three-degree-of-freedom hitch and ATV, and communication receivers and antennas mounted as specified by system integration requirements.[20] Subsystems are electrically linked, initialized, and calibrated. To finalize the process, a complete diagnostic check is performed in accordance with validated procedures.[21] The reference magnetometer is placed in an area free of magnetic anomalies and local disturbances such as vehicles, power sources and buildings. This task typically requires four persons working approximately 8 hrs each.

Task three consists of SOCS operations (traversing the preprogrammed route, and acquiring data from sensors, navigation, and three-degree-of-freedom hitch) conducted in accordance with the test plan provided in Appendix B. Operations are typically performed with a team of four to five persons. No infrastructure is required at the site, because SOCS is designed to operate in remote areas; fuels, power supplies, and communications are all transported with the system.

The final task is data reduction and processing. This is done both on-site and at remote facilities. The level of effort required is a function of the area characterized, the sensors implemented, and the number of anomalies detected. A small quantity of sensor data is evaluated at the site as a part of the SOCS standard operating procedure for data quality assurance. The remainder of the data are stored and processed when SOCS has completed collecting data at the site. Each data set, stored in the IDEF format, is analyzed using algorithms described in Section 2 to assess the performance of the ATV, magnetometer array and GPR. At the completion of the data reduction and processing, subsystem assessment reports are generated. The content of each of those reports are described in Section 4.4.

4.3 Sampling Procedures

Sampling procedures for SOCS are variable and determined by the information collected during the initial investigation described previously. SOCS speed, direction, and route are dependent on parameters such as soil conditions, types of expected UXO, obstacles, etc. Five land plots were selected at the Southern Test Area of JPG to demonstrate and evaluate SOCS: These areas are identified in Figure 21. Tests performed at Tyndall AFB showed that collecting data in north-south and east-west directions provided the best results; therefore, routes were planned to follow a rectangular pattern oriented appropriately. The size of the UXO targets expected to be detected

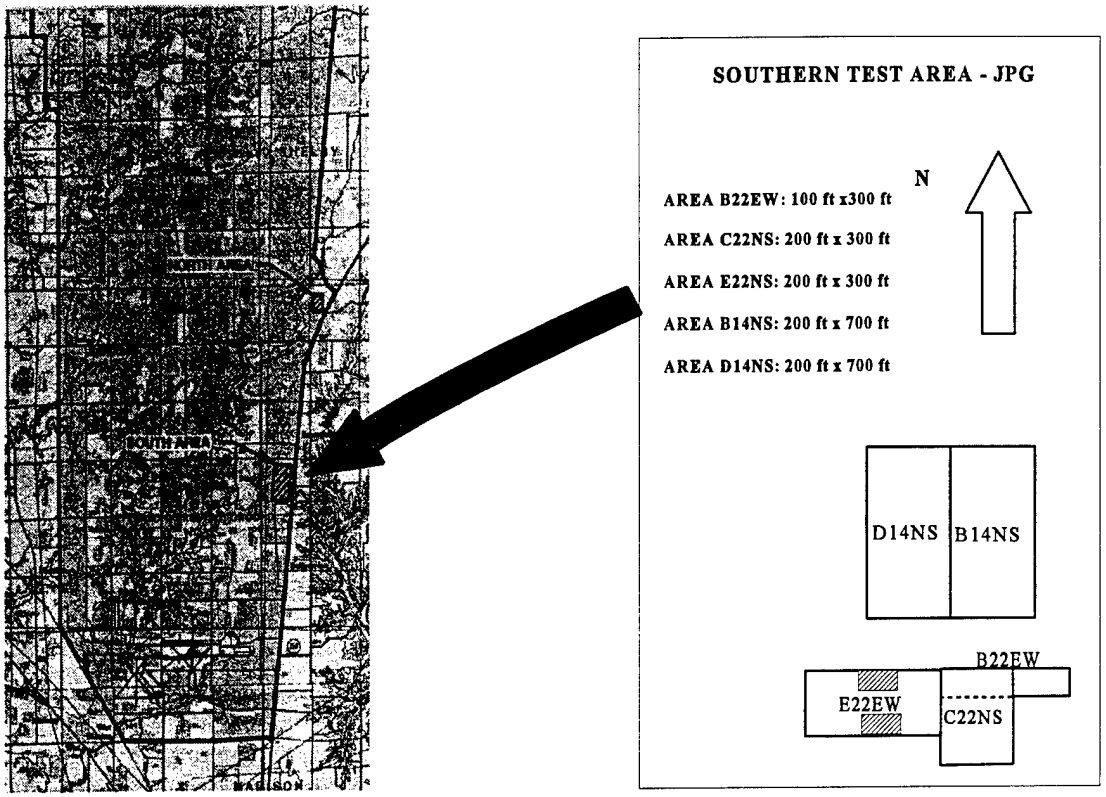

Figure 21. JPG Test Areas

at JPG dictated a horizontal spacing of 2.5 ft between the centerline of each SOCS path. Sampling rates of the magnetometers were set at 10 Hz and 20 Hz for the GPR. Sensor, navigation and hitch data are collected for up to 4 hrs before being downloaded and stored for reduction and analysis.

4.4 Analytic Procedures

Analytic procedures for analyzing SOCS performance centered around methods developed for the UXO clearance technology demonstrations performed at JPG.[4] From these methods, the statistics listed below are established as the basis for measuring the performance of SOCS.

- Probability of UXO Detection (P_d) - The ratio of targets reported as UXO by SOCS to the actual number of UXO buried at the test site. This provides a measure of the system's ability to detect buried UXO. A number approaching 1 is desirable.

- False Positives (FP) - Targets reported as UXO by SOCS that correspond to non-UXO items (e.g., fragments, construction material, etc.) buried at the site. This provides a measure of the system's ability to identify and discriminate between UXO and other objects typically found at a UXO site. Zero or a number close to zero is desirable.

- False Negatives (FN) - Targets reported as UXO by SOCS that do not correspond to any item buried at the site. Zero or a number close to zero is desirable.

- False Alarm Ratio (FA_{ratio}) - The ratio of the total number of false targets (positives and negatives) to the number of UXO detected at the site. This is a figure of merit that is used to relate system performance to actual UXO remediation. The false alarm ratio indicates the number of holes that would have to be dug to achieve the stated detection capability. A small number is desirable.

- False Alarm Rate (FAR) - The total number of false target (positives and negatives) per unit area.

- Location Accuracy (AR_{xy}) - Radial difference between the UXO position reported by SOCS and the actual UXO position.

- Depth Accuracy (AR_z) - Absolute difference between the UXO depth reported by SOCS and the actual UXO depth.

- Classification Ratio (P_c) - Ratio of the number of UXO reported by SOCS that are correctly classified as small, medium or large.

- Length Estimate - Accuracy of the CNR algorithms to determine the length of a detected UXO. This metric applies only to the GPR.

- Survey Precision - The ratio of the total area characterized by SOCS to the total site area.

5. Performance Assessment

5.1 Performance Data

To measure the ability of the ATV to traverse an area, an algorithm was developed to compare the planned SOCS route to the actual SOCS route recorded by the navigation system. Survey precision was calculated using the actual vehicle path multiplied by the MSP width and subtracting overlapping areas. To minimize the effects of GPS inaccuracies, INS position data was used to determine the ATV and MSP route. NTV tests performed prior to the SOCS project showed that the INS information was nearly identical to the actual path of the vehicle. Figure 22 is a graphical presentation of a SOCS route and the area characterized under autonomous control. Table 2 provides a summary of the survey precision results for Tyndall AFB and each of the test areas at JPG.

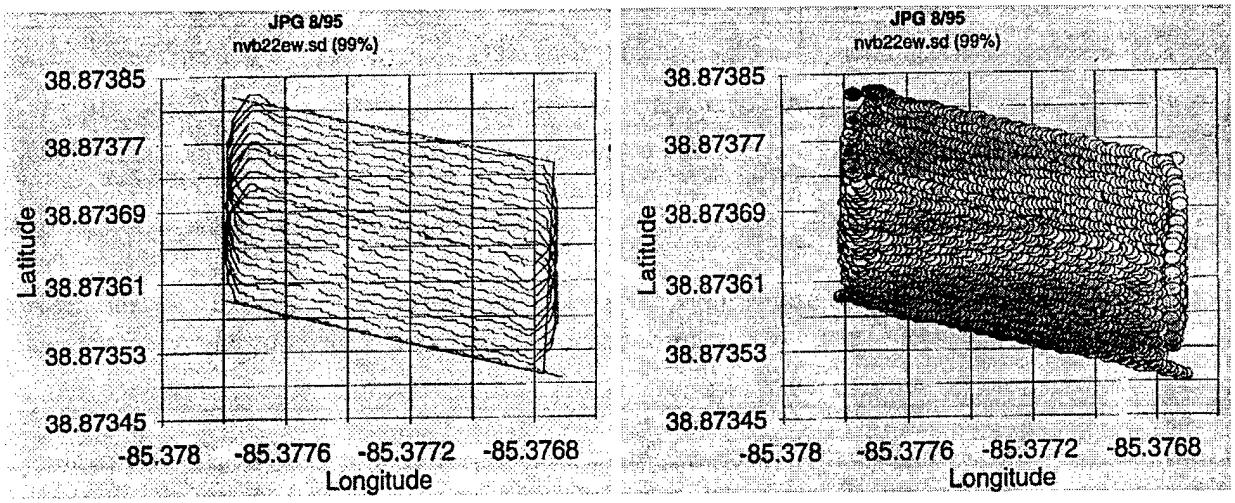

Figure 22. ATV Navigation Test Results

Table 2. SOCS ATV Test Results

Test Site	Area Characterized by SOCS	Notes
Tyndall AFB	99%	• No obstacles encountered. • Minor maneuvering problems in the sand due to system weight and carriage configuration - no corrective action necessary.
JPG		
B22EW	100%	• No obstacles - 100% of planned route completed. • Total survey time = 28 minutes. • Swath width = 1.25 meters.
C22NS	97%	• Two obstacles resulted in a planned route for 97% area characterization. • Completed 100% of planned route - good obstacle avoidance achieved. • Swath width reduced to .5 meters to obtain greater GPR data resolution. • System experienced difficulties making sharp turns. • Total Survey Time = 90 minutes
E22EW	96%	• Same notes as C22NS • Total Survey Time = 71 minutes
B14NS	64%	• Heavy rains, deep mud and mechanical problems prevented test completion. • Total Survey Time = 116 minutes
D14NS	74%	• Five obstacles located at test area. • Structural failure of ATV frame prevented test completion. • System followed nearly 100% of planned path and successfully avoided two obstacles prior to structural failure.

The data collected from each sensor were processed using the algorithms unique to that sensor. As described in Section 2, the GPR data is processed in a two-step process using a SAR method to identify detected anomalies and the CNR to discriminate and classify those anomalies. Initial results from testing at Tyndall AFB showed that 27 targets were reported as UXO within the approximately .7 acres surveyed. Of those, 12 corresponded to baseline targets. Table 3 provides a summary of the GPR metrics measured at a critical radius (R_{crit}) of 2.0 meters. Table 4 provides a comparison of each reported target information versus actual.

Table 3. GPR Results - Tyndall AFB
R_{crit} = 2.0 m

Total Number of Targets Reported by SOCS GPR	27
Total Number of Baseline Targets Detected	12
Total Number of Baseline UXO Targets Detected	8
Probability of UXO Detection (Pd)	47.1%
Accuracy of UXO Length Estimate (% of actual target length)	
Mean	33.4%
Standard Deviation	27.6%
Maximum	108%
Minimum	2.5%
False Positives (FP)	2
False Negatives (FN)	15
False Alarm Ration (FA_{ratio})	1.5
False Alarm Rate (FAR) per acre	24.6
Location Accuracy (AR_{xy}) (meters)	
Mean	.87
Standard Deviation	.389
Maximum	1.45
Minimum	.34
Depth Accuracy (AR_{z}) (meters)	
Mean	1.05
Standard Deviation	.313
Maximum	1.62
Minimum	.48

Table 4. Target Data and GPR Results - Tyndall AFB

TARGETS DETECTED WITH SOCS GPR

Baseline Target Information							Predicted Results	
No.	Name	Size	Orientation	Attitude	Depth (in)	Length (in)	Resonance Frequency (MHz)	Length (in)
1	155 mm projectile	M	160°	+30°	38.3	36	70.3	37.7
2	500 lb bomb	L	130°	0°	63.6	61	94.4	28.0
3	55 gal drum	L	120°	0°	33.8	48	48.9	53.9
4	55 gal drum	L	125°	+30°	41.5	48	56.4	46.8
5	2000 lb bomb	L	75°	-30°	55.1	90	58.2	45.4
6	8 in projectile	M	120°	-45°	18.7	30	71.3	37.0
10	practice bomb	S	165°	0°	42.5	25	80.6	32.8
15	practice bomb	S	0°	+30°	37.7	25	62.9	42.0
16	practice bomb	S	300°	0°	47.3	25	75.2	35.1
19	4.2 in mortar	M	270°	0°	23.9	19	114.6	23.1
21	steel pipe	S	90°	0°	46.5	24	79.6	33.2
22	steel pipe	S	90°	0°	60.7	36	85.9	30.7

Table 4. Target Data and GPR Results - Tyndall AFB

TARGETS NOT DETECTED WITH SOCS GPR

No.	Name	Size	Orientation	Attitude	Depth (inch)	Length (inch)	Resonance Frequency (MHz)	Predicted Length (inch)
7	81 mm mortar	S	330°	-35°	22.4	18		
8	81 mm mortar	S	225°	-45°	31.1	18		
9	8 in projectile	M	165°	0°	28.1	30		
11	practice bomb	S	unknown	-90°	18.9	25		
12	8 in projectile	M	0°	-30°	58.5	30		
13	60 mm mortar	S	330°	0°	16.2	8		
14	60 mm mortar	S	215°	-45°	12.7	8		
17	5 in rocket warhead	M	270°	+45°	24.1	18		
18	Russian mortar	M	340°	+30°	59.1	22.5		
20	steel pipe	S	90°	0°	7.3	12		

UXO Size: Large (L) > 205 mm principal diameter
Medium (M) 105 mm - 205 mm
Small (S) < 105 mm
Orientation: Forward/Nose direction: 0° - North, 90° - East, 180° - South, 270° - West
Attitude: 0° - principal axis parallel to surface, -90° - nose down, +90° - nose up
Depth: Distance below surface to center of mass

The IPT support contractors conducted further analyses to correct for variations in ATV velocity, MSP position and location errors induced by the GPS, and improper gain settings. The analysis of refined data showed nearly a 40 percent increase in P_d, a reduction in the FA_{ratio} by approximately 10%, and improved estimates for UXO length/size.[22]

The magnetometer data was processed using four times the noise threshold and the same R_{crit} as that for the GPR analysis. Tables 5 and 6 provide a summary of the magnetometer results achieved at Tyndall AFB.

Table 5. Magnetometer Results - Tyndall AFB
Signal to noise threshold = 4 (25 gamma)
R_{crit} = 2.0 m

Total Number of Targets Reported by SOCS Magnetometers	23
Total Number of Baseline Targets Detected	9
Total Number of Baseline UXO Targets Detected	8
Probability of UXO Detection (Pd)	47.1%
Baseline Targets Correctly Classified by Size	33.3%
False Positives (FP)	1
False Negatives (FN)	14
False Alarm Ration (FA_{ratio}) *Note: All false alarms reported at a 99% confidence level by the analyst.* False Alarm Rate (FAR) per acre	1.875 21.7
Location Accuracy (AR_{xy}) (meters)	
Mean	.96
Standard Deviation	.40
Minimum	.42
Max	1.8
Depth Accuracy (AR_{z}) (meters)	
Mean	.37
Standard Deviation	.24
Minimum	.01
Max	.76

Table 6. Target Data and Magnetometer Results - Tyndall AFB

TARGETS DETECTED WITH SOCS Magnetometer

Baseline Target Information						Predicted Results		
No.	Name	Size	Orientation	Attitude	Depth (in)	Size	Depth (in)	Confidence (%)
1	155 mm projectile	M	160°	+30°	38.3	L	63.0	99
2	500 lb bomb	L	130°	0°	63.6	L	63.4	99
4	55 gal drum	L	125°	+30°	41.5	L	61.0	99
5	2000 lb bomb	L	75°	-30°	55.1	L	85.0	99
6	8 in projectile	M	120°	-45°	18.7	L	38.2	99
7	81 mm mortar	S	330°	-35°	22.4	M	38.2	99
9	8 in projectile	M	165°	0°	28.1	L	28.7	99
11	practice bomb	S	unknown	-90°	18.8	L	33.9	99
12	8 in projectile	M	0°	-30°	58.5	L	68.1	99

Combining the data from each SOCS sensor, a composite set of targets was established and analyzed against the site baseline. Table 7 provides a summary of the overall performance of SOCS when tested at Tyndall AFB. The results show that the system was operating as designed, and the subsystems were properly integrated to perform the ESTCP demonstrations at JPG. The results also show that the magnetometers can not resolve two objects located in close proximity to each other. For example, target numbers 3 and 4 were reported as a single target.

Table 7. SOCS Results - Tyndall AFB
R_{crit} = 2.0 m

Total Number of Targets Reported by SOCS	50
Total Number of Baseline Targets Detected	16
Total Number of Baseline UXO Targets Detected	12
Probability of UXO Detection (Pd)	70.6%
False Positives (FP)	4
False Negatives (FN)	28
False Alarm Ratio (FA_{ratio}) False Alarm Rate (FAR) per acre	2.33 46.3
Average Location Accuracy (AR_{xy}) (meters)	.96
Average Depth Accuracy (AR_{z}) (meters)	.37

SOCS was demonstrated at JPG in September 1995. A total 6.86 acres were traversed within the JPG test areas described in Section 4.3. Due to subsystem problems (to be discussed later), data from both sensors was collected for an area approximately 1.04 acres - designated as Mission NS3. A complete analysis of mission NS3 was performed in accordance with the methods used to analyze the data collected from Tyndall AFB. The analysis results for Mission NS3 are provided in Table 8. Appendices C and D provide detailed information regarding the processing and analysis of the magnetometer array and GPR data collected at JPG.

Table 8. SOCS Performance - JPG Mission NS3
R_{crit} = 2.0 m
Magnetometer Signal to Noise Threshold = 4 (10 to 12 gamma)

	Magnetometer Array	GPR	SOCS Composite Data Set
Number of Targets Reported	21	22	43
Number of Baseline Targets Detected	4	6	10
Number of Baseline UXO Targets Detected	3	6	9
Number of Detected Baseline UXO Targets Correctly Classified for Size	0		
Accuracy of UXO Length Estimate (% of actual target length) Mean Standard Deviation Maximum Minimum		 81.8% 43.0% 147.0% 16.9%	
Probability of UXO Detection (Pd)	10.3%	20.7%	31.0%
False Positives (FP)	1	0	1
False Negatives (FN)	17	16	33
False Alarm Ratio (FA_{ratio}) False Alarm Rate (FAR) per acre	5.67 17.3	2.83 15.4	3.3 31.7
Location Accuracy (AR_{xy}) (meters) Mean Standard Deviation Maximum Minimum	 1.25 .41 1.67 .62	 1.26 .47 1.86 .53	 1.26 .45 1.86 .53
Depth Accuracy (AR_{z}) (meters) Mean Standard Deviation Maximum Minimum	 0.46 .28 .80 .01	 0.54 .55 1.7 .06	 .51 .46 1.7 .06

5.2 Data Assessment

The data collected and presented in Section 5.1 can be used to perform an assessment of each of the SOCS' major subsystems and the complete system. The following discussions focus on two primary measures of system performance: (1) ability of the SOCS ATV to autonomously tow a suite of sensor, and (2) capabilities of the sensor suite to accurately detect, identify, and characterize buried UXO.

ATV

The data collected using GPS/INS navigation and SIDCAPS provided a realistic assessment of the ATV's path planning, route following, and obstacle avoidance capabilities. When the ATV is operated at a site that has minimal obstacles and smooth to gently rolling terrain, nearly 100 percent of the area can be efficiently traversed. Under conditions where obstacles prevented 100 percent coverage, the ATV effectively navigated to avoid the obstacles. However, it was observed that the path execution software fails when the ATV encounters obstacles near the test area boundary or in the proximity of turns. A preliminary assessment indicates that this problem is inherent to the software and can be avoided during route planning.

Sensor Suite

The performance of the SOCS suite was not completely characterized during the ESTCP demonstration, and the test performed at JPG is not a realistic assessment of sensors' capabilities and limitations. Several problems were encountered during the demonstration that significantly affected the quality of the data collected and the effectiveness of the analysis techniques. These problems, listed below, were primarily attributed to subsystem reliability:

- Erratic data was identified in the files containing magnetometer and platform orientation information.
- Intermittent communications caused the system to re-initialize during data collection.
- Some position errors were identified in the navigation files that induced errors in the magnetometer and GPR data files.
- Structural and mechanical problems with the MSP forced an early termination of the tests.

Despite the problems encountered at JPG, sufficient data was collected at Tyndall AFB and JPG to make some preliminary assessments of the sensors' capabilities and identify future testing necessary to optimize system performance. Figures 23 and 24 show that SOCS has the capability to detect all sizes of UXO at depths of up to 1.5 meters. Moreover, the GPR and magnetometer provide complimentary UXO information; each detecting a different set of UXO at JPG.

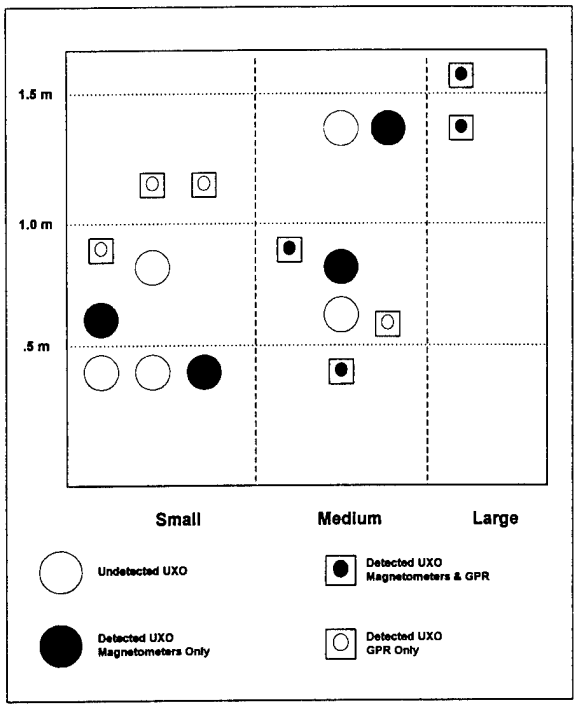

As expected, the magnetometer array is more proficient in detecting medium and large UXO buried below 0.5 meters; because, the analysis technique for magnetometer data can more readily identify long baseline dipoles than short baseline dipoles that are typical of smaller ordnance and surface debris. Further assessment of the magnetometer data collected from JPG indicates that the analysis software is unable to distinguish between multiple targets buried close together.

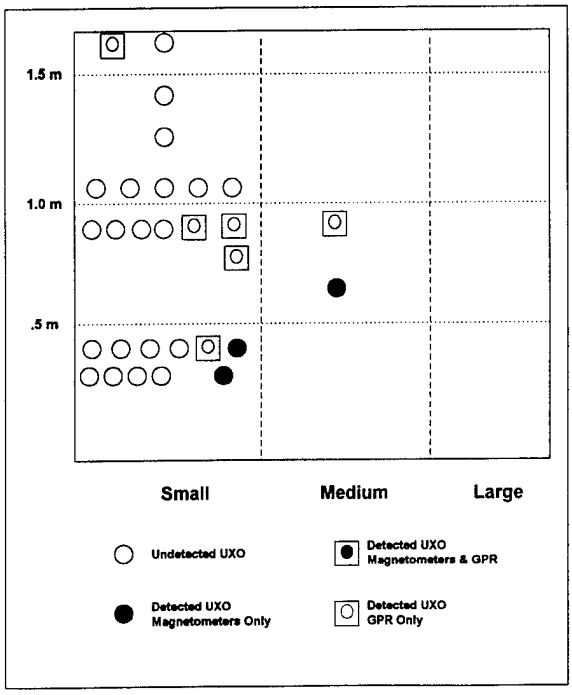

Figure 24. SOCS UXO Detection JPG Mission NS3

While this is not completely unexpected, the resolution of multiple dipoles was much less than predicted. The multiple dipoles also caused greater than expected depth and position errors. Additional tests are necessary to evaluate parameters such as sensor response rate, data sampling rate, and surveying speed and direction, and their effects on resolution of the magnetometer array. Appendix D provides an additional assessment of the magnetometer array.

Figures 23 and 24 also show that the SOCS GPR has the potential to be an effective sensor for detecting buried UXO. The poor predictions for target depth and location are attributed to several factors such as imprecise position data and lack of accurate soil property information. In at least two

cases, the GPR was able to resolve multiple targets in close proximity to each other. The CNR techniques were effective in reducing false alarms caused by surface and near-surface debris, and, as shown by the data in Table 3, is a promising technique for predicting the length of detected UXO. As with the magnetometers, further tests are necessary to fully evaluate the sensor's capabilities. Some of these tests include a study of: (1) the effects of varying soil electrical properties, (2) navigation precision and SAR focusing, (3) vehicle surveying rate and direction, (4) data sampling rate, and (5) gain slope settings for different soils and UXO sizes. A further discussion of the GPR analysis is provided in Appendix C.

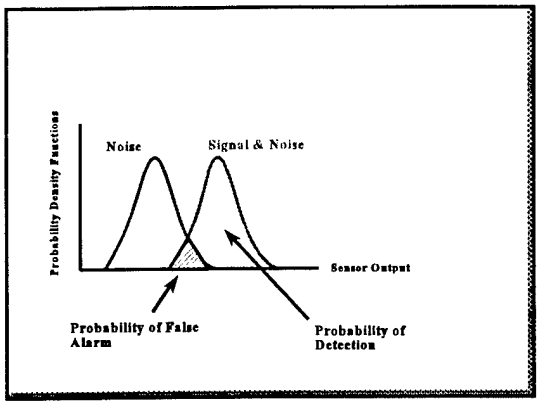

Figure 25. Sensor Performance Curves

In addition to specific tests described above, further testing must be performed to accurately characterize system, sensor, and geophysical noise induced to each sensor. These noise sources include ferrous components of the ATV, sensor electronics and power transmission equipment, MSP motion and vibration during operation, range clutter and debris, mineral deposits, antenna ringing, and varying soil conditions. Sensor Performance Curves such as the one depicted in Figure 24 must be created during rigorous system tests and collection of empirical data. These curves will provide an accurate determination of the detection capabilities of SOCS and its susceptibility to false alarms.

5.3 Technology Comparison

Comparing the performance of SOCS to other systems such as those described in References 4 and 5 does not provide a true measure of the system's value. As stated in Section 5.2, the reliability problems encountered at JPG did not permit the SOCS IPT to perform a comprehensive and realistic assessment of the systems' UXO detection, identification, classification, and localization capabilities. However, the results achieved from the Tyndall AFB tests do show that SOCS detection and discrimination capabilities are comparable to commercial systems, and that the testbed configuration has the potential to provide the Government with a characterization capability that has not been demonstrated to date. The autonomous feature is unique and provides the operator with increased safety during site investigations. Additionally, the open architecture design and standard data format structure of SOCS permits the continued study and advancement of both technology and methods. With further refinement of the SOCS technology, a commercial version of the system would be capable of characterizing up to 20 acres per day.

6. Cost Assessment

6.1 Cost Performance

If SOCS technology transitioned to commercial use, the expected operational costs of SOCS are listed in Table 9.

Table 9. Expected Operational Costs of SOCS Technology

Preparation & Mobilization		**System Operation & Maintenance**		**Demobilization & Data Analysis**	
Activity	Cost	Activity	Cost	Activity	Cost
Capital Equipment - One Time Purchase of SOCS	$600k	System Setup	$5k	System Packaging and Transport	$8k
Initial Site Investigation (search of UXO historical records, map terrain and locate obstacles, measure soil characteristics, and emplace survey control points)	$100k	System Operation and Data Acquisition	$2k per day	Data Reduction, Analysis, and Reporting	$2k per day
Support Equipment and Consumable Supplies	$10k	Routine Maintenance	$5k		
System Checkout and Transport	$15k				

6.2 Cost Comparisons to Conventional and Other Technologies

A direct comparison of costs for implementing conventional methods versus the SOCS technology does not provide a complete assessment of costs for UXO clearance. The conventional method for characterizing UXO sites, "mag and flag" (described previously), requires a much lower one-time investment for capital equipment, and overall lower costs for operation and maintenance. However, these lower costs are negated by increased remediation costs. Poor detection capability, high false alarms, and the inability to discriminate between UXO and debris (described in References 4, 5, and 6), force the Government to excavate every reported anomaly or accept significant liability for hazards to human health and property. The SOCS technology will provide the Government with more accurate UXO information that is expected to result in a substantial overall cost savings for UXO clearance.

7. Regulatory Issues

7.1 Approach to Regulatory Compliance and Acceptance

As discussed in Section 1.4, UXO clearance projects are executed in accordance with DoD 6055.9-STD with oversight from the Department of Defense Explosives Safety Board (DDESB). All equipment, systems and methods used at active, inactive, closing, or closed UXO sites are required to be approved by the DDESB. Specific performance requirements are not included in the DDESB document; however, future regulations are expected to establish minimum standards.

Since the tests at Tyndall AFB and JPG were the first demonstrations of SOCS, the public has not directly participated in the SOCS efforts. The SOCS IPT acknowledges that public acceptance of implemented technology is paramount to meeting the Government's plans for returning DoD property to the public, and all information obtained through the SOCS program will be distributed to the public via Technical Reports.

8. Technology Implementation

8.1 DoD Need

UXO is known to exist or is suspected at hundreds of sites throughout the United States. As stated in Section 1.1, the GAO estimated that cleanup costs could exceed $48 billion for the estimated 7 million acres. Since Reference 1 was issued, the scope of the UXO problem has been estimated to be more than 9 million acres and cleanup costs could be as high as $59.2 billion for DoD property and more than $200 billion for DoD property that was transferred to the Department of Interior.[23] The magnitude of the problem dictates the need for more effective, efficient, and economical methods for UXO clearance.

8.2 Transition

Characterizing a site is only one step in the UXO clearance process; however, the information obtained has significant impact on decisions to remediate at site, the level of the cleanup, costs, and determination of residual hazards. The demonstration of SOCS will lead to improvements in both Government and commercial technology, and implementing these technologies for characterizing UXO sites.

The SOCS program will continue as a cooperative effort between USAEC, NAVEODTECHDIV, USAF/WL, private industry, and academia. The system will be modified during FY 97 to improve reliability and durability. Additional tests are planned for late FY 97 at the Tyndall AFB and JPG to further characterize the system. Upon successful completion of these tests, SOCS will be used to perform limited site demonstrations to evaluate new commercial sensors, discrimination techniques, and operation procedures. Information from these tests and site demonstrations will be disseminated to the public.

9. Lessons Learned

While many of these lessons learned were discussed in Section 5, the following is a summary of the lessons learned during SOCS demonstration at JPG.

- A single sensor or system will not meet the needs for effective, economical UXO characterization. A compliment of sensors and deployment modes is necessary to operate in the varying environmental and geophysical conditions.

- Sensor performance is a function of many parameters such as soil properties, UXO and clutter profile, terrain, foliage, noise sources, data acquisition methods, etc... It is critical to accurately characterize each of these parameters in the environment where field operations are expected.

- An area can be autonomously traversed using the SOCS ATV technology. Efficiency can be improved by eliminating a line-of-sight restriction between the ATV and MCS. The path execution software needs to be revised to accommodate obstacles near turns and site boundaries.

- The MSP provides a platform for easy integration of different sensors. The carriage design reduces the system's ability to negotiate tight turns and rough terrain. Further tests are necessary to model and reduce motion and vibration. The cantilever design of the magnetometer mounts are subject to excessive motion; alternate designs should be considered. Noise sources such as ferrous objects mounted to the structure were discovered during operations at JPG; a comprehensive assessment of platform noise is required.

- GPR and CNR analysis techniques have the potential for effective target classification. The antenna weight is excessive and caused a structural failure of the ATV; implementation of a new design could reduce payload weight by more than 200 lbs. The cross polarized antenna requires data to be collected in two different directions, 45° apart; operating procedures need to be modified. Effectiveness of the GPR and the accuracy of the CNR techniques is greatly dependent on soil properties; a method for accurately measuring soil properties is required and the gain slope must be adjusted appropriately. The software for performing three dimensional SAR imaging is slow and requires excessive human intervention during data processing; develop or procure a completely automated software for SAR imaging.

- Magnetometers are effective instruments for UXO detection. Successful implementation of magnetometers requires rigorous characterization of noise sources; receiver operating curves are necessary for multiple configurations and operating condition. Procedures for operating the magnetometers are deficient; standard setup and operating procedures are required. The analysis techniques for the magnetometers are based on the detection of dipoles, which severely impedes the system's capability; refinement of the software is necessary.

- SIDCAPS provides adequate data acquisition for multiple sensors and ATV control and communications. Improvements can be made to increase data storage capacity, increase data transmission bandwidth to allow for real-time data assessment, and improve durability and weather protection.

10. References

1. General Accounting Office, "Future Years Defense Program: Optimistic Estimates Lead to Billions in Overprogramming", GAO/NSIAD-94-210, 29 July 1994.

2. U.S. Army, "U. S. Army Environmental Research and Development Requirements", Andrulis Report, 24 January 1994.

3. "Tri-Service Environmental Research, Development, Test and Evaluation Strategic Plan", January 1994.

4. U.S. Army Environmental Center, "Unexploded Ordnance Advanced Technology Demonstration Program at Jefferson Proving Ground (Phase I)", SFIM-AEC-ET-CR-94120, December 1994.

5. U.S. Army Environmental Center, "Unexploded Ordnance Advanced Technology Demonstration Program at Jefferson Proving Ground (Phase II)", SFIM-AEC-ET-CR-96170, June 1996.

6. U.S. Army Environmental Center, "Live Site Unexploded Ordnance Advanced Technology Demonstration Program", SFIM-AEC-ET-CR-96171, June 1996.

7. Naval Explosive Ordnance Disposal Technology Center, "Estimation of Size and Location of Buried Objects using Measurements Made with an Array of Magnetometers", NAVEODTECHDIV TR-294, February 1989.

8. U.S. Army Environmental Center, "Surface Towed Ordnance Locator System", SFIM-AEC-ET-CR-95042, February 1995.

9. U.S. Army Environmental Center, "System/Design Trade Study Report for the Navigation of the Airborne, Ground Vehicular and Man-Portable Platforms in Support of the Buried Ordnance Detection, Identification and Remediation Technology Program", SFIM-AEC-ET-CR-95043, March 1995.

10. "Path Planning and Path Execution Software for an Autonomous Nonholonomic Robot Vehicle", Master's Thesis, University of Florida, 1993.

11. U.S. Army Environmental Center, "Ground Penetrating Radar for Ordnance Contaminated Site Restoration", SFIM-AEC-ET-CR-95041, June 1996.

12. Battelle, "Subsurface Ordnance Characterization System: Ground Penetrating Radar Controller, Antenna and Non-Ferrous Towed Platform", DAAD05-93-D-7021, 24 May 1995.

13. U.S. Army Environmental Center, "Detection and Discrimination Techniques for Total Field Magnetometers and Multi-Axis Gradiometers (Final Report)", SFIM-AEC-ET-CR-95093, 2 November 1995.

14. U.S. Army Environmental Center, "Pulsed Electromagnetic Induction (PEMI) Scientific and Technical Report (Final)", SFIM-AEC-ET-CR-95092, 9 November 1995.

15. Naval Explosive Ordnance Disposal Technology Division, "Integrated Ordnance Detection and Remediation System Information Storage and Data Exchange Formats", 31 January 1995.

16. Battelle, "Interface Design Document - Subsurface Ordnance Characterization System: Ground Penetrating Radar Controller", DAAD05-93-D-7021, 11 May 1995.

17. Brown, E. and Crane C. III, "A System for Performing Site Characterization for Test Ranges Containing Unexploded Ordnance", UXO Forum 1996 - Williamsburg, VA, March 1996.

18. "The American Heritage® Dictionary of the English Language, Third Edition", Houghton Mifflin Company, 1992.

19. Naval Explosive Ordnance Disposal Technology Division, "Range Clearance Technology Assessment Report, Revision 1", 1990.

20. Wintec, Inc., "SOCS Interface Design Document", Contract F08637-94-C6042/A008, June 1995.

21. Wintec, Inc., "Test Procedures for Simultaneous Data Collection and Processing System (SIDCAPS) Functional Performance Testing", Contract F08637-94-C6042/A008, June 1995.

22. Battelle, "Final Report on SOCS GPR III", Contract N00174-95-D-0009/002, May 1995.

23. U.S. Army Concepts Analysis Agency, "Cost Analysis for Munitions Rule (CAMRULE)", CAA-MR-95-65, August 1995.

Appendix B

Test Plan/Procedures Document
for the
Subsurface Ordnance Characterization System (SOCS)

20 JUNE 1995

TEST PLAN/PROCEDURES DOCUMENT FOR THE SUBSURFACE ORDNANCE CHARACTERIZATION SYSTEM (SOCS) AT JEFFERSON PROVING GROUND PHASE II DEMONSTRATIONS 1995

Authors:

Debra M. Scroggins (NAVEODTECHDIV)
Ed Brown (Tyndall Air Force Base)

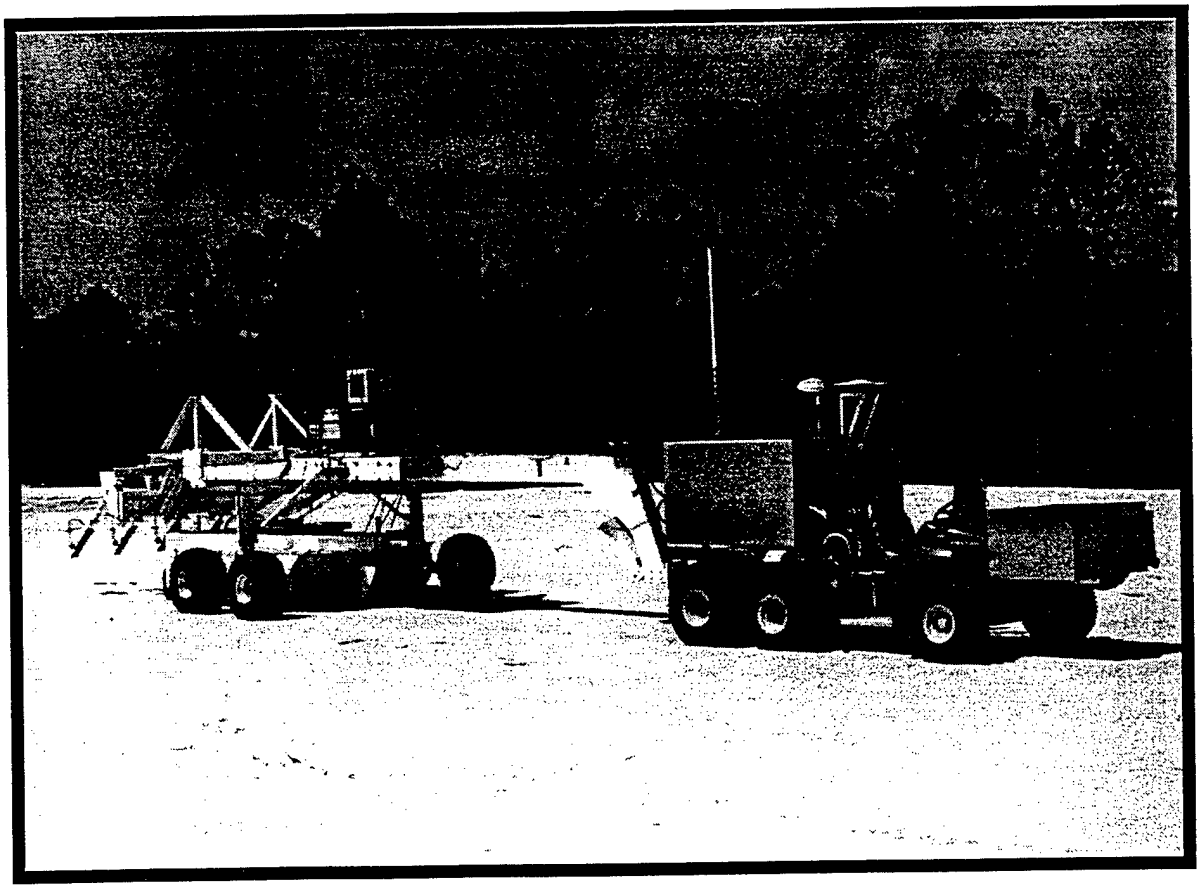

NAVAL EXPLOSIVE ORDNANCE DISPOSAL TECHNOLOGY DIVISION
2008 STUMP NECK ROAD
INDIAN HEAD, MARYLAND 20640-5070

TEST PROCEDURES FOR SUBSURFACE ORDNANCE CHARACTERIZATION SYSTEM (SOCS) AT JEFFERSON PROVING GROUND PHASE II DEMONSTRATIONS

1.0 SYSTEM IDENTIFICATION

The system to be tested in accordance with this document is the Subsurface Ordnance Characterization System (SOCS) being developed by the Naval Explosive Ordnance Disposal Technology Division (NAVEODTECHDIV) in Indian Head, Maryland and Wright Laboratory (WL/FIVCO) at Tyndall Air Force Base, Florida. SOCS is a test platform developed to evaluate the performance of new sensors and sensor combinations for the purpose of detecting, identifying and location buried unexploded ordnance (UXO) at active and formerly used defense sites.

2.0 SCOPE

This report documents overall performance testing of critical elements of SOCS functionality to be performed during initial testing of SOCS during August 1995 and demonstration of SOCS at Jefferson Proving Ground Phase II (JPG II) in Indiana during September 1995. The objectives of the JPG II demonstration are to: (1) determine SOCS' subsystem capabilities in a real-world environment, (2) identify reliability and durability issues, (3) determine which performance parameters are system specific and which are site specific, (4) evaluate the capability of acquiring ground penetrating radar (GPR) and magnetometer data simultaneously and (5) determine the performance of the sensors on SOCS in its current configuration.

3.0 SYSTEM OVERVIEW

In the defined SOCS operational scenario, site characterization is accomplished by means of an Autonomous Tow Vehicle (ATV) pulling a multi-sensor trailer containing a single GPR unit, an array of four cesium vapor magnetometer sensors and associated control electronics over the area to be characterized. The ATV currently consists of a John Deere Gator modified to minimize magnetic signature and incorporate autonomous capabilities. The ATV contains on-board navigation (inertial and differential Global Positioning System (GPS)) and vehicle control subsystems to support path traversal. A user interface is located in the Mobile Command Station (MCS) and provides the operator with system

status information and system control capability via a radio frequency communication link. The operator also has the ability to utilized local area network capabilities, floppy disks and/or tape transfers of operator entered information to initialize SOCS for subsequent autonomous operations.

Prior to conducting a survey, the operator designates a characterization area via the MCS, which is subsequently down-loaded to the ATV processing subsystem. The ATV then plans a survey path for the designated area and, upon operator consent, autonomously traverses the path with the sensor trailer in tow. In lieu of autonomous operations in situations where more control over SOCS is desired or required, SOCS can run a survey in tele-operated mode from the MCS by the operator. This tele-operated run might be performed to accommodate abnormal situations, missed area coverage, terrain or vegetation limitations, etc.

During a survey, SOCS' simultaneous data collection and processing system collects periodic samples of magnetometer and GPR output data and then stores the samples to a removable hard disk mass storage medium along with time and position stamps. The SOCS' equipment on the ATV also provides overall local sensor management including activation/deactivation, initialization, mode selection, etc. Other subsystems provide the remote control/operator interface capability at the MCS and determine precise sensor positions (relative to the ATV navigation subsystem determined position) for individual data samples based on the readings from the instrumented trailer hitch and GPR antenna housing rotations.

4.0 DETAILED TEST DESCRIPTION

The high level test procedures defined are intended to be performed by engineering and technician personnel familiar with the SOCS unit, using other system technical documentation generated under this effort (system specifications, user documentation, etc.)

4.1 Test Background

An informal operational test of the integrated SOCS system is planned during the mid-August 1995 time frame at JPG II. This test will occur prior to formal SOCS testing which is scheduled for mid-September 1995 at JPG II. The August test is intended only to verify basic system functionality including terrain traversal, navigation performance and data collection capability in a rugged environment.

4.2 Test Objectives

The specific objectives for the SOCS JPG II demonstration are as follows:

a. Verify the capability of the ATV/Sensor Trailer combination to autonomously traverse a planned path across terrain in the JPG site area, and evaluate sensor swath coverage of the traversed area.

b. Evaluate navigation subsystem performance in terms of deviation of the traversed path from the planned path.

c. Verify the capability of the data collection components to collect and store meaningful sensor data during path traversal, along with the associated time and position data.

d. Determine if ATV/Sensor trailer turning characteristics are based on system specifics or site parameters. (During Tyndall tests, the vehicle exhibited a skidding or sliding effect when making turns; this characteristic effected the shape of the turns, the sensor paths and the navigation ability. JPG II testing could determine whether this behavior was site specific due to the sand at Tyndall or is system dependent, which means this behavior would be exhibited at JPG also. Also, noise characteristics of the system have been determined for the Tyndall area only, testing at JPG could provide insight into the magnetic signature characteristics of the system itself.)

e. Identify reliability and durability issues that should be modified for real world environments. [The only environment SOCS has been tested in is the controlled test area at Tyndall AFB. This site is completely smooth, made of sand, and without any vegetation. The effects of a more hostile environment (terrain, vegetation, soil parameters) need to documented so required modifications can be incorporated.]

4.3 Applicable System Requirements/Specification References

Many of the documents generated under the SOCS effort were specifically written for particular SOCS subsystems. These subsystem documents are applicable when discussing testing, but of primary interest for the JPG II tests are the following specific system capabilities and associated SOCS System Specification paragraph references:

System Capability	Specification Paragraph
Platform Towing	3.2.1.3.1.2
Navigation	3.2.1.3.4.2
Vehicle Subsystem Control	3.2.1.3.4.3
Survey Travel Control	3.2.1.3.4.4
Data Collection/Storage	3.2.1.3.4.8

SOCS testing will provide implicit results of the basic operation of a number of subsystem supporting capabilities including the effectiveness of radio frequency communication, Differential GPS Navigation Support, Map Creation/Editing, Path Planning, etc.

4.4 Test Preparation/Set-up

The SOCS JPG II Demonstration will be performed at a former ordnance test range site on the JPG complex; SOCS will take data on the 80 acre site at JPG. The following preparations and setup activities are to be accomplished prior to execution of the test:

a. Brief test personnel on safety considerations for the planned test, and on actions to be taken in response to any hazardous or emergency situations.

b. Transport the ATV, sensor trailer, and MCS elements of SOCS and any required support equipment to a staging area adjacent to the designated JPG test site.

c. Set up the MCS in accordance with system technical documentation, and connect to a suitable source of 115 VAC 60 Hz power (local power system, gasoline or diesel powered generator, etc.)

d. Mechanically and electrically interconnect the ATV and sensor trailer.

4.5 Test Execution

Execution of the tests should be accomplished through performance of the following sequence of steps:

a. Enter site and survey specific parameters into the system via the main system Operator Interface in the MCS and download to the ATV navigation and path planning subsystems as part of the Inter-platform Data Set (IDS). This step includes determining where the GPS monument is located and calibrating SOCS' position to that monument.

b. Designate a search area (via entry of corner points) on a map display of the test site area at the Operator Interface in the MCS. Take note of specific obstacles on the survey area and include the coordinates of these obstacles in the layout of the site.

c. Download the designated search area to the ATV processing subsystem and initiate the path planning function.

d. Upload the planned path to the MCS, and review for acceptability; the planned path should avoid designated obstacles and maneuver the SOCS ATV to and from points of interest.

e. After acceptance of the planned path, command the ATV to autonomously travel to the survey starting point. This step may also be performed manually or in tele-operated mode if the situation is such that it is advisable not to operate in autonomous mode.

f. Command the ATV to execute autonomous traversal of the planned path, with desired sensors and associated data collection capabilities enabled, and with independent GPS position data recording enabled in the GPS element of the navigation subsystem.

g. Monitor (visually and on the MCS map display) SOCS autonomous path traversal, and initiate emergency stop function should the vehicle combination appear out of control or should any other unsafe situations occur. Also document any anomalies or deviations from expected system behavior observed during the survey, as well as any general impressions or observations about system performance.

h. After completion of autonomous path traversal by SOCS, download collected sensor and GPS data (through disk removal, output of data files through serial ports or via local area network connections, etc.) and power down the various SOCS subsystems.

i. Using independently supplied data analysis software, verify that sensor data (with time and location stamps) was appropriately stored in the correct formats throughout the survey period.

j. Using independently supplied GPS analysis software, post-process the collected GPS position data and create an overlay diagram of the actual traversed path on the map display of the planned path. Determine deviations (maximum and average or mean) between the planned and traversed paths. Using knowledge of sensor coverage patterns and locations (relative to the navigation reference frame), also evaluate the effective sensor coverage of the traversed area with respect to vehicle position, and plot the coverage swath on the survey site map display.

4.6 Data Collection/Results Documentation

Raw sensor and GPS position data will be automatically collected and stored by the applicable SOCS subsystems during the survey mission, in accordance with system initialization by the operator and the test execution procedures outlined in 4.5. The processed results will be documented for each run of the test. The documented results shall specifically include:

a. Time, date and number of tests run

b. General test conditions (weather, terrain, etc.)

c. Any observed safety issues or anomalies in system operation, or detected equipment malfunctions.

d. Operator observations or comments on overall system operation and performance.

e. The maximum and mean or average deviations of the traversed path versus the planned path, based on the post-processed results of the collected GPS position data.

f. Copies of plots of the planned path, the actual traversed path, and the sensor coverage swath overlaid on the survey area map display.

g. GPR and magnetometer data will be collected and passed on to respective post-processing team members.

4.7 Test Results Analysis

Results of individual test runs shall be analyzed to evaluate system performance relative to the test objectives delineated in Section 4.2. Any deficiencies in required functionality or associated performance of the system for the intended application shall be analyzed as to probable cause. If deemed appropriate and reasonable to accomplish by test management personnel, the cause(s) of suspected problems or performance deficiencies shall be fixed, and additional test runs made to evaluate the efficacy of the fix. Any detected deficiencies or problems which cannot be readily fixed to permit continued testing within the time frame of the JPG II demonstration shall be identified to program management personnel for determination of appropriate future action. The SOCS JPG II demonstration will be documented in a QUICK LOOK REPORT which will outline the specifics of the test, accomplishments, possible problems/resolutions and suggestions for future work.

Appendix C

SOCS GPR Analysis Quicklook Report

Final Report

on

SOCS GPR III

to

Naval Surface Warfare Center/ PRC Inc.

May 2, 1996

by

BATTELLE
505 King Avenue
Columbus, Ohio 43201

and

The Ohio State University ElectroScience Laboratory
1320 Kinnear Road
Columbus, Ohio 43212

Introduction

This report will summarize the results that Batteile and The Ohio State University ElectroScience Laboratory obtained by processing the GPR data received from the Surface Ordnance Characterization System (SOCS) when it collected data at Tyndall Air Force Base and Jefferson Proving Grounds. First we will discuss the results and then we will give a brief review of the process used to obtain the results.

Tyndall Results

Four complete GPR data sets were recorded at a test site at Tyndall Air Force Base. Known ordnance items were buried in sand at the test site. The SOCS vehicle drove over the test pad four times, twice driving primarily north-south and twice driving east-west. The parallel passes were approximately 1.5 to 2.0 meters apart. Figure 1 shows the paths followed during the east/west run and the north/south run used to create the SAR images below. Figure 2 shows the SAR image collapsed to two dimensions. The image shown is the sum of the absolute value of the image at each depth of the image. We have determined the coordinates and depths of the ordnance using the SAR images. In Figure 3, the known buried ordnance locations are marked with triangles and the targets found using the GPR SAR image are numbered and marked with Xs. The Ohio State University ElectroScience Laboratory (ESL) complex natural resonance (CNR) analysis to estimate the length of each target. Some of the locations marked on the map were eliminated by the CNR analysis when no resonances could be found.

A total of 38 possible targets were identified in the Tyndall data. Table 1 summarizes the Tyndall target information. The CNR analysis revealed that targets #3 and #4 are probably the same target and targets #15 and #16 are the same target. Two resonances were found at the coordinates of target #30. Of the 37 remaining locations, 16 are known ordnance items. There were 22 known ordnance items, therefore the detection rate was 16/22 or 73%. We are disregarding the 9 closely spaced plates along the southeast edge of the image. There were 22 false alarms, resulting in a false alarm rate of 22/37 or 59%.

Problems with the Tyndall Tests

There were several problems encountered during the SOCS GPR Tyndall tests that should be corrected for future tests.

One significant problem effecting the SAR imaging is an error in the recorded GPR antenna coordinates. The vehicle actually moved very smoothly, but the GPS positions recorded by the system are not always evenly spaced. Figure 4 shows the navigation points provided by SOCS GPS. They are not evenly spaced, so either the velocity of the vehicle varied, the time interval between positions varied, or the GPS positions recorded are not accurate. We believe the positions are not accurate because of the distortion of the target arcs in the raw data if we plot the raw time-domain data as a function of position. Figure 5 shows a waterfall plot of the raw time-domain waveforms as a function of scan index, i.e. uniform spacing is assumed. In Figure 5 there are clearly visible target arcs. However if we make a waterfall plot, see Figure 6, of the same raw time-domain waveforms as a function of the x-position of the GPR antenna as provided by SOCS, the target arcs become distorted. (Note that the same waveforms are plotted in both figures, but in Figure 5 the vehicle advances from left to right and in Figure 6 the vehicle advances from right to left.)

The error in the GPS position for each waveform will degrade the SAR image. To correct for this, a 30-point running average was used on the coordinates of each trace. This improved the SAR image, however there is still some position error, especially when the vehicle turns. In Figure 4, the GPR antenna positions are shown as dots and the averaged positions used for the SAR processing are shown as a smooth curve. The position system needs to be improved.

Another problem with the Tyndall tests is that during all of the SOCS GPR Tyndall tests, the gain on the system was set too high. This resulted in a portion of each time waveform being clipped off. Each time waveform was clipped off from 14.5 ns to 17.5 ns (5.75 to 8.75 ns after removing the system offset). Due to the improper gain setting, the arcs in the time domain data corresponding to shallow targets, less than approximately 0.6 meters, are incomplete or distorted, making it difficult to focus the shallow targets at the proper depth in the image. Some of the shallow targets are still detected from the arcs that appear at later times in the raw time-domain

data.

The spatial resolution in the direction perpendicular to the path of the vehicle could be increased by making the passes closer together. During the SOCS Tyndall tests, the passes were 1.5 to 2 meters apart and the targets appear unfocused in the direction perpendicular to the path. During the JPG tests the passes are less than a meter apart and the resolution is improved.

JPG Results

Battelle received five GPR data sets from SOCS from the JPG sites. Only one complete data set, C22, contained good GPR data. About one-third of a second data set, D14, was good, but this only consisted of 2 passes on each side of the region. During the remaining runs, the GPR system recorded invalid data for some unknown reason.

The path of the GPR antenna during the C22 run is shown in Figure 7. The parallel passes of the vehicle were designed to be 2.5 feet apart. Figure 8 shows the collapsed image of the C22 data. The potential target locations and estimated lengths are listed in Table 2. Figure 9 shows the potential target locations marked, as determined from the SOCS GPR SAR image. CNR analysis was used to eliminate clutter and estimate the lengths of the targets. The actual locations of the buried ordnance were not available to Battelle.

SOCS Data Processing

This section contains a brief description of the processing of the SOCS GPR data. Synthetic aperture radar processing of the time-domain GPR data consists of defining the volume to be imaged, collecting time domain GPR data, and constructing the SAR image. The image is constructed by summing, for each voxel in the volume, the data point from each bipolar time waveform that corresponds to the round trip time between the GPR antenna and the voxel.

In order to process the GPR data sets, the position of the GPR antenna is needed as a function of time. The SOCS GPR system records each received waveform along with the system time associated with that waveform. The position of the GPR antenna is determined from the

GPR time and the position and heading information supplied by a global positioning system (GPS) on the tow vehicle and sensors on the hitch. The sensors on the hitch detect the pitch, roll, and yaw angles of the hitch. The time, position of the GPS antenna, vehicle heading, and the hitch pitch, roll, and yaw are recorded 20 times per second.

The position of the GPS antenna, the vehicle heading, and the hitch roll, pitch, and yaw are used to calculate the position of the GPR antenna in UTM coordinates. Interpolation procedures are used to find the GPS antenna position and the hitch orientation at each GPR waveform time. A coordinate transformation is used to calculate the position of the GPR antenna at each GPR waveform time.

For each waveform of the GPR data and for each voxel in the volume of soil that is being examined, we must determine the round trip time for a signal to travel from the GPR antenna to the voxel and back to the GPR antenna. Once we determine this time, we determine the point in each time waveform that corresponds to a particular voxel. To construct the SAR image, for each voxel, we sum the points in each waveform whose time coordinate corresponds to the round trip time for that voxel.

The raw GPR waveforms include the antenna ringing, reflections from the surface, and a gain slope of 30 dB. The antenna ringing is removed by subtracting an average waveform from each waveform and the gain slope is removed by multiplying each time waveform by a -30 dB gain slope. After removing the antenna ringing and correcting for the gain slope in the raw time domain data, the waveforms can be viewed as a function of time or position and a target will appear as series of arcs. Figure 10 shows an example of the time domain response of the SOCS GPR to a target after we have subtracted the average waveform and removed the 30 dB gain slope. Four passes over the target are shown. The radar is nearest to the target in the second pass, where the response is the strongest.

Before forming the SAR image, the time waveform is shifted in time to place the beginning of the waveform at the surface of the ground. If the GPR antenna does not move significantly while the received signal is sampled, the round trip time is a function of the distance from the radar to the voxel and the velocity of the electromagnetic signal through the soil. The velocity of electromagnetic waves in the soil is v, equal to the speed of light divided by the

square root of the dielectric constant of the soil, ϵ_r.

The data from the GPR antenna is in the form $A(m,n)$, where A is an integer array, m is the position or waveform index, and n is the time index within the waveform. m ranges from 0 to the number of waveforms in the data set minus 1. n ranges from 0 to 255, the number of data points in each waveform minus 1.

If d is the one way distance from the GPR antenna at the mth position to the voxel centered at coordinates (x, y, z), the round trip time t for the voxel is

$$t(m,x,y,z) = 2 \frac{d(m,x,y,z)}{v} \qquad (1)$$

In the mth waveform, the time index of A that contains the data from the voxel at (x,y,z) is

$$n(m,x,y,z) = \frac{t(m,x,y,z)}{\Delta t} \qquad (2)$$

Δt is the time interval between data points in the GPR time domain waveforms. The resulting SAR image is

$$I(x,y,z) = \sum_{m=0}^{M-1} A(m, n(m,x,y,z)) e^{-2\beta d} \qquad (3)$$

The $e^{-2\beta d}$ term is to correct for the attenuation losses due to the soil conductivity, where

$$\beta = \frac{\sigma}{2} \frac{1}{\sqrt{\epsilon_r}} \sqrt{\frac{\mu_0}{\epsilon_0}} . \qquad (4)$$

σ is the soil conductivity. In the SOCS GPR data processed so far, we have ignored the effects of

the soil conductivity when constructing the image.

In general, the velocity in the soil may not be constant. The velocity may be a function of depth in the soil. Measurements of the dielectric constant and conductivity of the soil at the site at Tyndall Air Force Base indicate that the dielectric is approximately constant all depths with which the GPR is concerned. However, at JPG the measured dielectric constant of the soil is greater than at Tyndall and increases with depth. This complicates the calculation of the propagation time because the changing dielectric constant changes the velocity and also the path of the radar signal. The path becomes curved and the time it takes a signal to travel through the soil increases. The change is taken into account when doing the SAR processing with the following procedure.

If the dielectric constant of the soil is not constant, the propagation velocity in the soil is some function $v(x)$. For a voxel at depth d and angle of incidence θ, geometrical optics can be used to determine the path that connects the radar and a selected voxel. The radial distance r from the radar antenna is given by

$$r(d,\theta) = \int_0^d \sin\theta \frac{v(x)}{\sqrt{v_0^2 - v(x)^2 \sin^2\theta}}\, dx \qquad (5)$$

for $0 \geq \theta < \pi/2$. v_0 is the initial velocity in the soil at depth $x=0$. The two-way propagation time is then,

$$t(r,d) = \int_0^d \frac{v_0}{v(x)\sqrt{v_0^2 - v(x)^2 \sin^2\theta}}\, dx \qquad (6)$$

However, when processing the GPR data, we do not know θ. We know the depth of the voxel, d, and the radial distance between the voxel and the radar, r. We must invert Equation 5 to solve for θ and then substitute θ into Equation 6 to find the two-way propagation time.

If the velocity can be approximated as a linear function of the form,

$$v(x) = v_0 - \alpha x \tag{7}$$

the integrals in Equations 5 and 6 can be evaluated exactly.

To invert Equation 5, for each voxel depth, we create a vector containing the radial distances, r_i, for the angles $\theta = (\pi/2)\, I/n$, where $n=1000$. For each depth we have r as a function of θ. To get θ as a function of r, we use an interpolation procedure which performs a linear interpolation on vectors with an irregular grid. This interpolation procedure gives us θ_i for the known radial distances r_i, allowing us to calculate the two-way time from Equation 6.

The Ohio State ElectroScience Laboratory measured the dielectric constant at Jefferson Proving Grounds 6 feet south of marker A24 as a function of depth . The measured dielectric constant and the dielectric constant derived from the linear approximation of the velocity used for the SAR processing are shown in Figure 11. Battelle used this approximation to create the SAR images for the SOCS JPG data.

Processing Steps

The following steps are necessary to process a SOCS GPR data set and determine the possible target locations and lengths.

1. Obtain the *NAV.DAT*, *PLAT.DAT*, and *GPR.DAT* files from SOCS and transfer them to our computer (133 MHZ Pentium).

2. Run a conversion program to combine the *NAV.DAT*, *PLAT.DAT*, and *GPR.DAT* files into one *GPR.XYG* file consisting of each radar waveform and the position of the GPR antenna for each waveform.

3. Run the SAR imaging program on the *GPR.XYG* file to create an image of the volume beneath the area covered by the file.

4. View the SAR image and mark possible target locations by positioning the cursor over the position and clicking the mouse. The program will save the target locations in a target file.

5. Send the target locations and the raw GPR data, the *GPR.XYG* file, to ESL for complex natural resonance processing. If ESL finds a resonance frequency, they return the resonance frequency and estimated electrical length for each target location.

6. Create a table using EXCEL containing all of the information required in the STD file and then convert the information into an ascii file in the STD file format.

Battelle has written a computer program in IDL, an interactive data language, to perform the processing of the SOCS GPR raw data. The program allows the operator to perform steps 2, 3, and 4. The Ohio State University's ElectroScience Laboratory has computer programs to perform the complex natural resonance analysis to determine the targets' electrical lengths.

Notes about the STD Files

The information included in the STD files is shown in Tables 3 and 4. The actual STD files are being sent with this report on a disk. The resolution in the data processed so far has not be sufficient to determine target azimuth, target declination, or target type. The target electrical length is estimated using the complex natural resonance. The electrical length is usually approximately 10% longer than the physical length, but the electrical length is used here to determine target size. The target size is small if the electrical length is less than 11 inches. The target size is medium if the electrical length is greater than 11 inches but less than 26 inches. The target size is large if the electrical length is greater than 26 inches. We do not currently have a systematic method of estimating our confidence in size. If we found a resonance, we gave it a 75% confidence.

Additional Work

In the future, several modifications could be made to the processing program in order to further automate and speed up processing of the SOCS GPR data. We would like to write and implement code to automatically locate targets using a thresholding algorithm which tabulates possible target locations. We would also like to integrate the complex natural resonance calculation into the main processing program.

Table 1. Tyndall Target Information.

Targets Found using SOCS Tyndall Data Files ew.dat and ns.dat:										
Found Targets	x UTM	y UTM	Latitude (deg)	Longitude (deg)	Depth (m)	Known Ordnance No.	Known Ordnance Depth	Damping Factor (Np/ns)	Frequency (Mhz)	Length (inch)
B1	646998 06	3316416.5	29 9698097	85.4764294	1 4			-5 55E-02	74 90	27 01
B2	646997 94	3316413.5	29 9697826	85.476431	1 4		1 542	-6 29E-02	81 50	24 82
B3	646998 06	3316410 5	29 9697555	85.4764302	1.4	21	1.181	-3 64E-02	76 25	28 43
B4	647000 56	3316410.75	29 9697575	85 4764043	1 8	21	1 181	-9 09E-02	81 05	25 12
B5	647001 13	3316420	29 9698409	85 4763971	1			-1 02E-01	83 45	24 35
B6	647001 38	3316415	29 9697957	85.4763952	1.2	22	1 542	-6 45E-02	61 60	33 19
B7	647002 06	3316427 25	29 9699062	85.4763865	1.4			-1 52E 01	146 55	14 63
B8	647004 06	3316431	29 9699398	85.4763652	1 4			-4 97E-02	46 40	43 56
B9	647007 25	3316410.5	29 9697544	85.476335	1 2			-4 77E-02	77 35	26 21
B10	647005 44	3316405	29 969705	85.4763545	1 4			-5 53E-02	73 35	27 64
B11	646998 31	3316401.25	29 9696721	85 4764289	1 6			-7 53E-02	74 20	27 27
B12	646995 69	3316397.75	29 9696408	85 4764565	1 4			-4 90E-02	61 10	33 11
B13	646996 75	3316392.25	29 9695911	85 4764463	1 6			-1 69E-02	27 00	74 91
B14	646999 56	3316390 5	29 9695749	85 4764174	0 8		1 485	-5 24E 02	49 70	41 25
B15	646999 94	3316387 75	29 9695501	85 4764139	1		1 485	-4 65E-02	79 80	25 89
B16	647001 94	3316387.25	29 9695453	85 4763932	1		1 485	-3 82E 02	91 10	22 22
B17	647003 81	3316385	29 9695248	85.4763741	1		1 485	-5 09E-02	61 75	44 68
B18	647010 75	3316385 5	29 9695285	85.4763022	1	13	0 411	NA	NA	NA
B18	647010 75	3316385 5	29.9695285	85.4763022	1	14	0 323	NA	NA	NA
B19	647014 25	3316399	29 9696499	85.476264	1	3	0 859	-6 91E-02	45 50	45 62
B19	647014 25	3316399	29.9696499	85.476264	1	4	1.054	-6 91E 02	45 50	45 62
B20	647017 31	3316402.5	29.9696811	85.4762319	0 6			-1 53E-01	128 40	15 76
B21	647015 44	3316415 5	29 9697986	85.4762494	1.2	5	1.399	-4 59E-02	48 30	41 87
B22	647017.13	3316423.75	29 9698728	85.4762308	2			-3.77E-02	51 70	39 15
B23	647021 69	3316432.25	29.9699489	85 4761824	0.6	8	0 79	-1 28E-01	134 70	15 38
B24	647024 25	3316429	29 9699193	85 4761563	1	7	0 568	-1 08E-01	115 50	17 52
B25	647029	3316417	29 9698105	85 4761087	1 4			9 91E 02	71 00	28 49
B26	647035.56	3316427.25	29 9699022	85 4760394	1	10	1 08	-6 11E-02	69 75	29 59
B27	647038.25	3316425.25	29 9698838	85.4760118	1.2			-6 58E-02	56 65	35 74
B28	647042.38	3316424	29.969872	85.4759691	0.8	9	0.715	-7.79E 02	54 55	37 23
B29	647034	3316414.5	29.9697873	85.4760573	1	6	0.475	-6 58E-02	53 15	39 17
B30a	647040	3316408.5	29 9697325	85.4759959	1.2	17	0.613	-2 46E-02	82 20	24 61
B30b	647040	3316408.5	29.9697325	85.4759959	1.2	17	0 613	-3 61E-02	38 60	52 37
B31	647036 81	3316394.5	29.9696066	85.4760309	1.2	15	0.958	-5.92E-02	62 30	32 47
B32	647032	3316396.75	29.9696274	85.4760804	1.6			-6 00E-02	88 20	23 06
B33	647029.94	3316403.25	29.9696863	85.4761009	2.4	19	0.608	-6.16E-02	106 25	19 22
B34	647029.44	3316390.5	29.9695714	85.4761078	1.2	1	0.974	-8.18E-02	49 50	40 97
B35	647020.63	3316394.5	29.9696085	85.4761986	1.2			-6 89E-02	65 85	32 60
B36	647021.13	3316384.75	29.9695205	85.4761947	1.2	2	1.616	-6.12E-02	45 70	44 21
B37	647023	3316382.5	29.9695	85.4761757	1.2		1.616	-1.03E-01	83 70	24 16
B38	647039 56	3316381.25	29.9694867	85.4760042	1.6			NA	NA	NA
B39	647041 19	3316400	29.9696557	85 4759848	1.4	16	1 2	-3 93E 02	71 50	28 34

Table 2. JPG Target Information.

Targets Found using SOCS JPG Data File c22ns3:

Target #	x UTM	y UTM	Latitude (deg)	Longitude (deg)	Depth (m)	Damping Factor (Np/ns)	Frequency (MHz)	Length (inch)
2	640764.63	4303946.5	38.8731077	85.3773286	0.2	-0.0598	26.8	57.7339
4	640760.94	4303969	38.873311	85.3773665	0.2	-0.0246	22.5	68.853
5	640741.06	4304004.5	38.873634	85.3775883	0.8	-0.0579	33.3	46.4758
6	640747.81	4303962.5	38.8732545	85.3775191	0.4	-0.0382	19.7	78.7725
7	640742.06	4303972	38.873341	85.3775834	0.8	-0.0781	46.5	33.316
9	640750.94	4303947	38.8731144	85.3774862	1	-0.0426	35	44.2627
10	640770	4304001	38.8735978	85.3772555	0.6	-0.0726	86.6	17.8839
11	640747	4304033.5	38.8738942	85.3775139	0.6	-0.0654	27.8	55.8268
13	640749.44	4304002	38.8736101	85.3774922	0.8	-0.0334	23.6	65.6438
14	640746.31	4304003.5	38.8736241	85.377528	0.2	-0.0539	40.3	38.4098
15	640762.06	4303990.5	38.8735045	85.3773492	0.4	-0.0616	103	15.0407
16	640779.19	4303964	38.873263	85.3771572	0.8	-0.1068	73.8	20.9918
17	640775.88	4303970.5	38.8733221	85.377194	0.8	-0.0236	25.7	60.216
18	640771.75	4303955	38.8731831	85.3772448	0.2	-0.0562	37.8	40.9642
19	640762.06	4303975	38.8733649	85.3773523	0.2	-0.0775	35	44.2627
21	640763	4303959	38.8732206	85.3773448	1	-0.0932	122.1	12.6853
22	640768.5	4303991	38.873508	85.3772748	0.8	-0.0276	25.9	59.8722
23	640775.5	4304023.5	38.8737996	85.3771875	0.8	-0.0872	66.3	23.3841
24	640780.13	4304023	38.8737943	85.3771343	0.6	-0.0479	28.3	54.8387
25	640779.88	4304018.5	38.8737538	85.3771381	0.8	-0.1048	65	23.8337
26	640774.81	4304007	38.8736511	85.3771988	0.4	-0.0697	42	36.8856
27	640777.25	4303996	38.8735516	85.377173	0.6	-0.048	25	61.9677

Table 3. Tyndall STD File Information.

File No	Resonance Frequency (MHz)	Estimated Electrical Length* (inches)	x (utm) (meters)	y (utm) (meters)	Latitude (deg)	Longitude (deg)	Target Depth (meters, NMEA)	Target Azimuth (Deg)	Target Declination (deg)	Target Size** (S,M,L)	Target Type	Confidence in Size (%)	Confidence in Type (%)
B1	74 9	27 01	646998 1	3316417	29.96981	85 47643	-1 4	NA	NA	L	NA	75	NA
B2	81 5	24 82	646997 9	3316414	29 96978	85 47643	-1 4	NA	NA	M	NA	75	NA
B3	76 25	28 43	646998.1	3316411	29 96976	85 47643	-1 4	NA	NA	L	NA	75	NA
B4	81 05	25 12	647000 6	3316411	29 96976	85 4764	-1 8	NA	NA	M	NA	75	NA
B5	83 45	24 35	647001.1	3316420	29.96984	85 4764	-1	NA	NA	M	NA	75	NA
B6	61 6	33 19	647001 4	3316415	29.9698	85.4764	-1 2	NA	NA	L	NA	75	NA
B7	146 55	14 63	647002.1	3316427	29 96991	85.47639	-1 4	NA	NA	M	NA	75	NA
B8	46.4	43 56	647004.1	3316431	29 96994	85.47637	-1 4	NA	NA	L	NA	75	NA
B9	77 35	26 21	647007.3	3316411	29 96975	85.47634	-1.2	NA	NA	L	NA	75	NA
B10	73 35	27 64	647005 4	3316405	29 96971	85 47635	-1 4	NA	NA	L	NA	75	NA
B11	74 2	27 27	646998 3	3316401	29 96967	85 47643	-1 6	NA	NA	L	NA	75	NA
B12	61 1	33 11	646995 7	3316398	29 96964	85 47646	-1 4	NA	NA	L	NA	75	NA
B13	27	74 91	646996 8	3316392	29 96959	85 47645	-1 6	NA	NA	L	NA	75	NA
B14	49 7	41 25	646999 6	3316391	29 96957	85.47642	-0 8	NA	NA	L	NA	75	NA
B15	79 8	25 89	646999 9	3316388	29 96955	85 47641	-1	NA	NA	M	NA	75	NA
B16	91 1	22 22	647001 9	3316387	29 96955	85.47639	-1	NA	NA	M	NA	75	NA
B17	61 75	44 68	647003 8	3316385	29 96952	85.47637	-1	NA	NA	L	NA	75	NA
B19	45 5	45 62	647014.3	3316399	29.96965	85.47626	-1	NA	NA	L	NA	75	NA
B20	128 4	15 76	647017 3	3316403	29 96968	85 47623	-0 6	NA	NA	M	NA	75	NA
B21	48 3	41 87	647015.4	3316416	29 9698	85.47625	-1 2	NA	NA	L	NA	75	NA
B22	51 7	39 15	647017.1	3316424	29 96987	85.47623	-2	NA	NA	L	NA	75	NA
B23	134 7	15 38	647021 7	3316432	29 96995	85 47618	-0 6	NA	NA	M	NA	75	NA
B24	115 5	17 52	647024 3	3316429	29.96992	85.47616	-1	NA	NA	M	NA	75	NA
B25	71	28.49	647029	3316417	29 96981	85.47611	-1 4	NA	NA	L	NA	75	NA
B26	69 75	29 59	647035 6	3316427	29 9699	85 47604	-1	NA	NA	L	NA	75	NA
B27	56 65	35 74	647038 3	3316425	29.96988	85 47601	-1 2	NA	NA	L	NA	75	NA
B28	54 55	37 23	647042.4	3316424	29 96987	85 47597	-0 8	NA	NA	L	NA	75	NA
B29	53 15	39 17	647034	3316415	29 96979	85.47606	-1	NA	NA	M	NA	75	NA
B30a	82 2	24 61	647040	3316409	29 96973	85 476	-1 2	NA	NA	L	NA	75	NA
B30b	38 6	52 37	647040	3316409	29 96973	85 476	-1 2	NA	NA	L	NA	75	NA
B31	62 3	32 47	647036.8	3316395	29.96961	85.47603	-1.2	NA	NA	L	NA	75	NA
B32	88 2	23 06	647032	3316397	29.96963	85 47608	-1 6	NA	NA	M	NA	75	NA
B33	106 25	19 22	647029 9	3316403	29 96969	85.4761	-2 4	NA	NA	M	NA	75	NA
B34	49 5	40 97	647029 4	3316391	29 96957	85.47611	-1.2	NA	NA	L	NA	75	NA
B35	65 85	32 60	647020 6	3316395	29 96961	85.4762	-1.2	NA	NA	L	NA	75	NA
B36	45.7	44 21	647021 1	3316385	29.96952	85.47619	-1.2	NA	NA	L	NA	75	NA
B37	83 7	24.16	647023	3316383	29 9695	85 47618	-1.2	NA	NA	M	NA	75	NA
B39	71 5	28 34	647041.2	3316400	29 96966	85 47598	-1 4	NA	NA	L	NA	75	NA

**Small < 11 inches, Medium >11 inches and < 26 inches, Large >26 inches

*Electrical Length is approximately 10% longer than physical length, but electrical length was used here to determine size, S, M, or L

Table 4. JPG STD File Information.

File No	Resonance Frequency (MHz)	Estimated Electrical Length* (inches)	x (utm) (meters)	y (utm) (meters)	Latitude (deg)	Longitude (deg)	Target Depth (meters, NMEA)	Target Azimuth (Deg)	Target Declination (deg)	Target Size** (S,M,L)	Target Type	Confidence in Size (%)	Confidence in Type (%)
2	26 8	57 7339	640764 6	4303946.5	38 87311	85.37733	-0 2	NA	NA	L	NA	75	NA
3	NA	NA	640768 9	4303948 5	38 87313	85 37728	NA	NA	NA	NA	NA	NA	NA
4	22 5	68 853	640760 9	4303969.0	38.87331	85 37737	-0 2	NA	NA	L	NA	75	NA
5	33 3	46 4758	640741.1	4304004.5	38 87363	85 37759	-0 8	NA	NA	L	NA	75	NA
6	19 7	78 7725	640747 8	4303962 5	38 87325	85 37752	-0 4	NA	NA	L	NA	75	NA
7	46 5	33 316	640742 1	4303972 0	38 87334	85 37758	-0 8	NA	NA	L	NA	75	NA
8	27 8	55 7264	640734 6	4303956 5	38 87320	85 37767	NA	NA	NA	L	NA	75	NA
9	35	44 2627	640750 9	4303947 0	38 87311	85 37749	-1	NA	NA	L	NA	75	NA
10	86 6	17 8839	640770 0	4304001 0	38 87360	85 37726	-0 6	NA	NA	M	NA	75	NA
11	27 8	55 8268	640747 0	4304033 5	38 87389	85 37751	-0 6	NA	NA	L	NA	75	NA
12	25 8	60 0463	640735 4	4304025 0	38 87382	85 37765	NA	NA	NA	L	NA	75	NA
13	23 6	65 6438	640749 4	4304002 0	38 87361	85 37749	-0 8	NA	NA	L	NA	75	NA
14	40 3	38 4098	640746 3	4304003 5	38 87362	85 37753	-0 2	NA	NA	L	NA	75	NA
15	103.	15 0407	640762 1	4303990 5	38 87350	85.37735	-0 4	NA	NA	M	NA	75	NA
16	73 8	20 9918	640779 2	4303964.0	38 87326	85.37716	-0 8	NA	NA	M	NA	75	NA
17	25 7	60 216	640775 9	4303970 5	38 87332	85.37719	-0 8	NA	NA	L	NA	75	NA
18	37 8	40 9642	640771 8	4303955 0	38 87318	85 37724	-0 2	NA	NA	L	NA	75	NA
19	35	44 2627	640762 1	4303975 0	38 87336	85.37735	-0 2	NA	NA	L	NA	75	NA
20	41	37 7852	640763 0	4303962 0	38 87325	85 37734	NA	NA	NA	L	NA	75	NA
21	122 1	12 6853	640763 0	4303959 0	38 87322	85 37734	-1	NA	NA	M	NA	75	NA
22	25 9	59 8722	640768 5	4303991 0	38 87351	85 37727	-0 8	NA	NA	L	NA	75	NA
23	66 3	23 3841	640775 5	4304023 5	38 87380	85 37719	-0 8	NA	NA	M	NA	75	NA
24	28 3	54 8387	640780 13	4304023	38 87379	85 37713	-0 6	NA	NA	L	NA	75	NA
25	65	23 8337	640779.88	4304018.5	38.87375	85.37714	-0 8	NA	NA	M	NA	75	NA
26	42	36 8856	640774.81	4304007	38.87365	85.3772	-0 4	NA	NA	L	NA	75	NA
27	25	61 9677	640777.25	4303996	38.87355	85.37717	-0 6	NA	NA	L	NA	75	NA

**Small <11 inches, Medium >11 inches and < 26 inches, Large >26 inches

*Electrical Length is approximately 10% longer than physical length, but electrical length was used here to determine size, S, M, or L

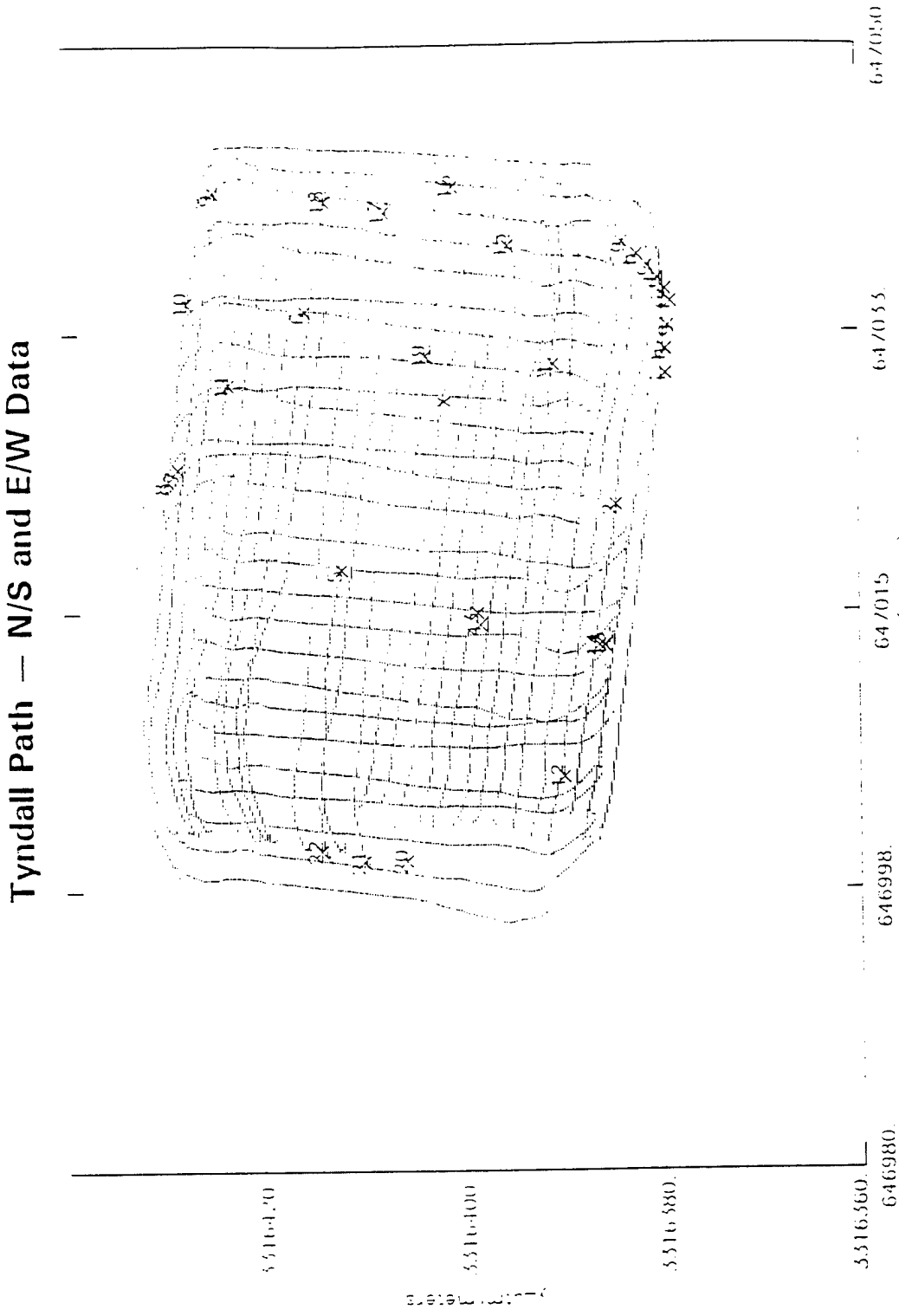

Figure 1. SOCS GPR Tyndall Path - N/S and E/W Data.

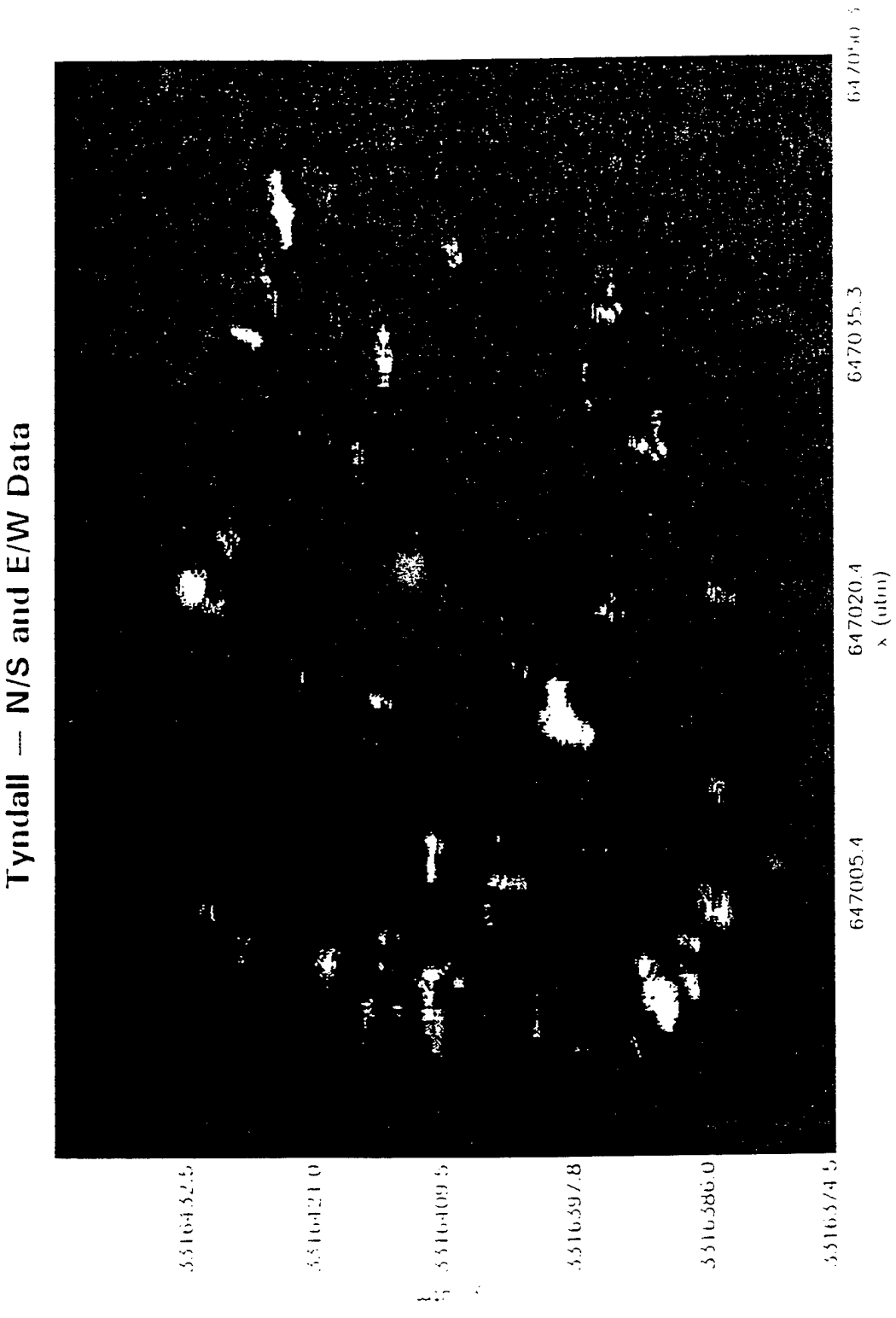

Figure 2. SOCS GPR Image Tyndall - N/S and E/W Data.

Figure 3. SOCS GPR Tyndall Actual Ordnance and Found Target Locations

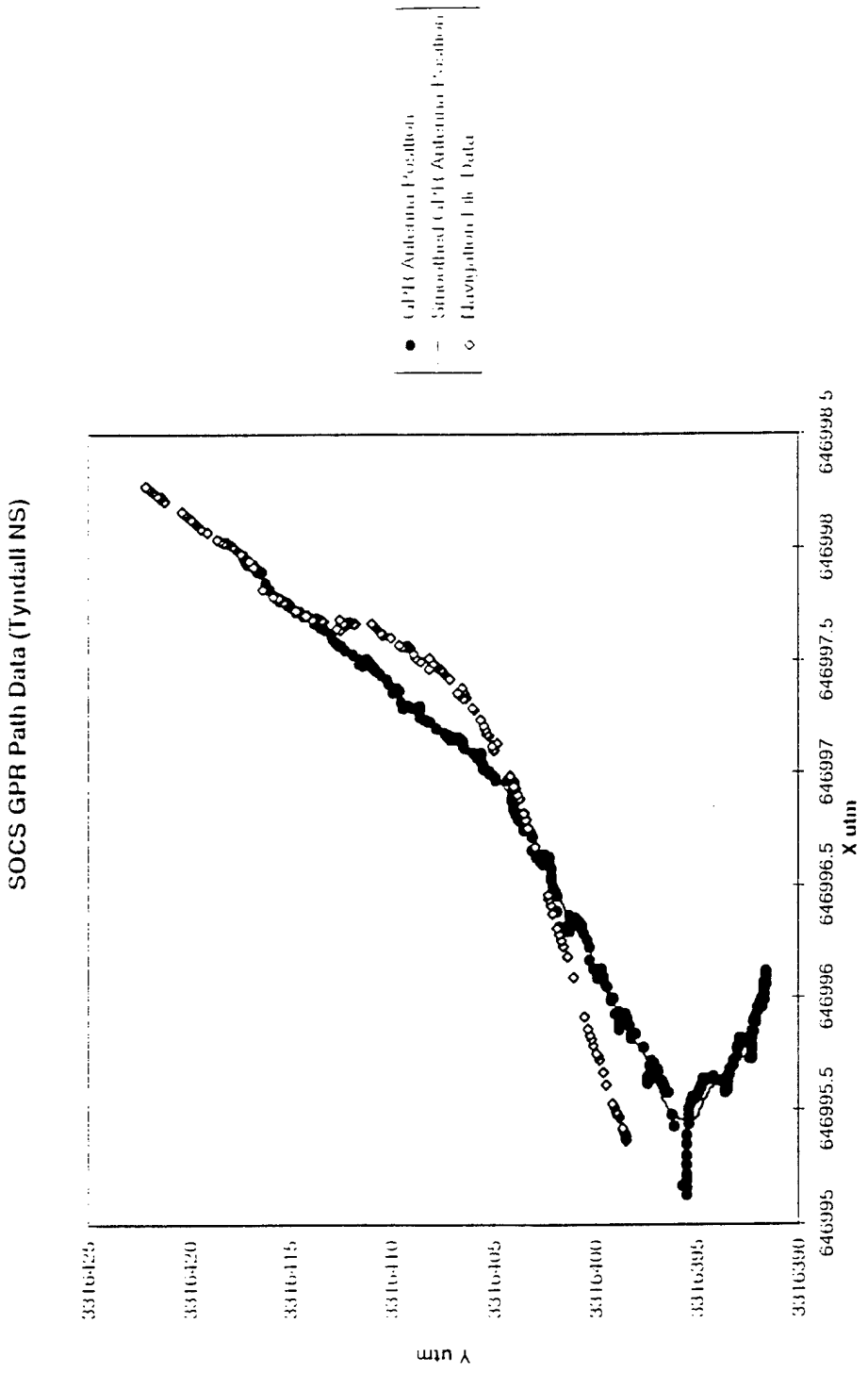

Figure 4. SOCS GPR Original and Smoothed Path (Tyndall ns)

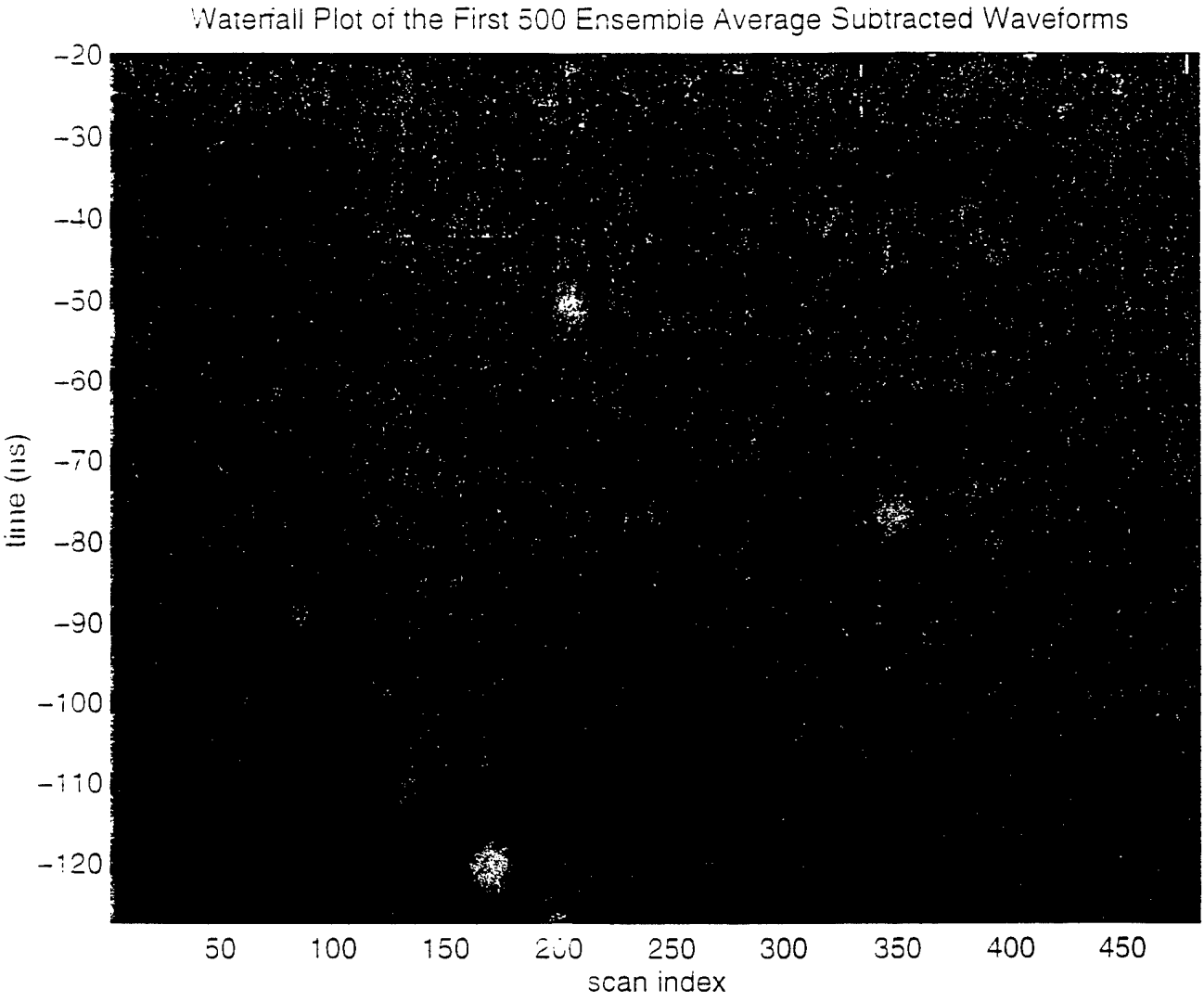

Figure 5. Waterfall Plot of Time-Domain GPR Data as a Function of Scan Index

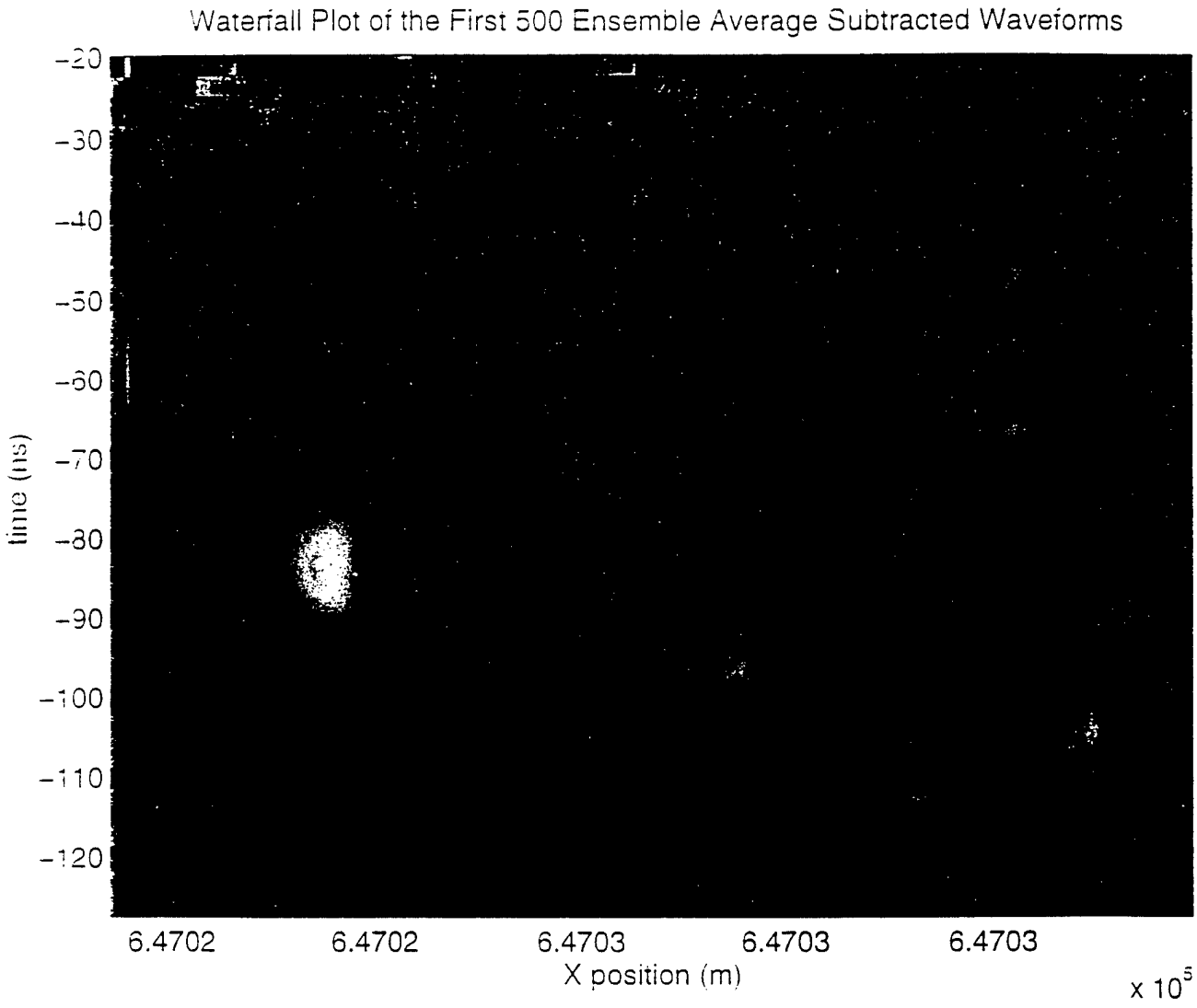

Figure 6. Waterfall Plot of Time-Domain GPR Data as a Function of GPS Position.

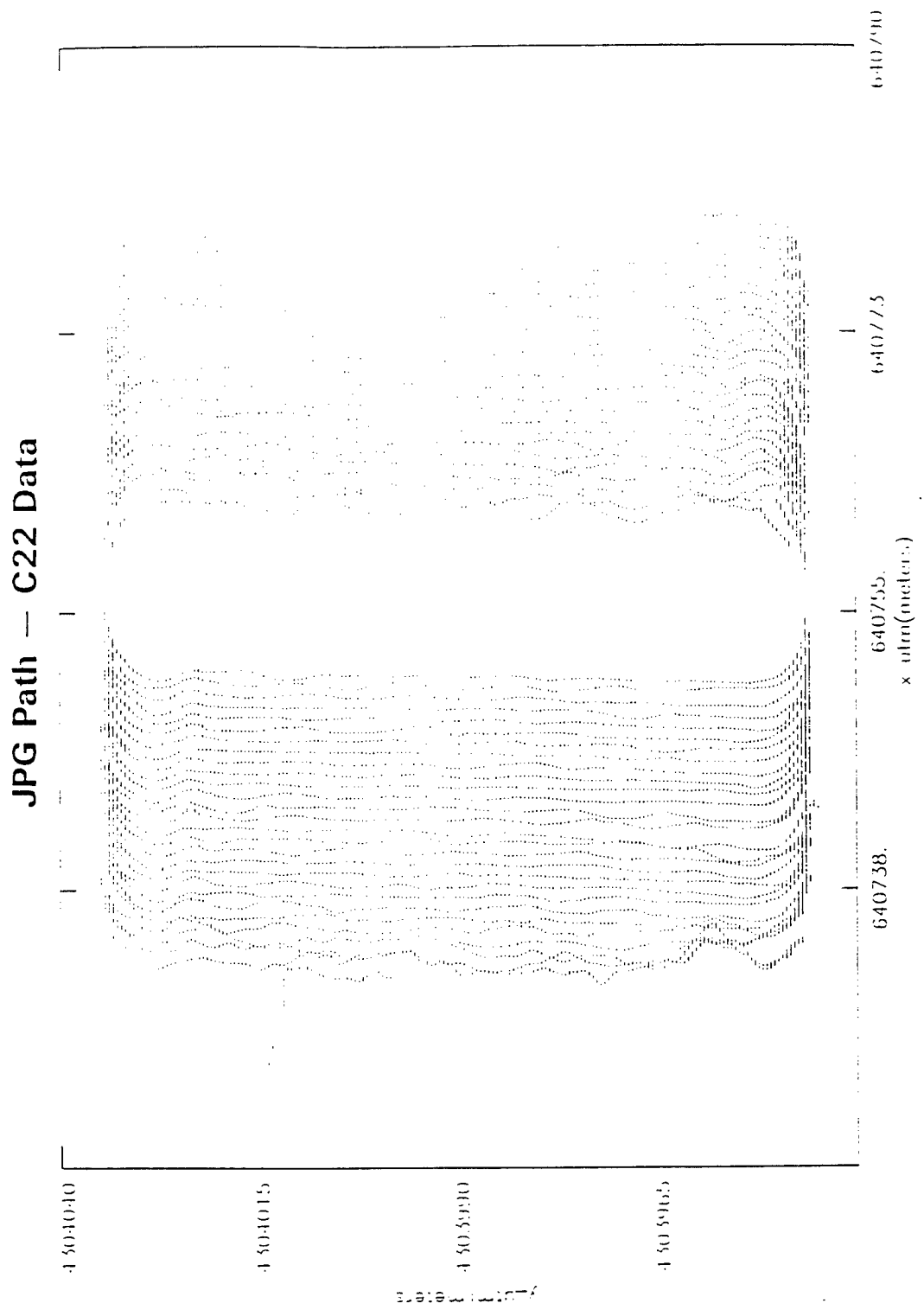

Figure 7. SOCS GPR JPG Path - C22 Data.

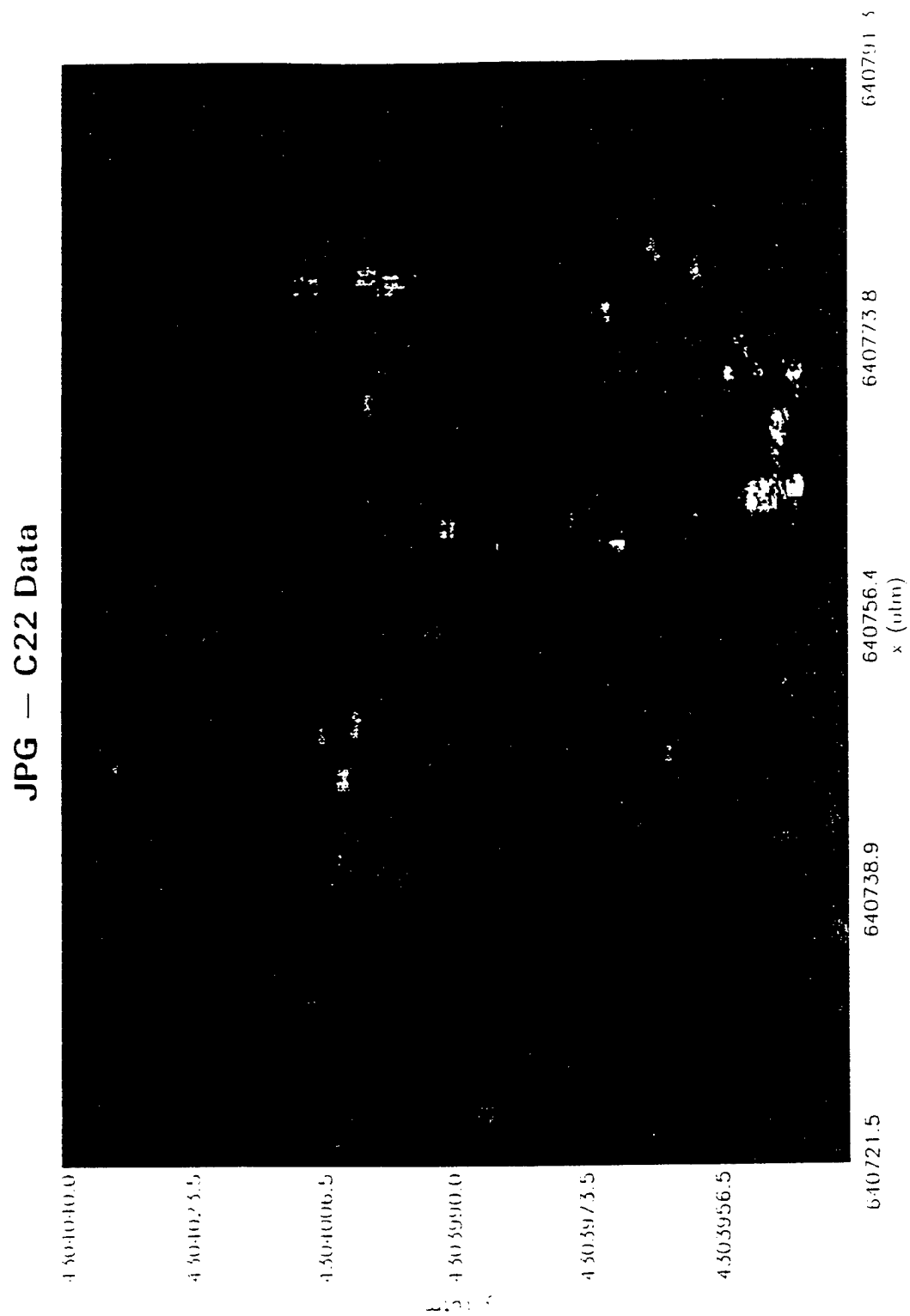

Figure 8. SOCS GPR Image JPG - C22 Data.

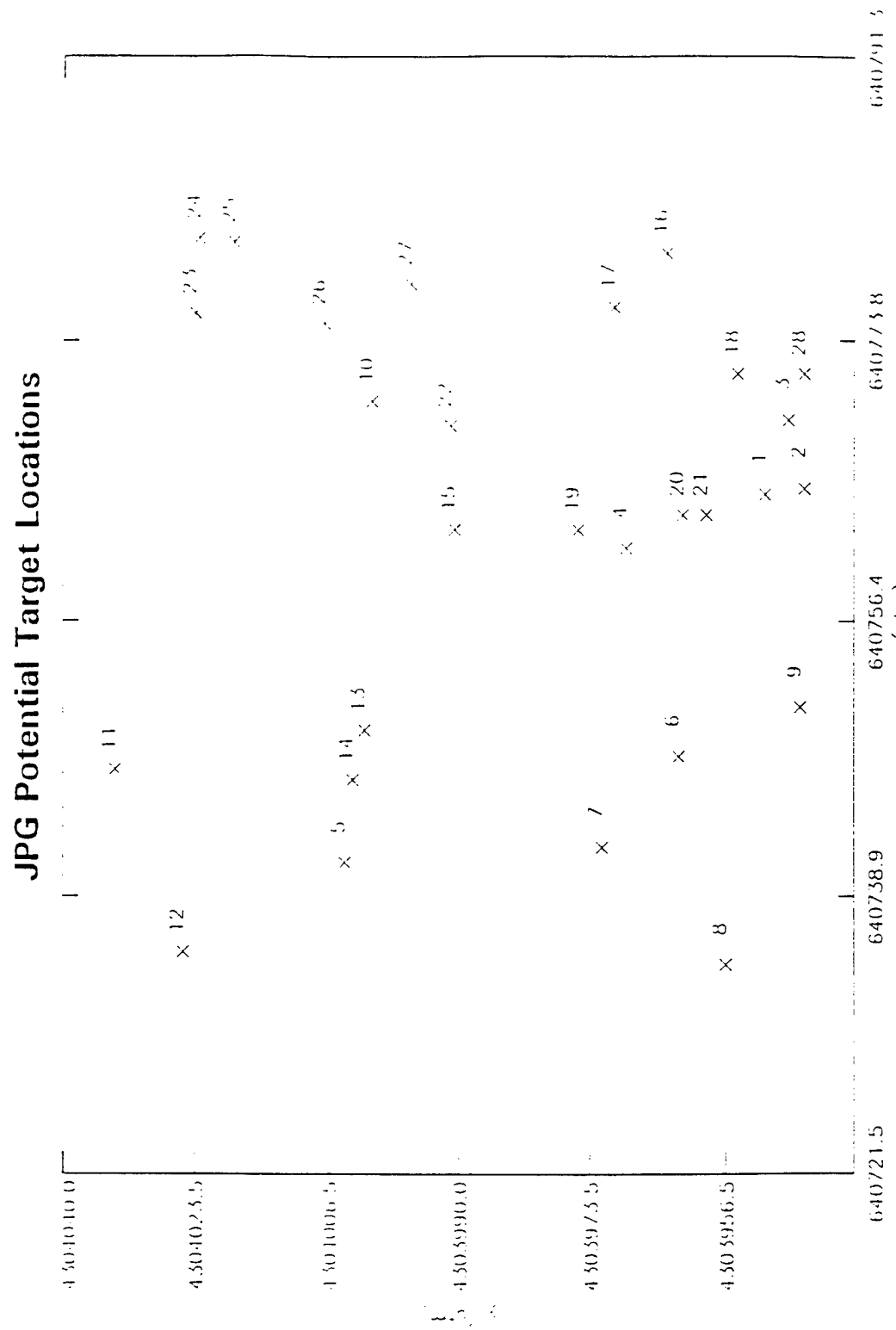

Figure 9. SOCS GPR JPG Potential Target Locations.

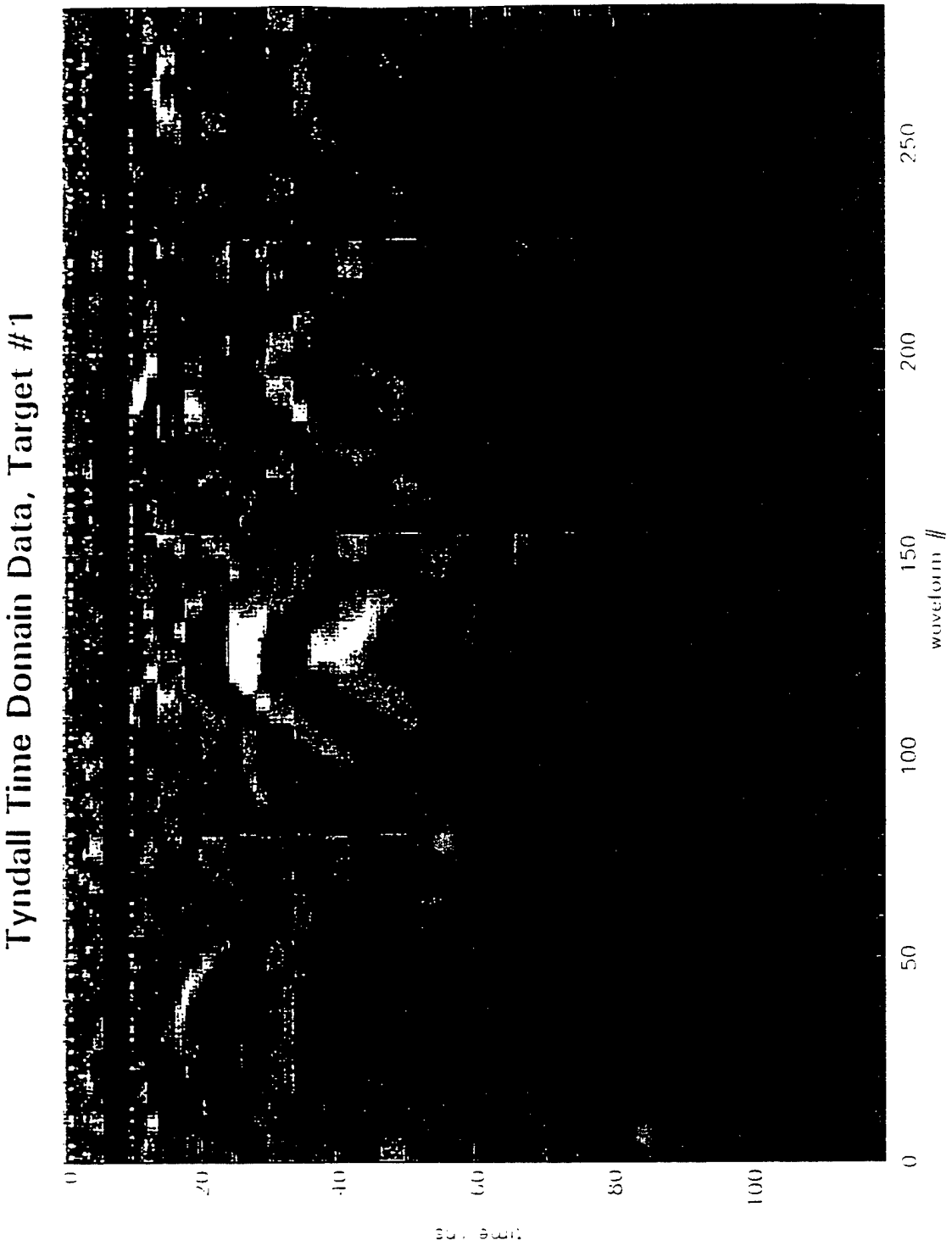

Figure 10. SOCS GPR Tyndall Time Domain Data, Target #1.

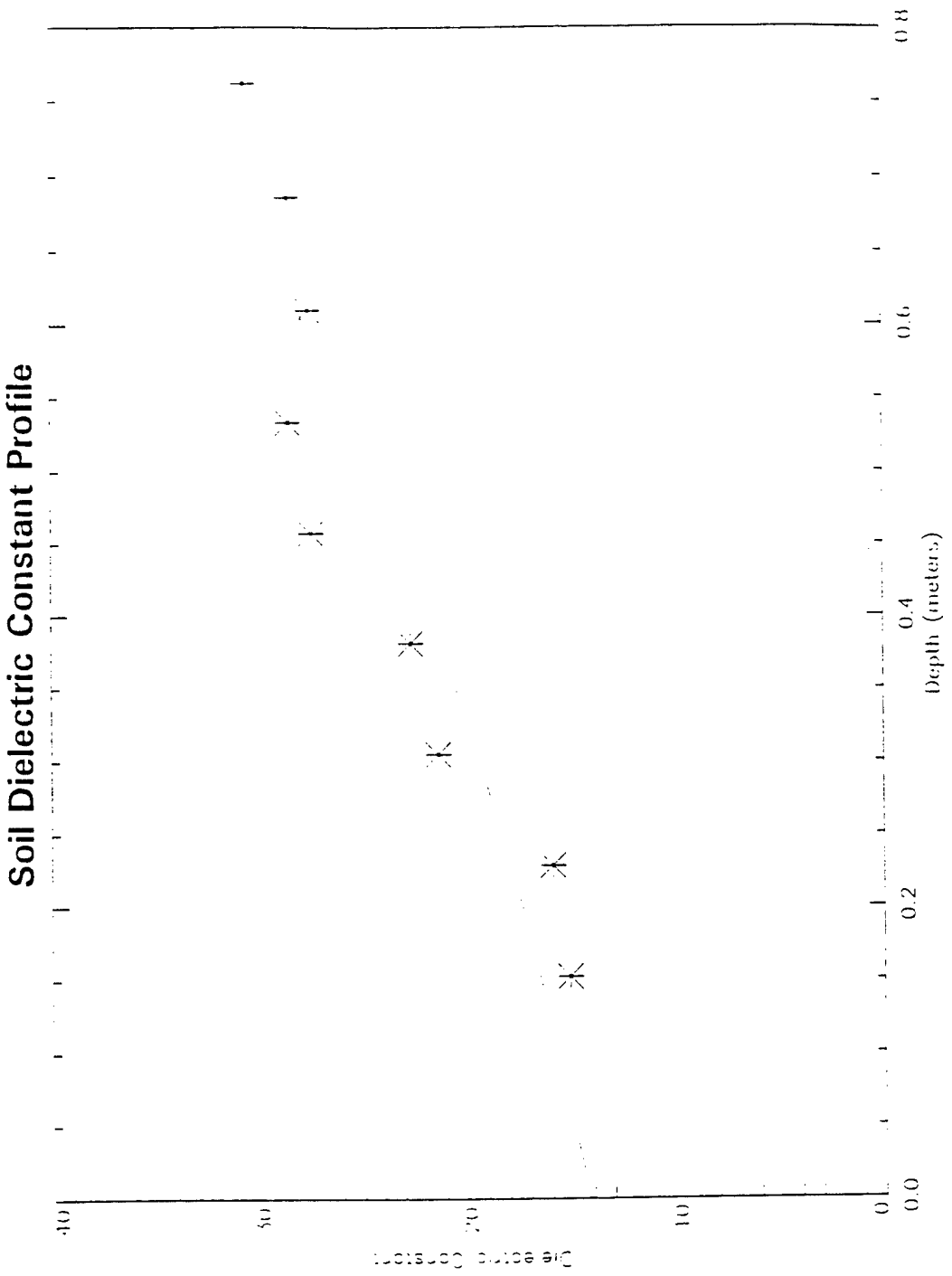

Figure 11. JPG Soil Dielectric Constant Profile.

Appendix D

SOCS Magnetometer Quicklook Report

VA-072-050-95-TR

SOCS DEMONSTRATION AT JEFFERSON PROVING GROUND: QUICK LOOK DATA SUMMARY

15 NOVEMBER 1995

ROBERT DiMARCO
DOUGLAS DePROSPO

AETC Areté Engineering Technologies Corporation
1725 JEFFERSON DAVIS HIGHWAY, SUITE 707
ARLINGTON, VIRGINIA 22202

TABLE OF CONTENTS

LIST OF FIGURES

1.0 INTRODUCTION

From September 13 through September 18, 1995, NAVEODTECHDIV deployed the Subsurface Ordnance Characterization System (SOCS) at Jefferson Proving Ground in Indiana to exercise the system and collect data on the 80-acre UXO demonstration site. Pursuant to our contract with PRC, AETC supported this deployment, providing personnel in the field to analyze data quality and process magnetometer data. In this report we summarize results of the analysis of these data, along with results from the data acquired with SOCS in late August. The purpose of this short report is twofold: (1) to document the data collected, and (2) to create a record of the current status of SOCS data, as determined in the analysis, for comparison with future data sets.

In section 2 of this report we first describe the missions run by SOCS during the August and September test periods. Navigation tracks for each mission are shown and the area covered is reported in local grid and absolute coordinates. Next, the mapping of magnetometer data to spatial positions is discussed. A problem observed in positioning the magnetometers through turns is traced to a problem in recording the vehicle heading. Directional offsets are then calculated. We conclude that changes made during the test to mitigate ferrous contamination near the sensors reduced the directional offset to levels that are too small to be determined without separate testing. Amplitude images of mapped magnetometer data for each mission are shown next. Then noise levels for the magnetometers are estimated; the lowest noise levels seen in the data are consistent with the SOCS specifications (< 1 nT). Target processing for each mission was accomplished using *Magproc* (*Magproc* output for these data are given in the form of STD files on the diskette attached to this report). The final subsection compares *Magproc* fits for targets that were seen in more than one mission. Results and conclusions are summarized in section 3.

2.0 DATA AND ANALYSIS

2.1 SOCS MISSIONS

The SOCS missions run during the August and September tests are summarized in Table 1. The 80-acre demonstration site is divided into a rectangular grid with grid boxes being identified by the designation of the point in the northeast corner. All grid boxes are 100 feet by 100 feet (except along the southern edge of the site). The grid is rotated a few degrees clockwise from the directions of UTM x and y, but we will refer to grid axes as being north-south and east-west. The grid points on the east-west axis are designated by letters, A through O, where A is the furthest east. Along the north-south axis the grid points are designated by number from 1 to 26. In this report we use a local coordinate system with the origin at grid point A1 and the negative x and y axes pointing along the grid west and south, respectively. For example, the grid point C22 is at relative x = -200 and y = -2100 feet.

The naming convention for the SOCS files encodes the grid designation for the northeast corner of the planned area, followed by the dominant direction of travel. When more than one mission was run over the same area the file name is extended by a numeral indicating the repetition number. For example the mission **C22ns1** has its northeast corner at the grid point C22. The dominant direction of travel was north-south and this was the first mission on this area.

Mission	Date	Grid Squares	Track Spacing (ft)	Comments
C22ns1	August 26	3 X 2	4	no magnetometer data
C22ns2	August 26	3 X 2	4	shift in absolute position
B22ew	August 26	3 X 1	4	shift in absolute position
C22ns3	August 29	3 X 2	2.5	incomplete
E22ew	September 15	3 X 2	4	
B14ns	September 16	7 X 2	4	incomplete
D14ns	September 18	7 X 2	4	incomplete

Table 1. Summary of SOCS Data Missions at JPG

During August, four missions were recorded. Three of these were run with an incorrect position for the GPS base station (**C22ns1**, **C22ns2**, **B22ew**). This error results in the absolute positions in the navigation file being incorrect by a constant offset (in this case the recorded positions were about 43.7 feet to the south and 1.2 feet to the west of the actual positions). However, the relative navigation positions are correct within the file. Analysis results from these data sets need to be corrected when comparing to absolute ground truth. The positioning problem was noticed in the field and corrected before mission **C22ns3** was recorded. This mission was run with 2.5 foot spacing between tracks, as opposed to the normal 4 foot spacing, to increase the spatial resolution of the GPR

data. This mission ended early due to equipment malfunction. The **C22ns** missions and the **B22ew** mission overlapped in some areas, in Section 2.7 we will compare *Magproc* output for the targets in the overlapping areas.

During the period from September 15 to September 18 three more missions were recorded. **E22ew** covered six grid boxes and contained two obstacles (trees). The other two missions were planned to cover 14 grid boxes, covering this area would require mission times over 2 hours. However, both of these missions ended early due to equipment problems. Figure 2-1 shows the positions from the navigation file for all of the missions (only one of the **C22ns** missions is shown). The reported latitude and longitude have been converted to 80-acre grid coordinates to make it easier to see the relative positions; plots can also be made in units of latitude and longitude or UTM coordinates if desired. Note that the **B22ew** mission data are plotted at their reported positions which contain an offset error as noted above. These data should be shifted higher relative to the other points.

Individual mission tracks are shown in Figures 2-2 through 2-8. As in the previous figure the navigation points have been transformed to the 80-acre grid coordinate system. In these figures a dot is plotted at each point as reported in the navigation file. The density of points along the track is high enough that the lines appear solid much of the time. However, at more or less regular intervals there are short periods (of up to a second) when the position does not update. This causes the short gaps visible in the tracks. Most of the missions contained obstacles (trees) which SOCS had to steer around. For this field exercise the locations of the obstacles were determined with the SOCS GPS and the track planning software laid out paths to circumvent them.

In the individual mission plots there are numbered points (marked by diamonds) which comprise the corners of the areas covered. The locations of these points in local coordinates, UTM, and latitude/longitude are given in Table 2 so that the area covered during the field exercise can be determined.

	Local xy (ft)		UTM (m)		Lat/Lon (deg*100+ min)	
C22ns1						
1	-200.2	-2154.0	640782.96	4304018.61	3852.42524	-8522.62615
2	-200.7	-2429.2	640775.92	4303935.02	3852.38013	-8522.63205
3	-393.7	-2423.9	640717.44	4303941.45	3852.38417	-8522.67240
4	-389.2	-2147.8	640725.69	4304025.21	3852.42936	-8522.66567
C22ns2						
1	-201.9	-2153.1	640782.48	4304018.92	3852.42541	-8522.62648
2	-203.0	-2431.9	640775.18	4303934.27	3852.37973	-8522.63257
3	-397.6	-2435.4	640715.97	4303938.05	3852.38235	-8522.67346
4	-391.5	-2146.0	640725.06	4304025.81	3852.42969	-8522.66610

Table 2. Boundary Points of Area Surveyed

B22ew						
1	-109.2	-2148.5	640810.74	4304018.02	3852.42465	-8522.60695
2	-105.3	-2235.1	640809.76	4303991.61	3852.41039	-8522.60795
3	-374.6	-2232.4	640728.01	4303999.14	3852.41525	-8522.66438
4	-375.9	-2143.8	640729.83	4304026.09	3852.42980	-8522.66280
C22ns3						
1	-207.4	-2115.0	640781.73	4304030.62	3852.43174	-8522.62685
2	-191.3	-2382.3	640779.97	4303949.03	3852.38766	-8522.62908
3	-254.8	-2387.6	640760.53	4303949.01	3852.38784	-8522.64252
4	-271.0	-2121.2	640762.27	4304030.33	3852.43177	-8522.64032
5	-305.6	-2112.4	640751.99	4304033.88	3852.43379	-8522.64738
6	-290.5	-2385.0	640749.75	4303950.70	3852.38886	-8522.64995
7	-346.3	-2389.4	640732.70	4303950.75	3852.38905	-8522.66174
8	-366.4	-2117.7	640733.39	4304033.78	3852.43392	-8522.66024
E22ew						
1	-415.2	-2104.4	640718.87	4304039.04	3852.43690	-8522.67021
2	-416.2	-2300.0	640713.70	4303979.65	3852.40485	-8522.67452
3	-698.7	-2296.5	640627.97	4303987.78	3852.41007	-8522.73369
4	-734.0	-2097.3	640622.21	4304049.15	3852.44329	-8522.73692
B14ns						
1	-133.1	-1317.5	640824.24	4304271.04	3852.56128	-8522.59451
2	-141.5	-1992.5	640804.84	4304066.20	3852.45075	-8522.61044
3	-196.1	-1988.5	640788.34	4304068.78	3852.45230	-8522.62182
4	-193.9	-1317.5	640805.77	4304272.56	3852.56228	-8522.60726
5	-237.9	-1307.5	640792.64	4304276.69	3852.56463	-8522.61629
6	-239.0	-1976.6	640775.59	4304073.48	3852.45497	-8522.63057
7	-296.5	-1980.5	640758.05	4304073.71	3852.45526	-8522.64270
8	-295.9	-1303.5	640775.12	4304279.35	3852.56624	-8522.62837
D14ns						
1	-293.5	-1323.5	640775.36	4304273.24	3852.56293	-8522.62828
2	-299.1	-1988.5	640757.06	4304071.35	3852.45399	-8522.64342
3	-378.8	-1984.5	640732.93	4304074.55	3852.45596	-8522.66005
4	-366.5	-1317.5	640753.32	4304276.88	3852.56511	-8522.64347
5	-411.2	-1307.5	640740.02	4304281.01	3852.56748	-8522.65262
6	-422.3	-1982.5	640719.77	4304076.24	3852.45700	-8522.66914
7	-465.2	-1974.6	640706.93	4304079.74	3852.45901	-8522.67797
8	-497.0	-1781.4	640702.09	4304139.20	3852.49119	-8522.68058
9	-489.8	-1301.6	640716.28	4304284.79	3852.56975	-8522.66898

Table 2. Boundary Points of Area Surveyed (cont'd)

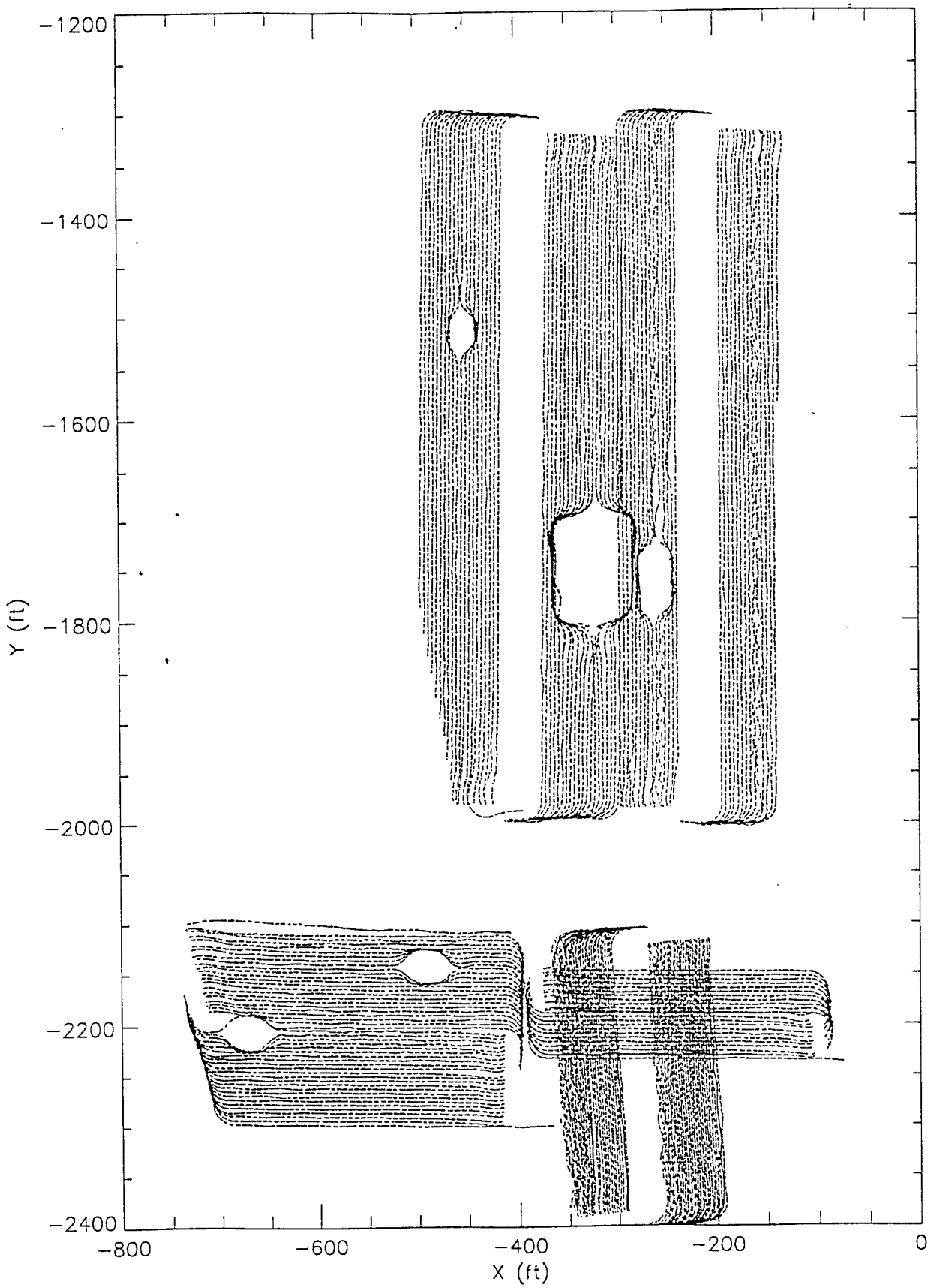

Figure 2-1. Navigation positions in local grid coordinates for missions: **B22ew**, **C22ns3**, **E22ew**, **B14ns**, and **D14ns**.

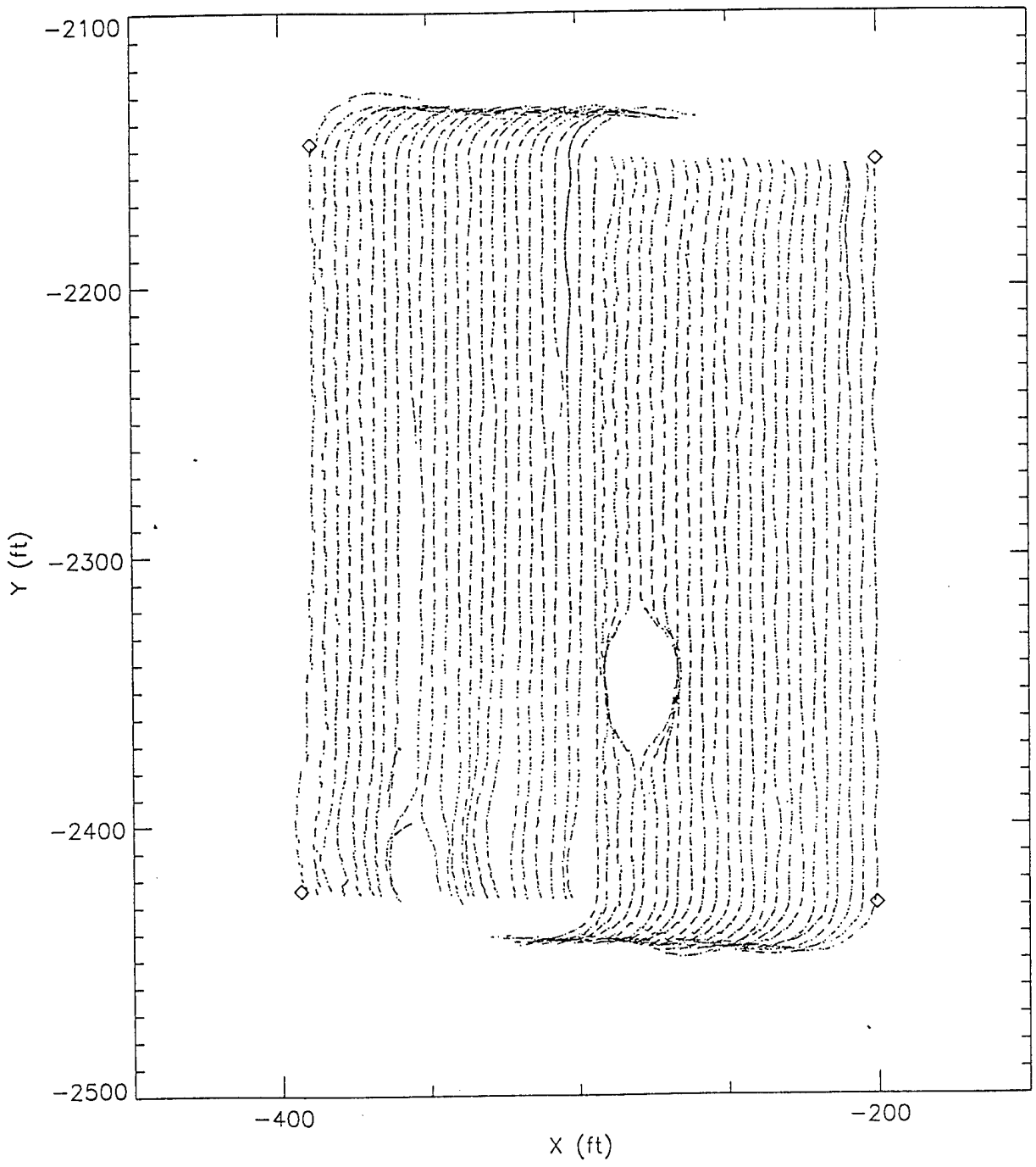

Figure 2-2. Navigation positions in local grid coordinates for mission **C22ns1**. Diamonds are the points listed in table 2.

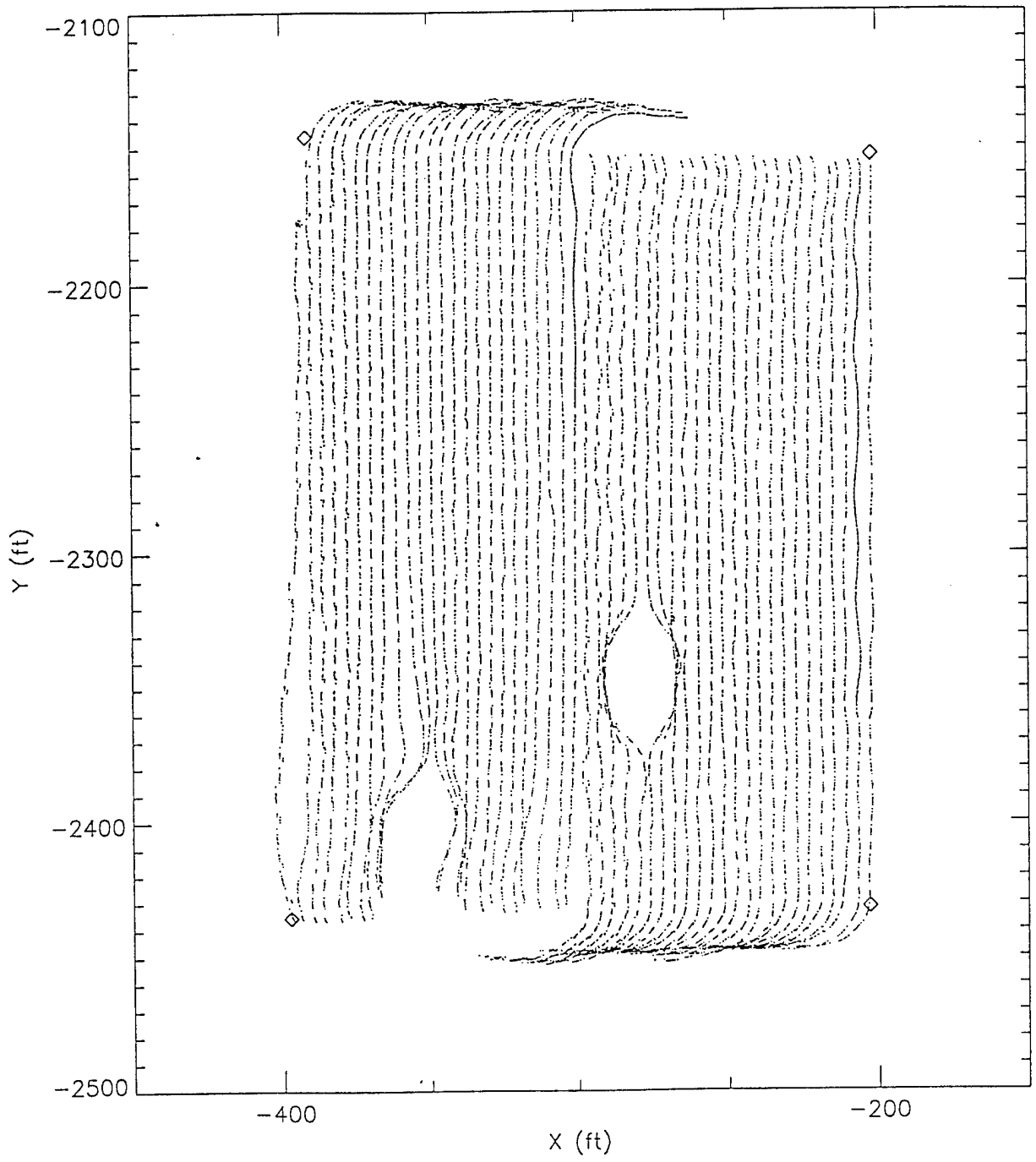

Figure 2-3. Navigation positions in local coordinates for mission **C22ns2**. Diamonds are the points listed in table 2.

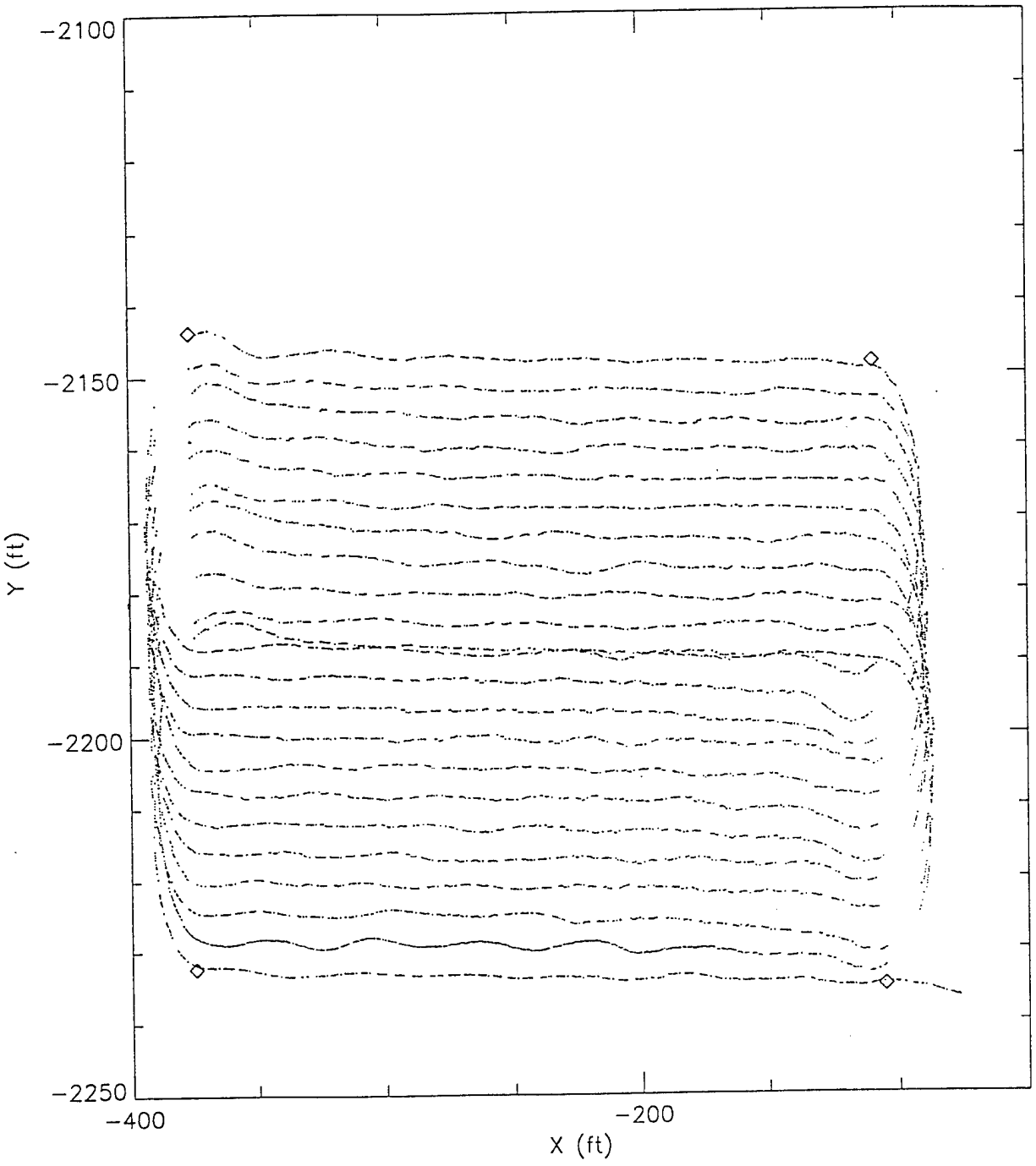

Figure 2-4. Navigation positions in local grid coordinates for mission **B22ew**. Diamonds are the points listed in table 2.

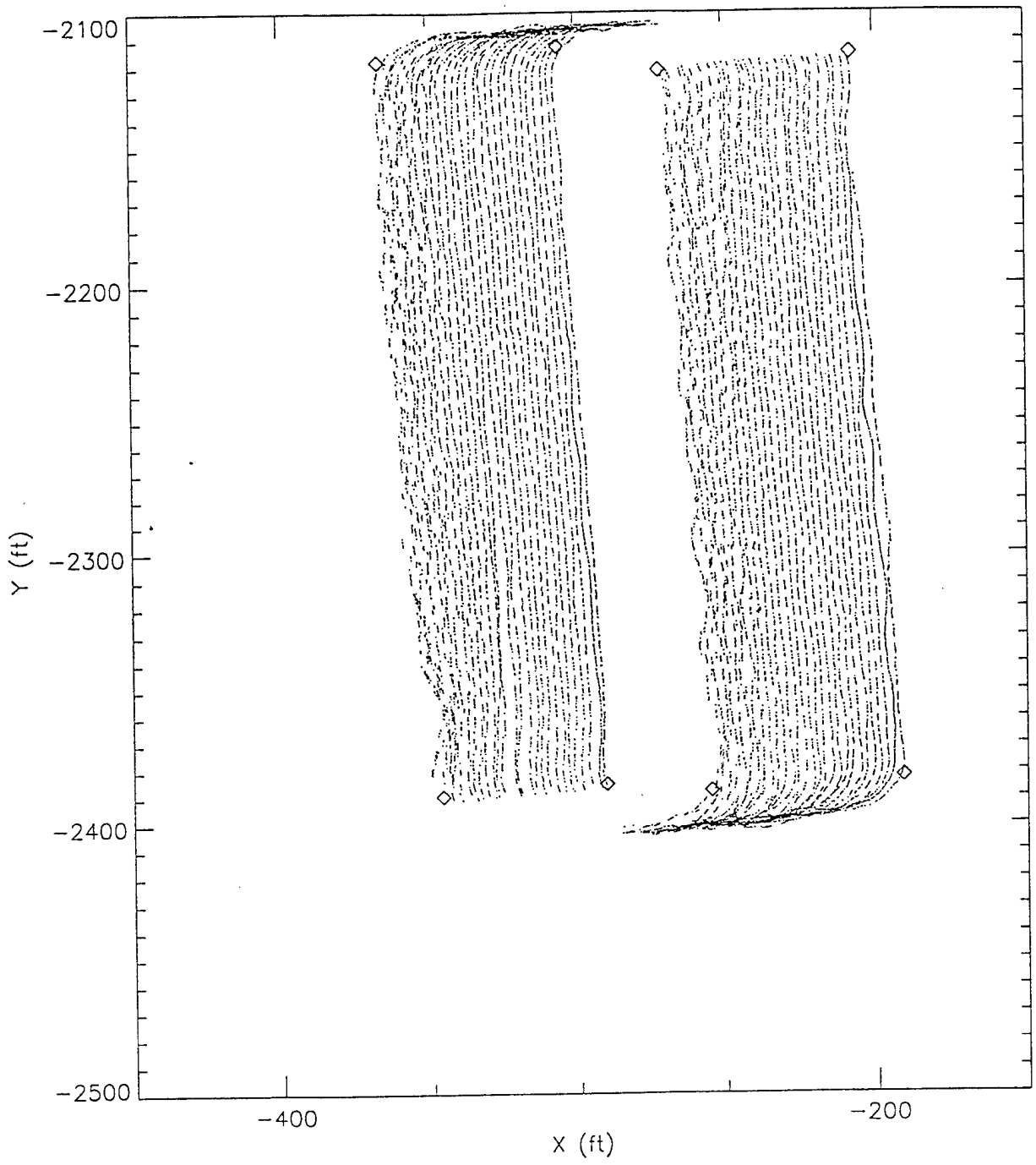

Figure 2-5. Navigation positions in local grid coordinates for mission C22ns3. Diamonds are the points listed in table 2.

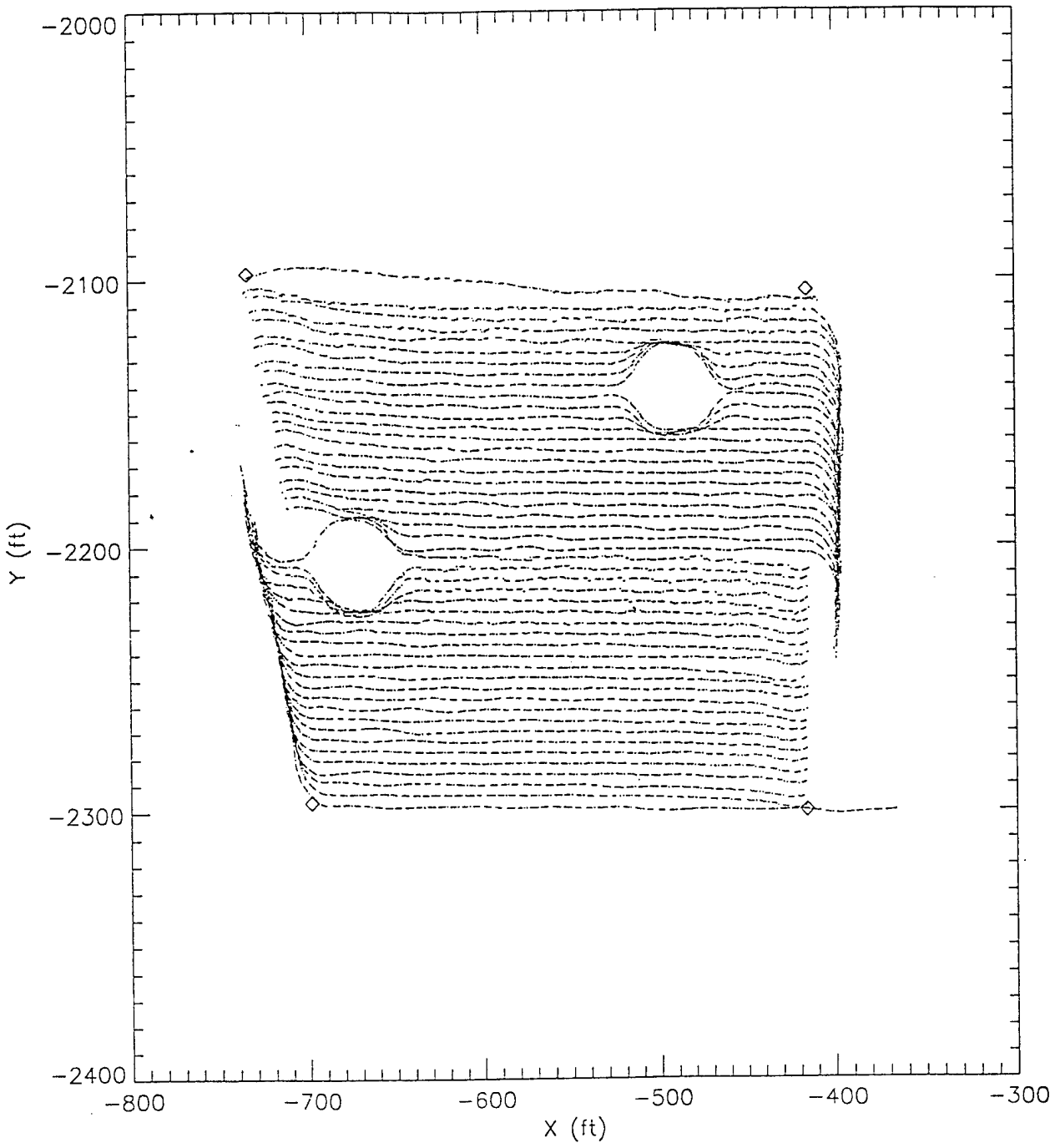

Figure 2-6. Navigation positions in local grid coordinates for mission **E22ew**. Diamonds are the points listed in table 2.

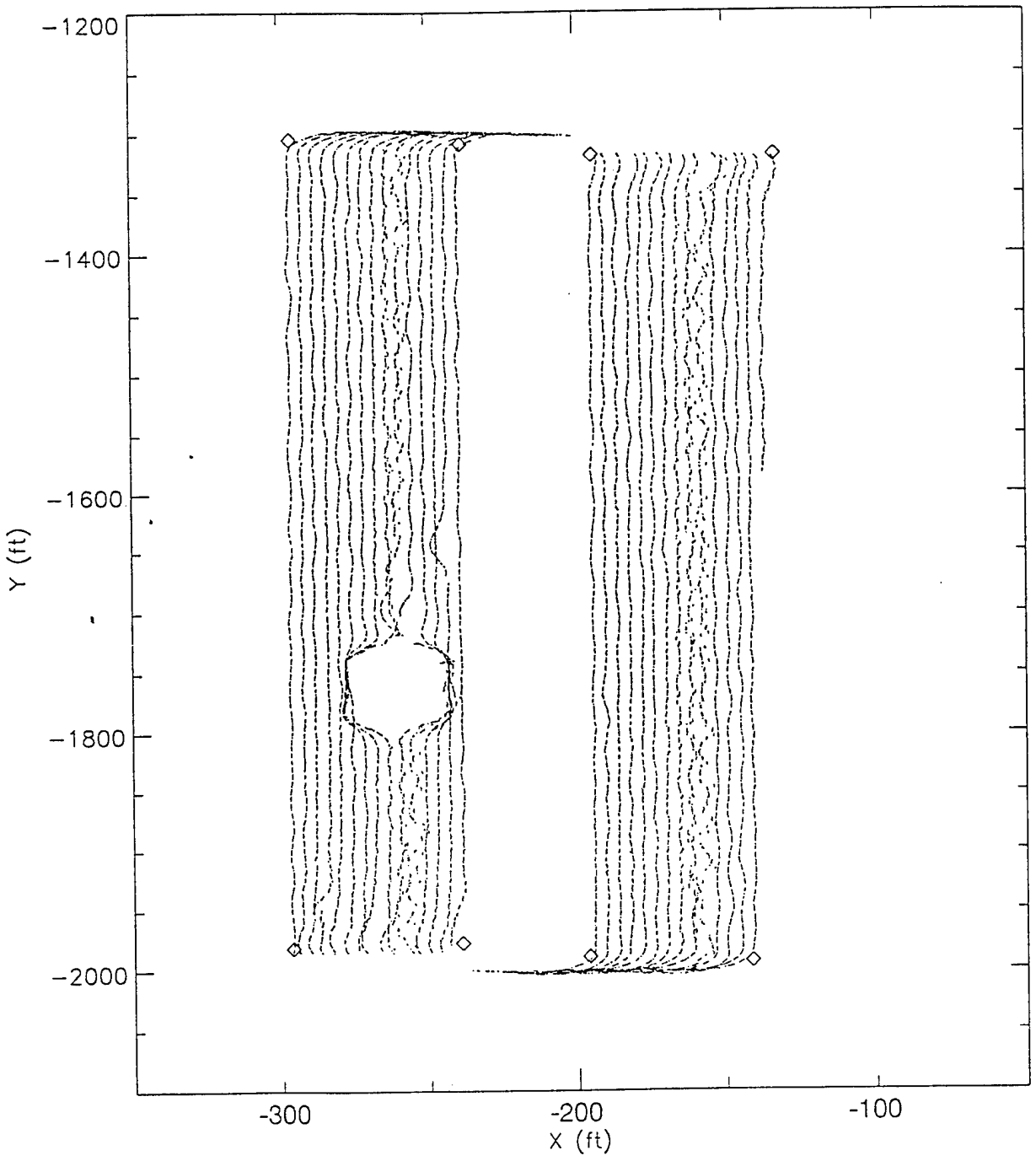

Figure 2-7. Navigation positions in local grid coordinates for mission **B14ns**. Diamonds are the point listed in table 2.

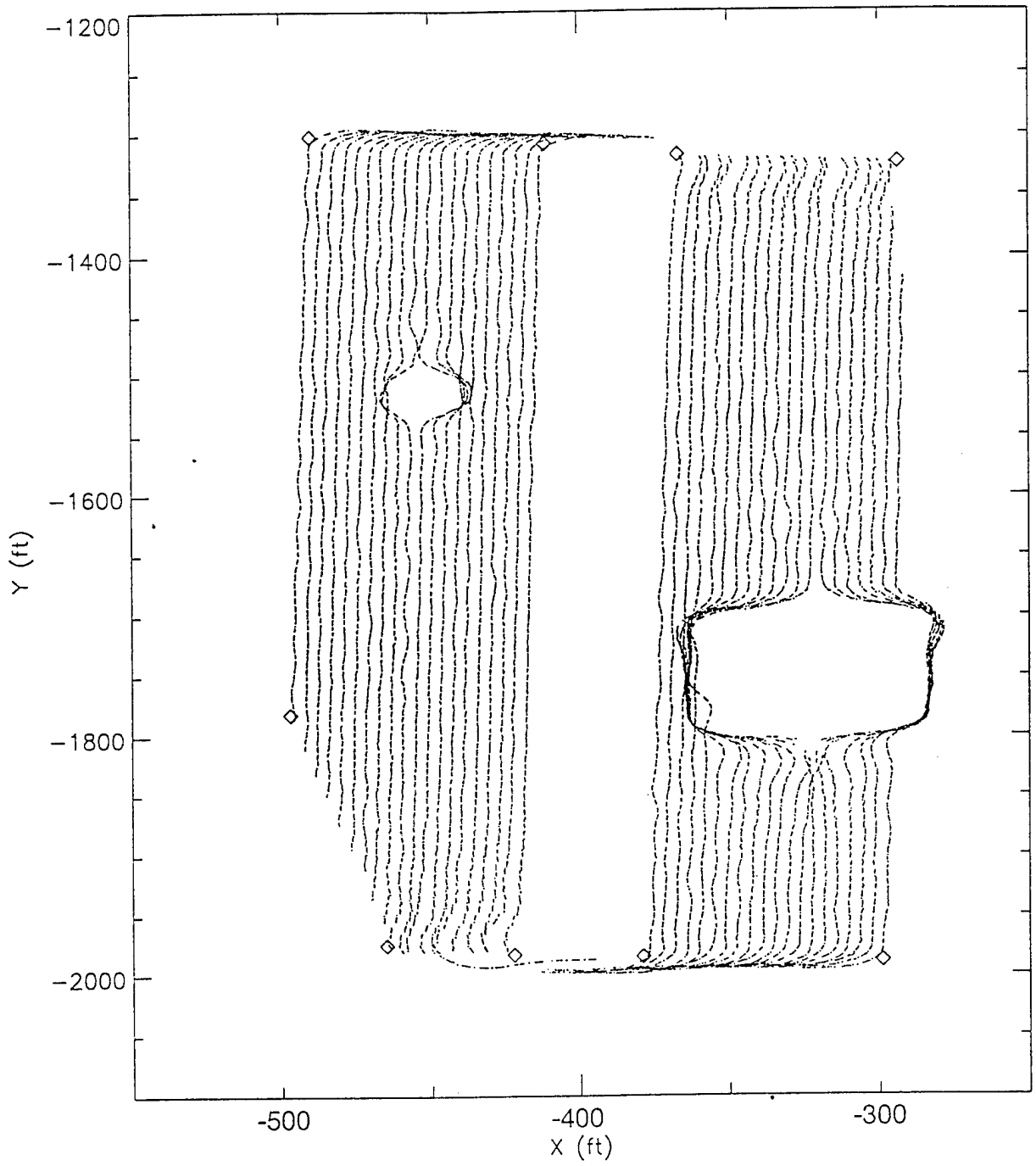

Figure 2-8. Navigation positions in local grid coordinates for mission **D14ns**. Diamonds are the points listed in table 2.

2.2 MAGNETOMETER MAPPING

The positions during this field exercise, for both the real-time navigation and the recorded data, were determined using a combination of GPS and inertial navigation information. This updated software from the University of Florida resulted in improved straightness in the SOCS path compared to previous data from tests at Tyndall AFB. In addition to improving the quality of the path, the new software eliminates the need for frequent stops to update the position. On one occasion, during mission **B14ns** (Figure 2-7), the path began to oscillate along the track and the operator stopped the vehicle to allow the Kalman filter to reset. This oscillating track can be seen near the x-positions -160 and -260 ft. After resetting the filter this problem did not recur. The oscillations in the path visible near the end of mission **C22ns3** (Figure 2-4) occurred due to equipment problems.

The figures described above show the position of the GPS antenna as reported in the navigation file. The positions of the magnetometers are determined from this information, the vehicle and trailer orientation data in the platform file, and the known location of the magnetometers on the trailer. Figure 2-9 shows the magnetometer positions for part of a typical mission, **E22ew**, overlaid on the navigation positions (black). Each of the four magnetometers is shown with a different color. As in the previous figures a dot is printed at each data location. The magnetometer data are recorded at 20 Hz and the locations are extrapolated between navigation positions so the paths appear solid. The magnetometer cart typically follows the tow vehicle so the navigation positions are usually covered up, except where the vehicle turns. The four magnetometers are 18 inches apart (covering 4.5 feet) which at the typical 4 foot spacing between tracks yields good coverage of the field. Just below relative y of -2200 feet is the border between tracks heading to the right (upper section) and tracks heading to the left (lower section).

Note that as the SOCS vehicle turns, to avoid the tree in the upper part of Figure 2-9, the magnetometer positions seem to wiggle around the path. This effect is more obvious in Figure 2-10, which shows the vehicle track in black and the mapped path of one magnetometer in red. Field observations of the actual magnetometer locations indicate that they are in fact moving smoothly through the turns. It appears that the problem in mapping the magnetometer locations is due to a slow updating of the vehicle heading channel. Figure 2-11 shows the vehicle heading (upper panel) and yaw of the trailer hitch (lower panel) channels versus time as the vehicle enters a turn. The hitch yaw increases smoothly to a maximum of about 30 degrees, then levels out and drops back down as the trailer follows the tow vehicle out of the turn. The vehicle heading starts to change smoothly, then seems to stick for up to 2/3 of a second before updating to the expected angle. During this period the mapping software sees the yaw angle of the trailer hitch increasing while the heading is not changed. Thus the trailer seems to be moving sideways and the magnetometer positions drift to the side. When the heading angle updates, the magnetometers "jump" back into proper position. The heading sticks several times during the turn, although the effect on the magnetometer positions is not as obvious later in the turn since the hitch yaw is not changing as fast. The cause of the problem with the vehicle heading is under investigation.

2.3 DIRECTIONAL OFFSET DUE TO SOCS

In previous SOCS data from Tyndall AFB it was noticed that magnetometer D (the starboard outside sensor) exhibited a shift in median field level from the other sensors. Also, the directional offset for

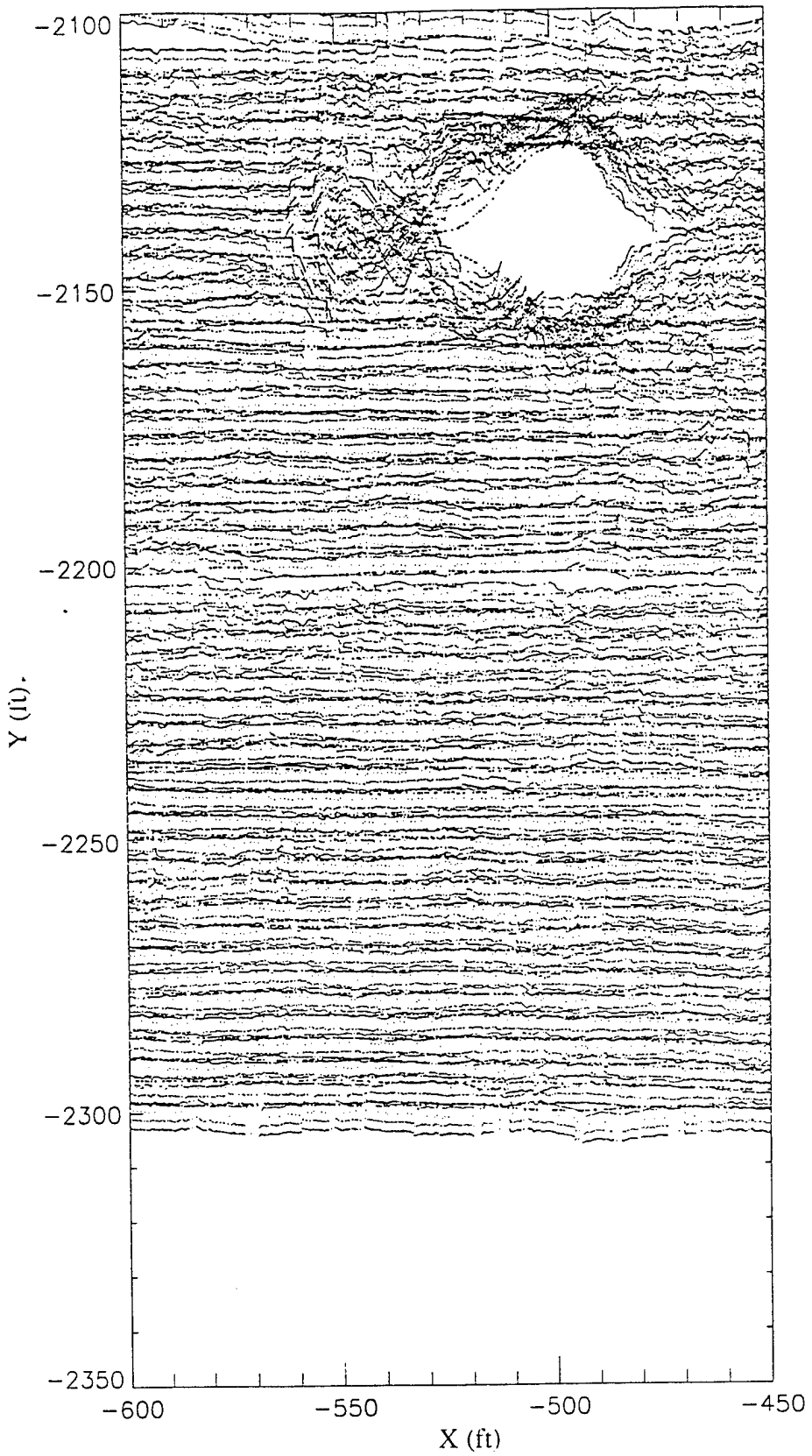

Figure 2-9. Navigation positions (black) and mapped magnetometer positions (color) in local grid coordinates from mission **E22ew**.

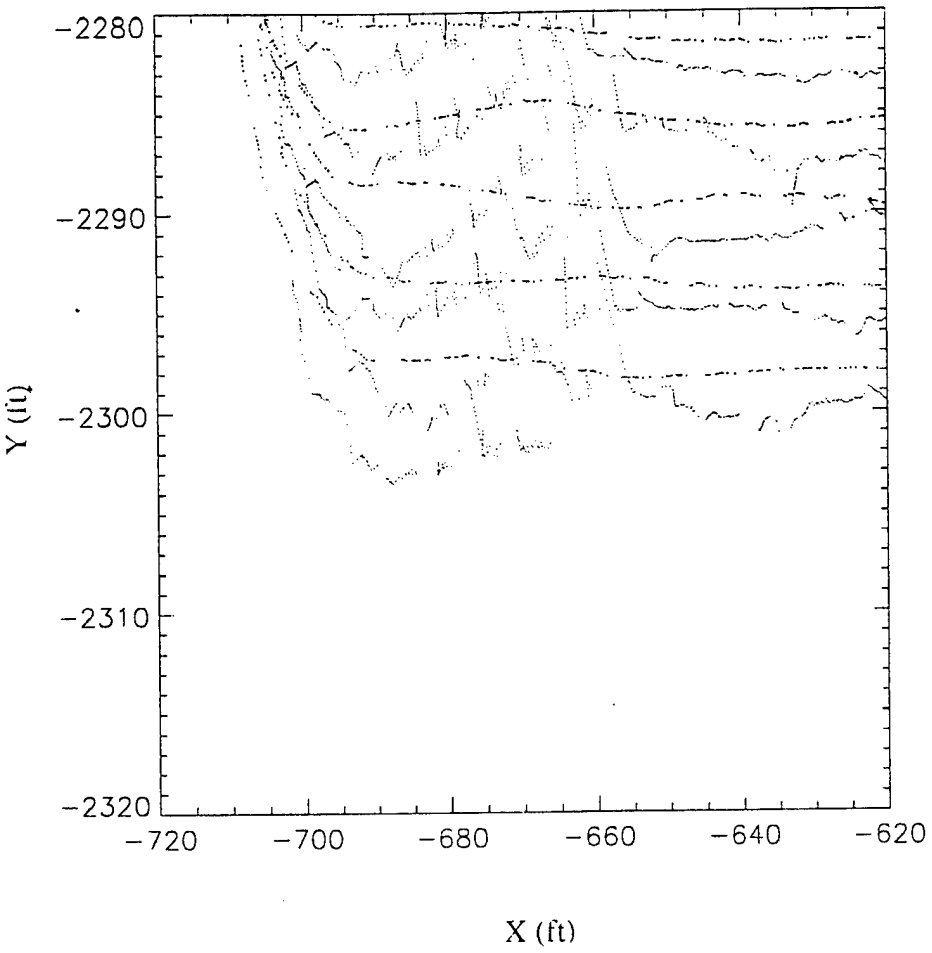

Figure 2-10. Navigation positions (black) and mapped magnetometer positions (red) as the tow vehicle turns north (upwards) from mission **E22ew**.

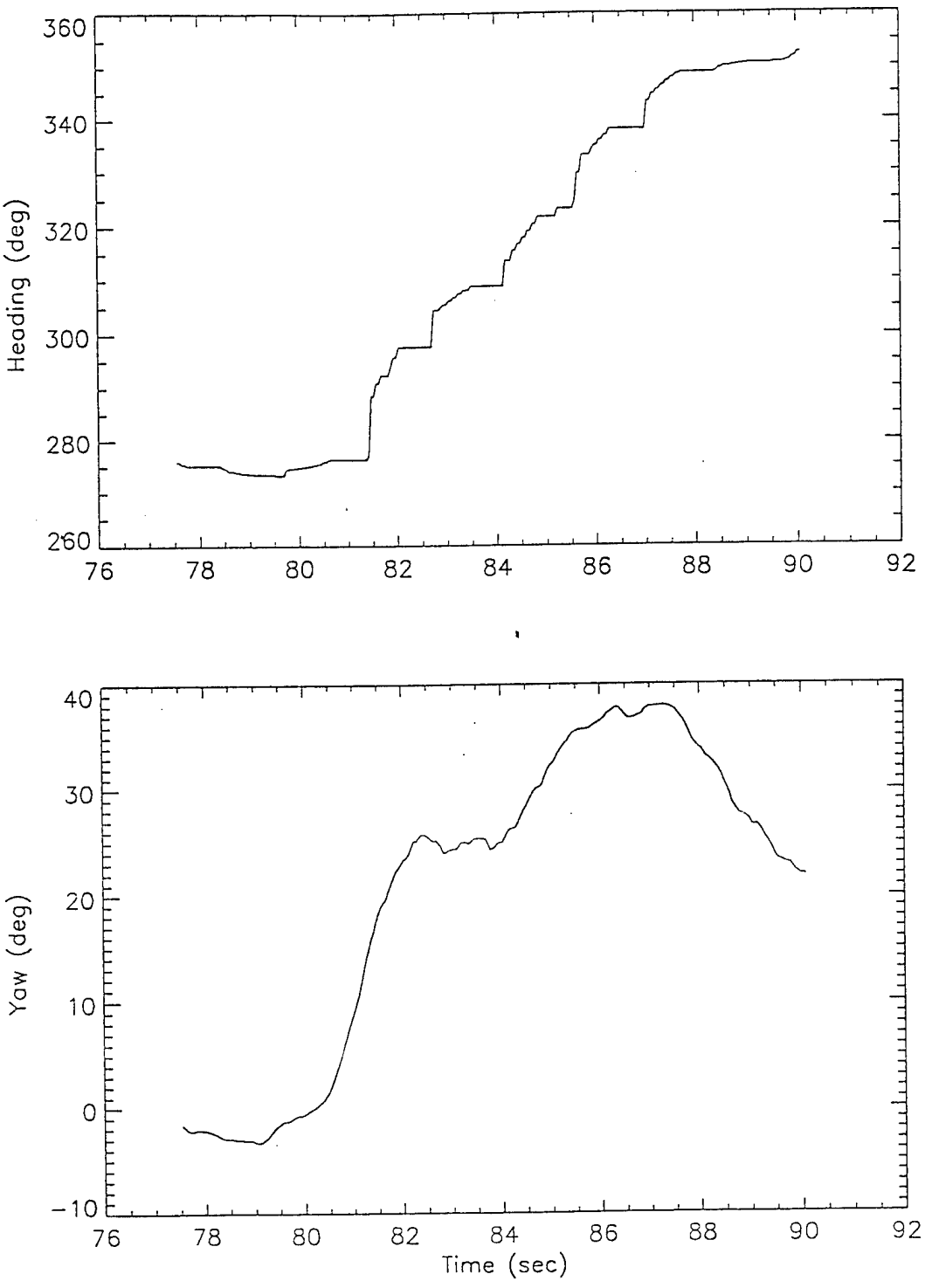

Figure 2-11. Vehicle heading (upper panel) and yaw of the trailer hitch (lower panel) as a function of time as the tow vehicle turns from west to north.

this sensor was larger than for the other three. Before taking data in September the trailer was examined with a Schonstedt gradiometer to determine if there was a magnetic source near sensor D. In this way it was determined that the small bubble level mounted near each magnetometer contained a small threaded bolt. In the case of sensor D this bolt was magnetized. The level of magnetization was small, but since the bolt was only a few inches from the sensor it had a significant effect on the data. After removing the bubble level near sensor D, this magnetometer's median field levels and directional offset became consistent with the other three magnetometers. This change is documented in Table 3 which lists the directional medians for the four sensors and in Figure 2-12 which displays the directional offset for the 6 missions where magnetometer data were collected. Prior to removing the bubble level between runs **B22ew** and **E22ew**, sensor D offsets were larger than and inconsistent with those of the other sensors. After removing the magnetic source, the offsets are all consistent. Similarly, the median level for sensor D, which had been different from the median level of the other sensors by 10 nT is now in the same range as for the other sensors. **Although the other three bubble levels did not appear to be magnetized, we strongly recommend removing them. It is likely that their connecting bolts are also ferrous and so they may become magnetized at some point in the future.**

Mission	Magnetometer: Median field for each direction (nT)			
	A	B	C	D
C22ns2	54463.0	54462.3	54464.7	54469.1
	54461.2	54460.9	54462.2	54476.2
B22ew	54430.9	54430.2	54432.3	54439.6
	54429.6	54429.3	54430.4	54442.7
C22ns3	54416.2	54415.6	54416.8	54430.3
	54418.2	54417.4	54419.5	54427.4
E22ew	54440.2	54439.7	54441.7	54441.2
	54441.6	54440.2	54441.8	54441.2
B14ns	54434.8	54434.2	54436.0	54435.7
	54433.7	54433.3	54434.8	54434.2
D14ns	54440.7	54440.1	54442.2	54441.4
	54437.6	54437.3	54438.7	54438.0

Table 3. Median Magnetic Field for Each Direction of Travel

Figure 2-12 indicates that directional offsets of several nT are still being seen in the data. It is not clear if this remaining offset is a directional shift due to residual magnetic fields from SOCS or if it reflects an environmental shift in the average field over the survey area. Note that the shifting

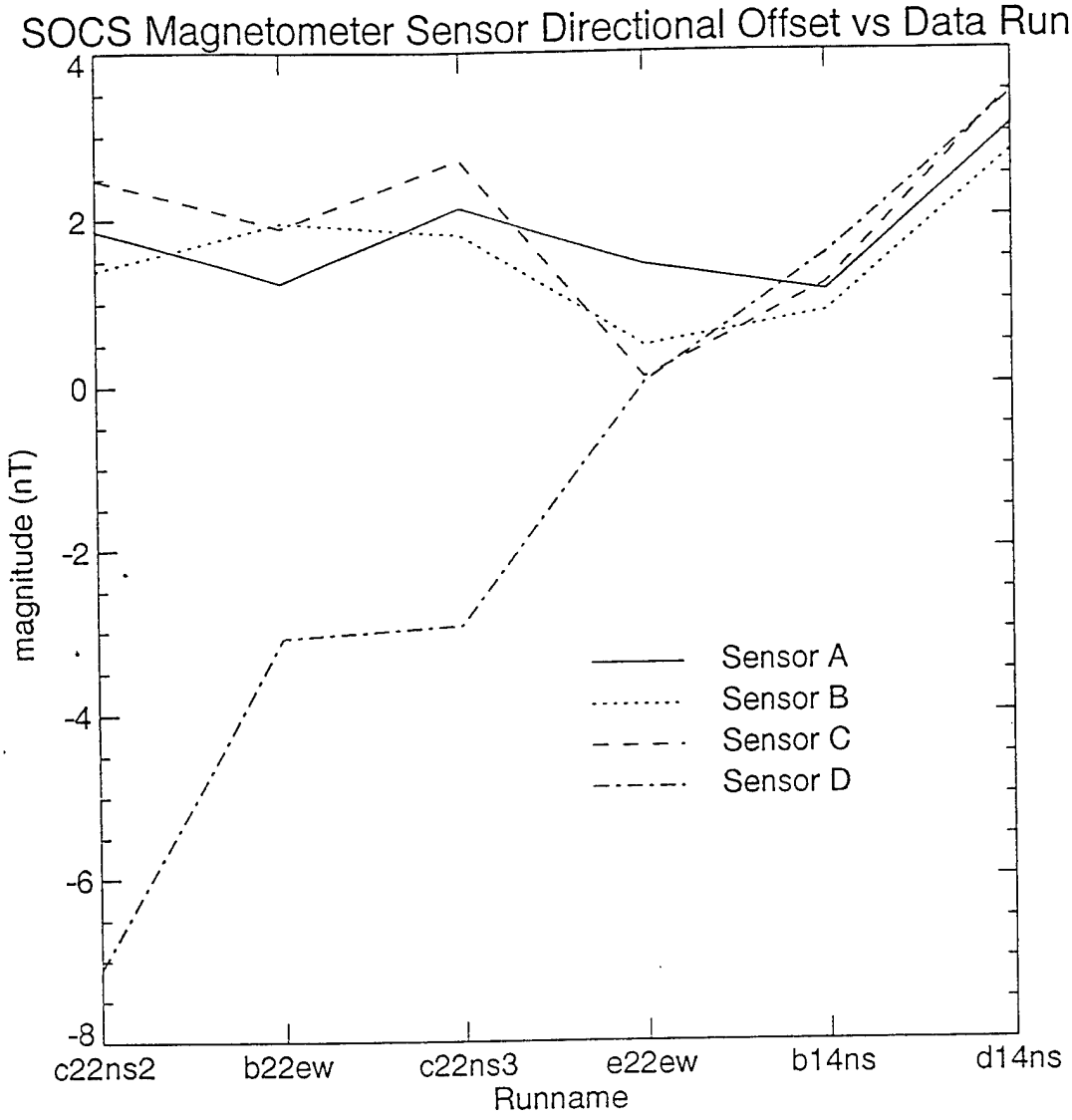

Figure 2-12. Absolute directional offset from *Magproc* versus run number. Ferrous bolt near sensor D was removed between missions **C22ns3** and **E22ew**.

racetrack path of the SOCS survey splits the mission area into two halves; for one half SOCS is traveling in one direction, for the other half the direction is reversed. If a gradient in the measured field exists over the region, we would expect to see different median levels for the data from the two directions. The offsets seen in Table 3 for the last few missions are small enough, a few nT, that we cannot determine whether they are caused by spatial shifts in the field or by SOCS. Thus, we can only conclude that the remaining residual field contamination from the SOCS tow vehicle and trailer is at or less than a few nT.

We recommend a special test to document the remaining directional offset in SOCS. For this test SOCS would cover a set of tracks (in a magnetically clean area) moving in both directions. Covering the same tracks in both directions would eliminate the effects of any environmental spatial gradients, allowing a direct calculation of the directional offset. For this test a reference magnetometer would be required so that temporal changes in the Earth field can be removed.

2.4 MISSION AMPLITUDE IMAGES

The magnetic data processor works directly on the mapped magnetometer data which is irregularly spaced. In order to make color images of the amplitude data these mapped points were interpolated to a uniform grid. An amplitude plot of the whole area covered is shown in Figure 2-13. Separate plots for each mission are shown in Figures 2-14 - 2-19. For all of these amplitude data the median field has been removed separately for the two directions of travel of each sensor in each mission.

An amplitude image of the whole field, as in Figure 2-13, often provides a good perspective for determining larger scale features (e.g., geologic features, drainage beds, fence lines, roads) which may not be evident in plots of individual missions. In this case the coverage was rather sparse for this purpose. There are some weak features trending east-west which are seen continuing across the boundary between the missions **B14ns** and **D14ns**, for instance near relative y positions -1700 and -1900 feet. Also, there is a linear band of anomalies, possibly an old fence line, extending from roughly (-250,-2400) to (-300, -2100). The banding seen in the **E22ew** mission data (between -700 and -400 relative x) is due to uncompensated temporal drift in the Earth field during the mission. This banding also hides features in the combined images since adjoining edges of different missions do not have the same zero level.

Amplitude maps for the individual missions are shown in Figures 2-14 through 2-19. Note that in these images the scales of the x and y axes are not the same, so features are distorted. The crosses and numbers on the images refer to anomalies detected and fit with *Magproc*; these will be discussed in Section 2.6. In several of the missions there is a banding of the data perpendicular to the direction of travel (e.g., **E22ew** and **D14ns**). This is caused by temporal drift of the Earth field amplitude during the time of the mission. Because of the race track pattern of the SOCS navigation a slow temporal shift in the field produces a double set (one for each direction) of amplitude changes across the measured area.

The **C22ns** region was measured twice and this region overlaps the **B22ew** area. The overlap is evident comparing Figures 2-14, 2-15 and 2-16 (recall that positions for the first two missions are shifted south of their actual locations by about 44 feet). Targets in this overlapping region are discussed in Section 2.7.

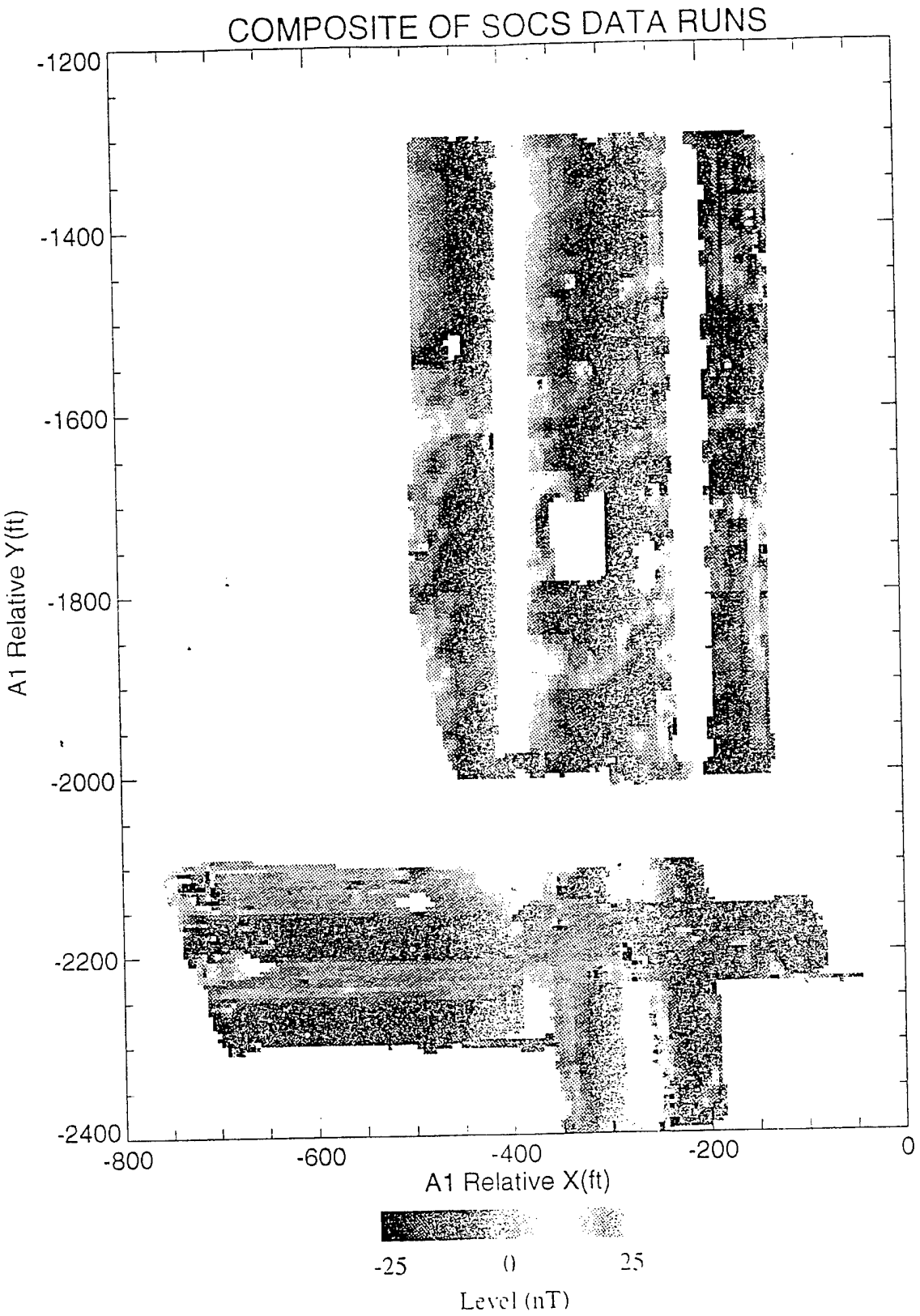

Figure 2-13. Interpolated magnetic amplitude image of area covered by SOCS missions.

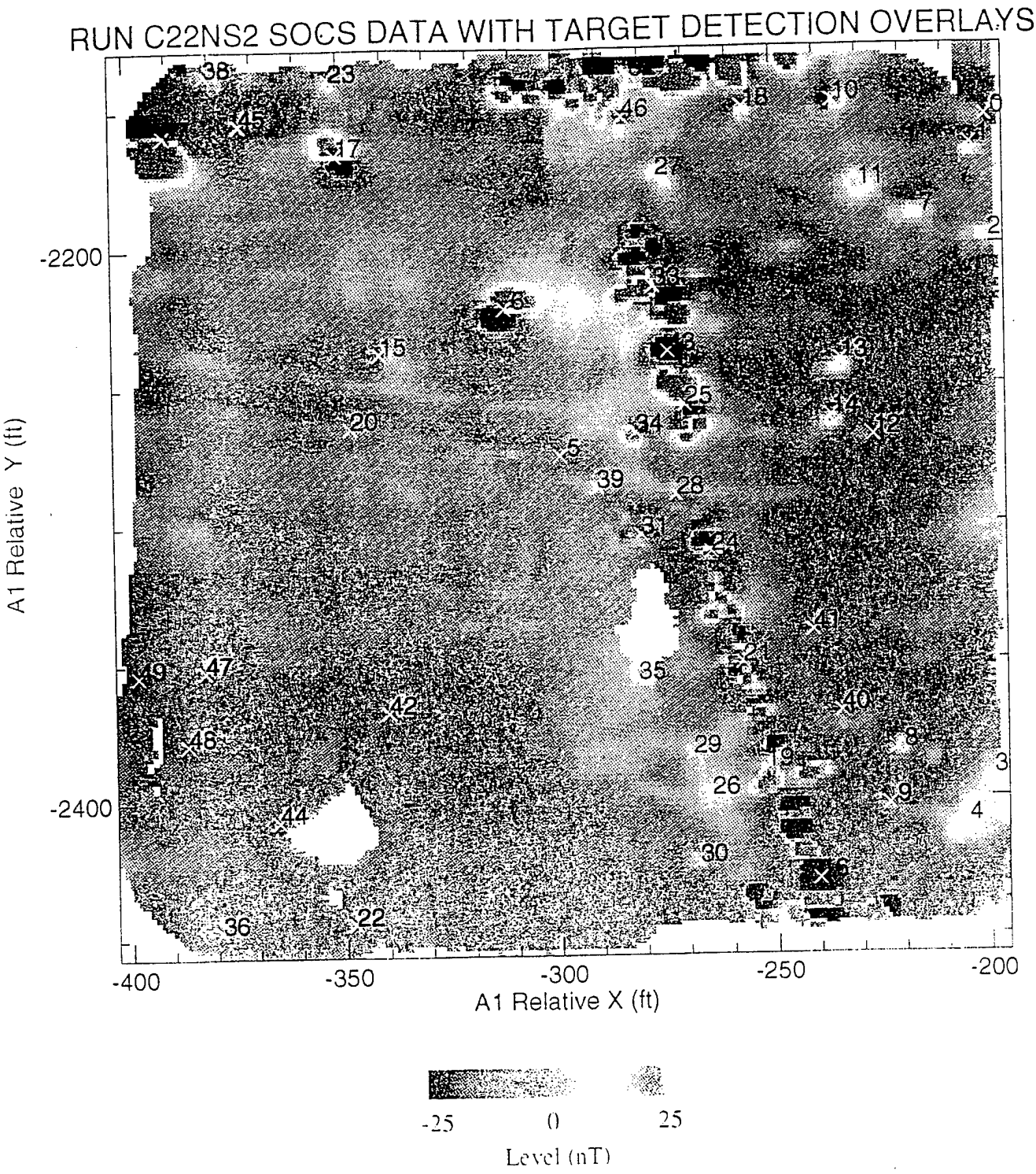

Figure 2-14. Interpolated magnetic amplitude image of mission **C22ns2** data. X's mark the locations of *Magproc* fits, the numbers refer to the order of the fits in the STD file.

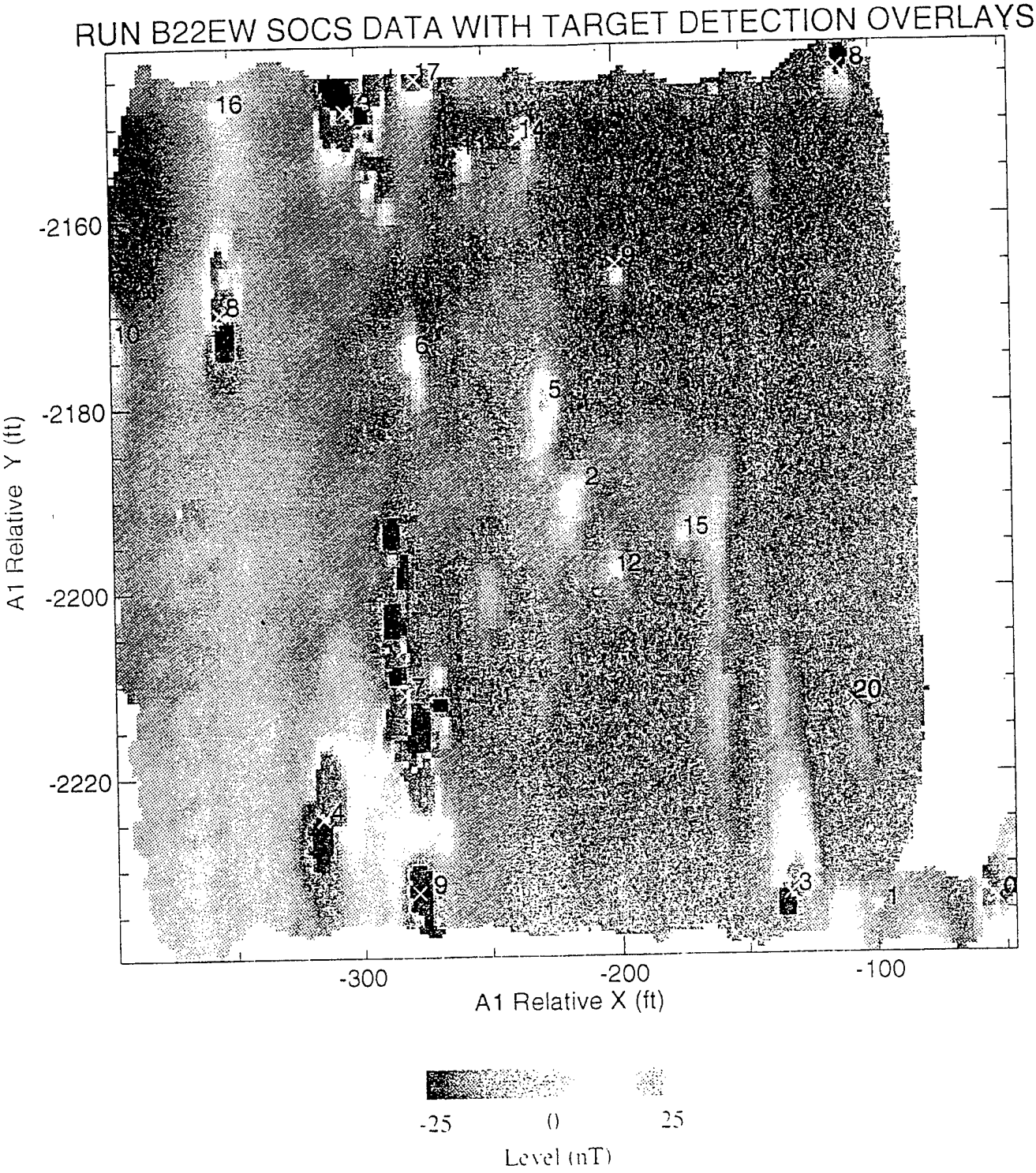

Figure 2-15. Interpolated magnetic amplitude image of mission **B22ew** data. X's mark the locations of *Magproc* fits. the numbers refer to the order of the fits in the STD file.

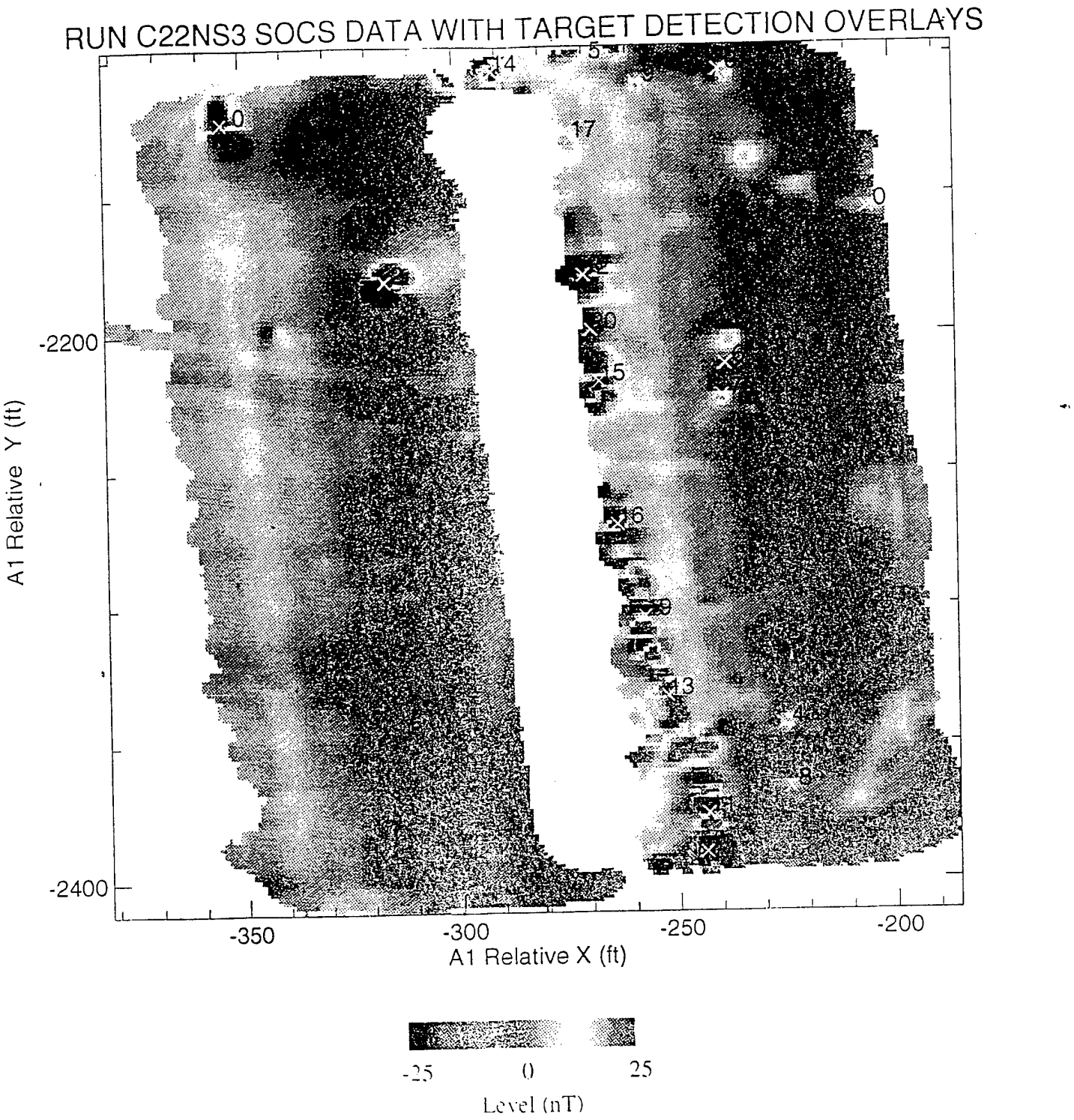

Figure 2-16. Interpolated magnetic amplitude image of mission **C22ns3** data. X's mark the locations of *Magproc* fits, the numbers refer to the order of the fits in the STD file.

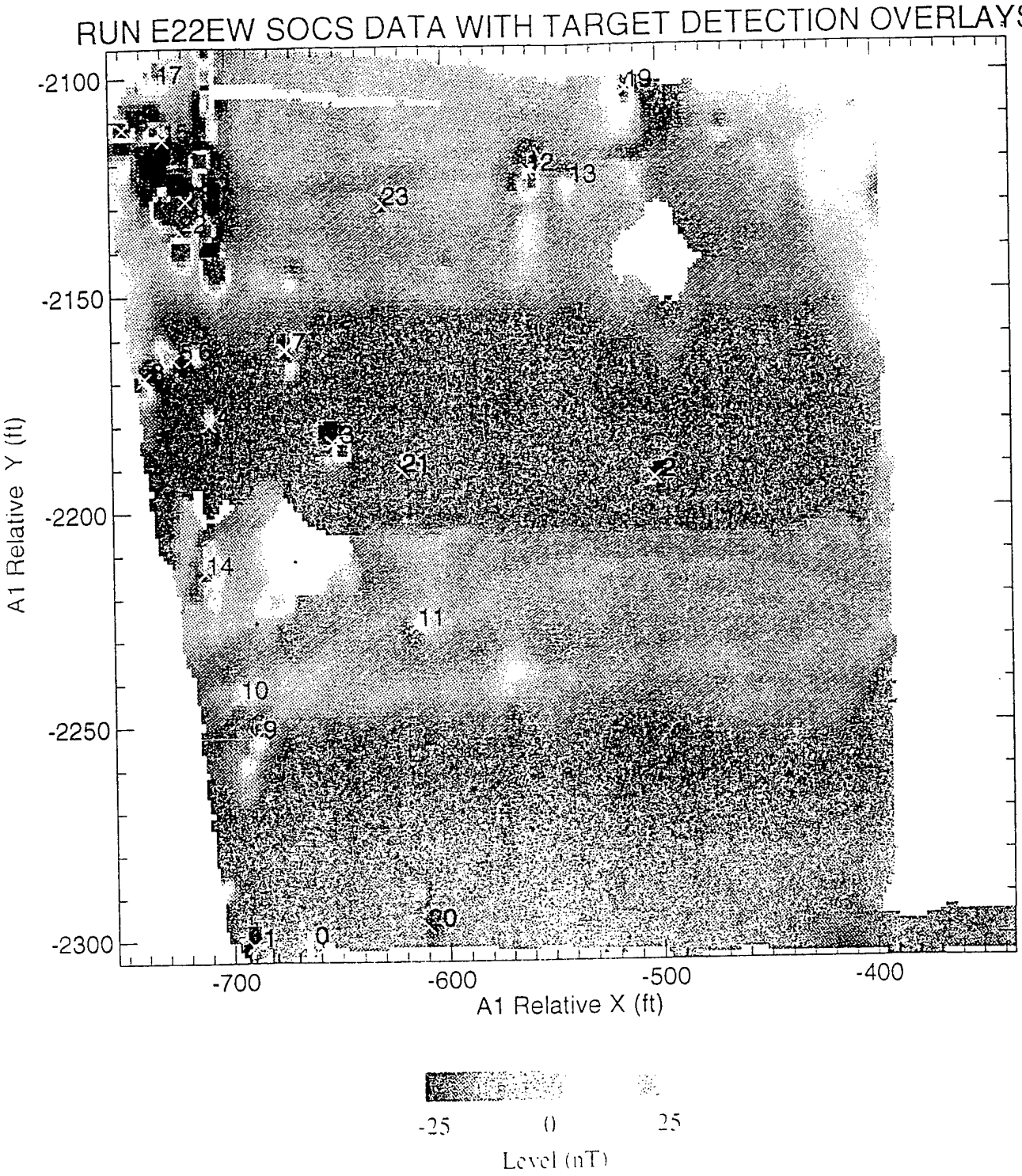

Figure 2-17. Interpolated magnetic amplitude image of mission **E22ew** data. X's mark the locations of *Magproc* fits, the numbers refer to the order of the fits in the STD file.

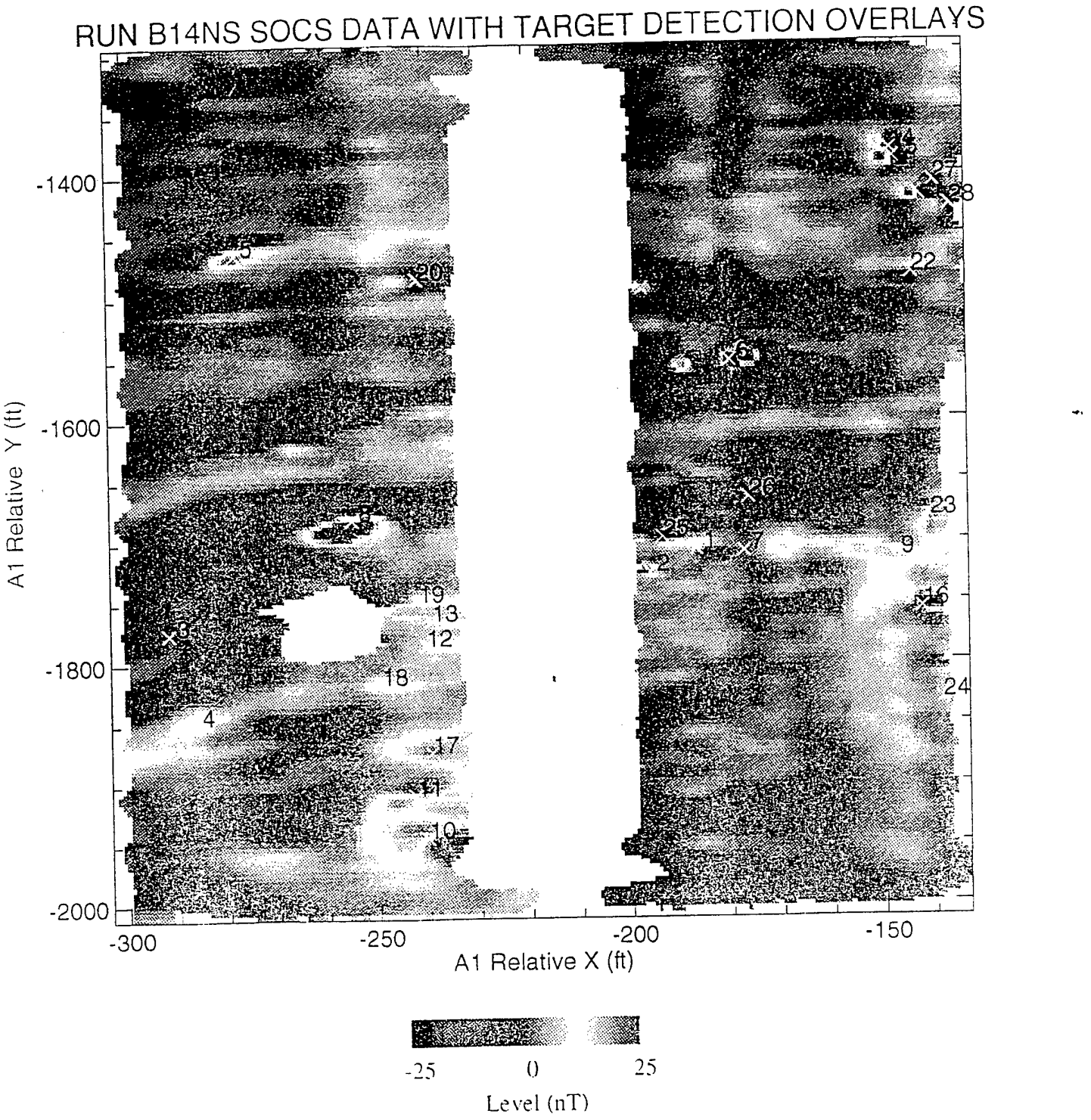

Figure 2-18. Interpolated magnetic amplitude image of mission **B14ns** data. X's mark the locations of *Magproc* fits, the numbers refer to the order of the fits in the STD file.

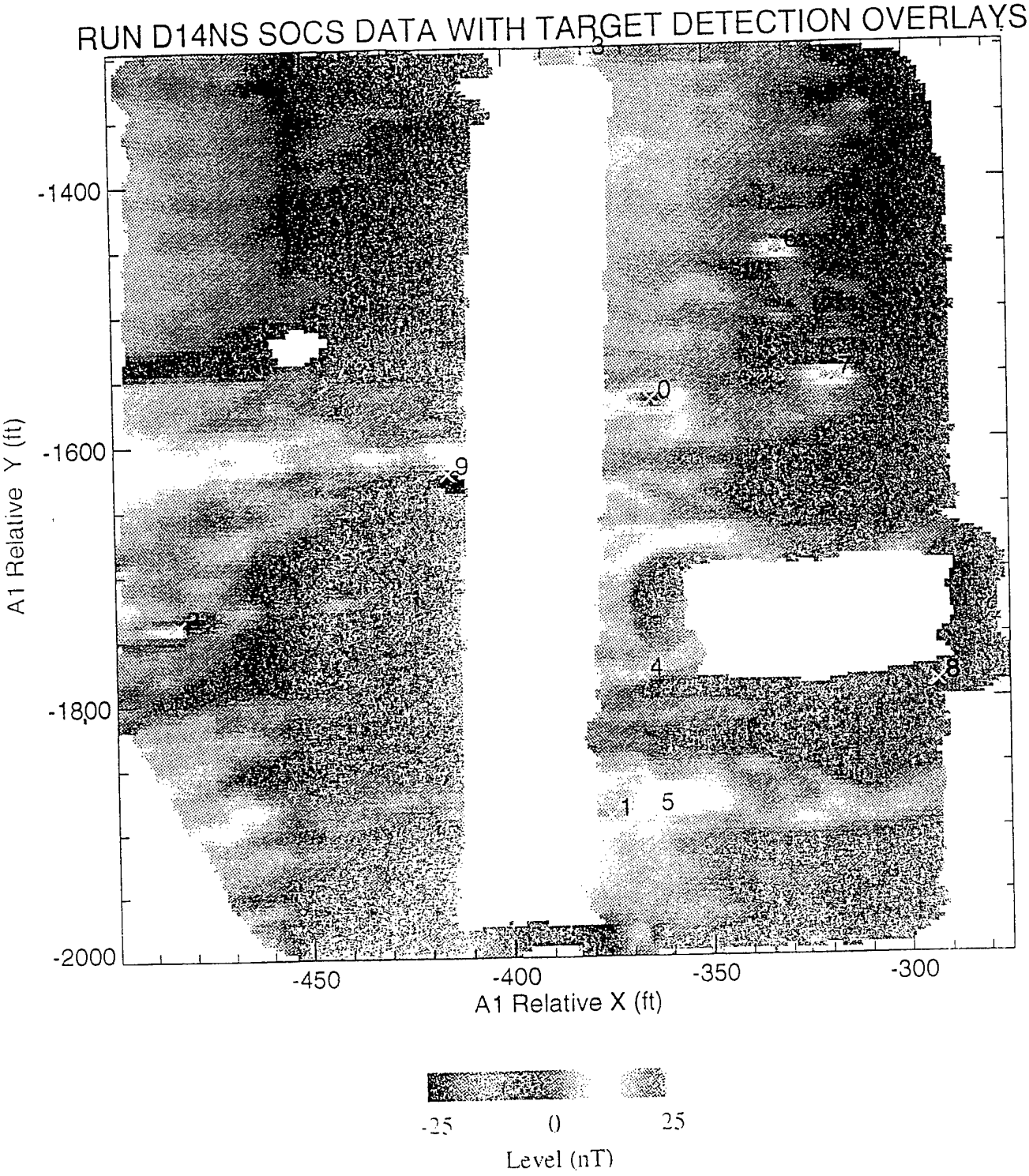

Figure 2-19. Interpolated magnetic amplitude image of mission **D14ns** data. X's mark the locations of *Magproc* fits. the numbers refer to the order of the fits in the STD file.

2.5 MAGNETOMETER NOISE LEVELS

Noise levels for the six missions are summarized in Table 4. These noise levels are calculated in *Magproc*. The algorithm used rank orders all magnetometer readings and then finds the median. The change in amplitude for a set fraction of the points about the median is used to determine the noise level. Thus, the reported noise is an estimate of the gaussian noise field ignoring large amplitude fluctuations. This method of estimating the noise, rather than the usual *rms* deviation, is used because it is insensitive to the large amplitude signals from the targets. A more detailed discussion of this method of estimating noise may be found in DeProspo, 1995, (ref (1)).

Mission	Magnetometer: Average noise (nT)			
	A	B	C	D
C22ns2	2.7	2.7	2.7	2.8
B22ew	4.6	4.4	4.4	3.5
C22ns3	5.4	5.5	5.5	5.5
E22ew	6.7	6.7	6.6	6.7
B14ns	4.0	3.9	3.9	3.9
D14ns	5.1	5.1	5.1	5.2
D14ns (ref mag)	2.8	2.8	2.8	2.7
D14ns (ref mag, quiet area) - noise averaged over all sensors: 1.0 nT				

Table 4. Average Noise Level for Each Magnetometer

Note in Table 4 that there is a much greater difference in noise levels between missions than between sensors on a particular mission. The largest changes in noise level between missions is caused by uncompensated temporal drift of the Earth field during the run. This is evident in the difference in noise levels for missions **C22ns2** and **C22ns3**. Although the two missions covered essentially the same area, the estimated noise during **C22ns3** was greater by a factor of two. It is clear from the image of this mission (Figure 2-16) that a temporal shift of about 15 nT occurred due to a change in the Earth field during **C22ns3**. Of the data collected by SOCS only the last mission, **D14ns**, had coincident reference magnetometer data that could be used to subtract out the temporal drift. A time series of the reference magnetometer data during this mission is shown in Figure 2-20. During the mission the amplitude of the Earth field changed by over 10 nT. Data from this mission was reprocessed with the temporal field drift removed. Figure 2-21 shows a comparison between the original (upper image) and reprocessed (lower image) amplitude data. The noise result is listed in Table 4 with the heading **D14ns** (ref mag). The noise level was reduced by almost a factor of two from 5.1 to 2.8 nT. The noise level for the reprocessed data is consistent with the lowest levels seen during the field exercise in mission **C22ns2** (there was little temporal drift in the field during this mission). Other missions with high noise levels also appear to be influenced by temporal drift in the

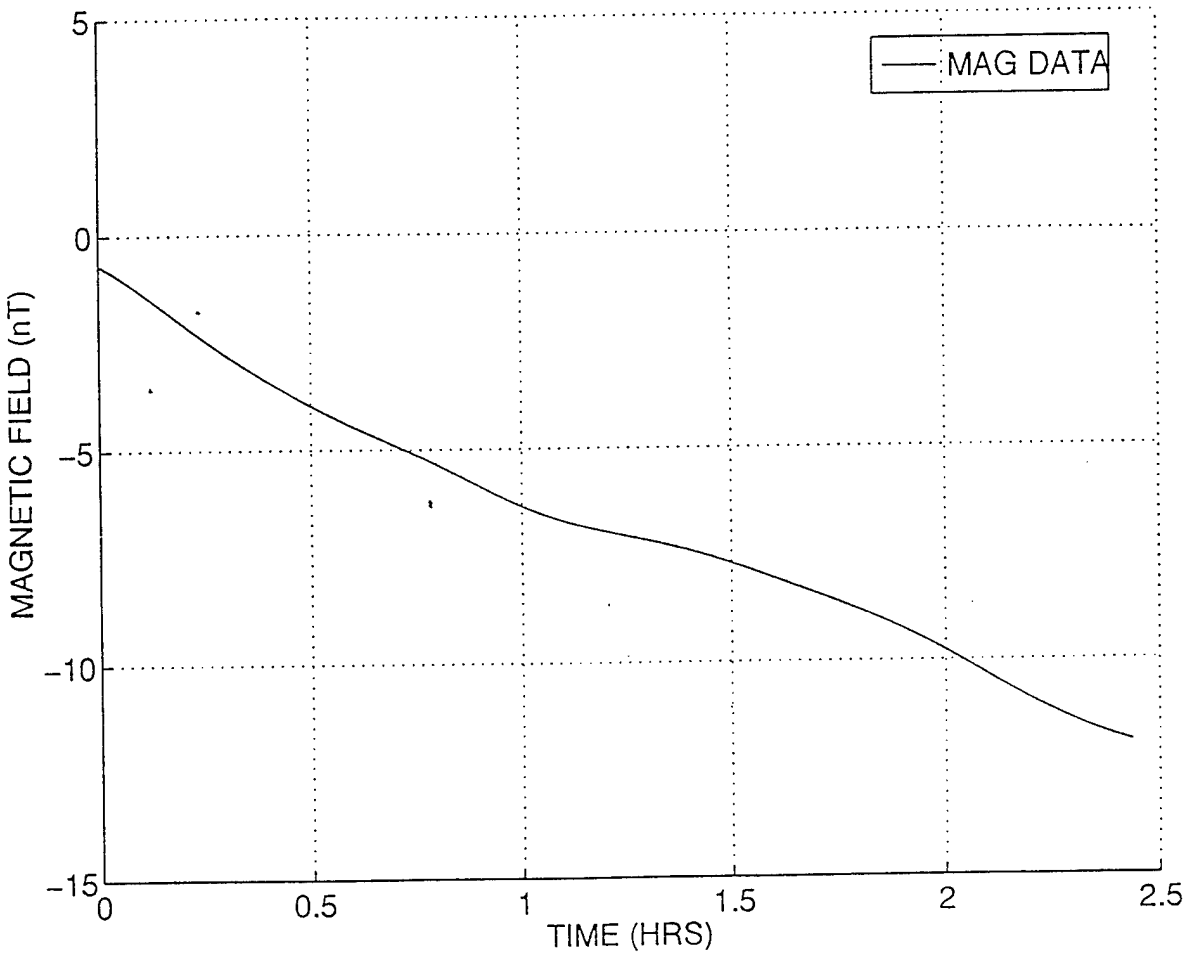

Figure 2-20. Time series of reference magnetometer data collected during mission **D14ns.**

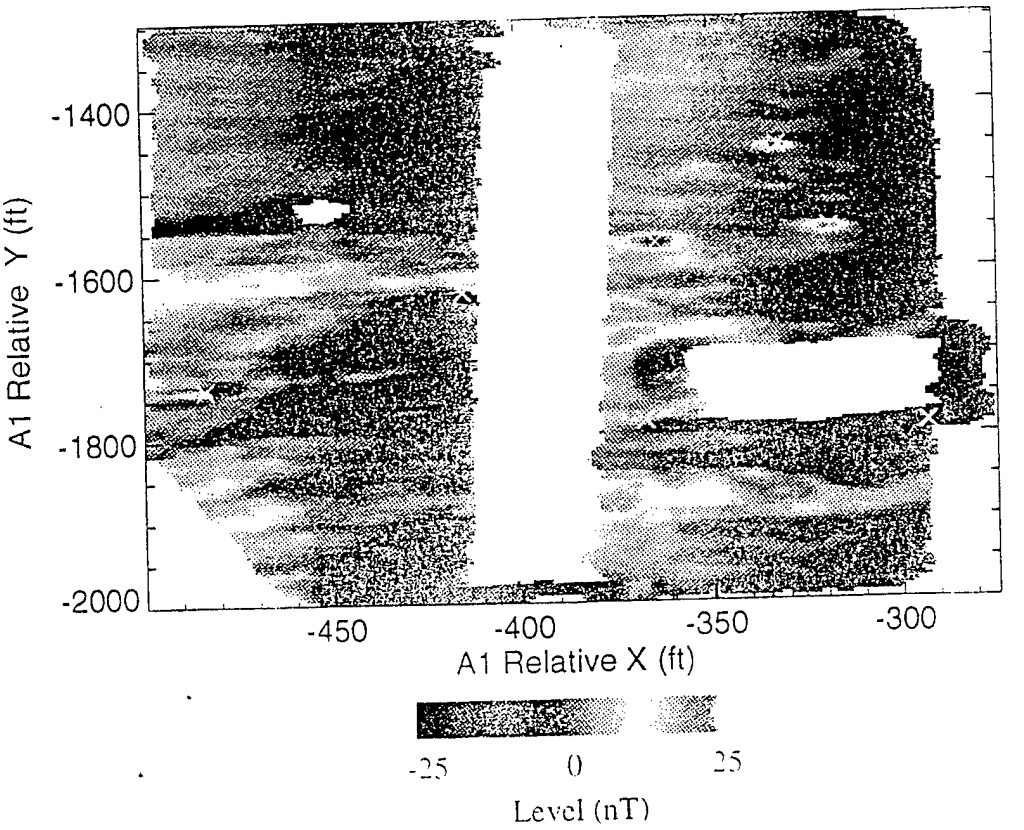

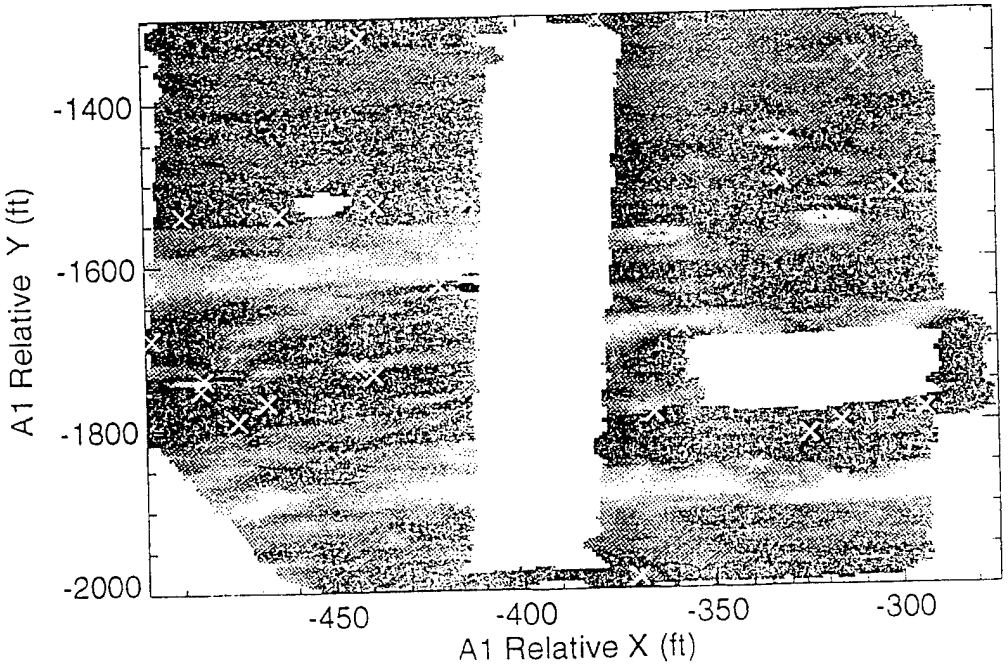

Figure 2-21. Interpolated magnetic amplitude images of mission D14ns without (upper panel) and with (lower panel) reference magnetometer correction.

field (this is apparent in the color amplitude plots). **It is recommended that the reference magnetometer be fully integrated into the SOCS data taking operation so that reference data are available routinely.**

The remaining noise levels are well above the quoted instrument noise levels for the magnetometers (< 0.1 nT). It appears that this noise is dominated by spatial environmental fluctuations. To check this we isolated data from the (relatively) quiet area in the northbound legs of the reprocessed **D14ns** mission, between roughly -1480 and -1350 in y (see Figure 2-21). There were about 25,000 magnetometer points in the area selected which covered about a third of an acre. The noise level for this area was 1 nT, calculated by the same algorithm as used for the whole mission. The increased level seen over the whole mission is due to the spatial features evident in the amplitude image. In our previous experience at JPG, on the 40-acre site, the lowest noise levels we saw with a hand held magnetometer were in the range of 0.5 to 1.0 nT. The foregoing analysis would seem to indicate that the system noise level for SOCS is at or below 1 nT. However, it may be that some of the noise which appears to be environmental may actually be system noise that is spatially correlated. For instance, the areas with higher noise may be rougher and the observed noise increase may be due to the magnetometers bouncing. **A SOCS field measurement program to determine the system noise and isolate its causes is highly recommended.**

2.6 TARGET PROCESSING

All of the field data were run through the SOCS automatic magnetometer processing code *Magproc* (version 1.2). Results in the form of STD files are included on the diskette attached to this report. The locations of the detected anomalies are marked with crosses in the amplitude plots (Figures 2-14 - 2-19), the numbers refer to the order of the anomalies in the STD files.

Mission **C22ns2** had a large number (49) of detected anomalies. In part this is due to the low noise level and consequently lower exceedence threshold than other missions (the current version of *Magproc* uses a threshold of four times the estimated noise level). Also, this area contains a linear region of positive and negative anomalies running from the southern edge almost to the northern edge and trending west. In this region the dipole association algorithm has trouble matching pairs. A large number of the reported anomalies are single pole exceedences. Some of these single pole anomalies appear to be valid targets (such as 11, 7, and 2), while others are probably just environmental fluctuations (such as 4, 26, and 29). There are also several strong isolated dipoles which are target like (6, 7, and 17). This mission was run north-south but there are several features running east-west across the field. One consists of two roughly parallel lines running from the western edge, between anomalies 15 and 20, almost to the eastern edge of the area. This feature may be an old track or road, or it may be caused by a system noise source (such as a small amplitude jump as the trailer goes over a bump).

The mission **B22ew** covers some of the same area as the previous mission. The noise level was higher, apparently because of a long scale environmental feature which has a larger field on the western edge and grades to a smaller field to the east. Seventeen anomalies were detected; most of them appear to be caused by compact objects. The northern part of the linear feature seen in **C22ns2** and many of the same isolated targets are also seen in this mission. These overlapping targets are discussed in the next section.

C22ns3 was meant to cover the same ground as **C22ns2**, but was ended early due to equipment problems. During this mission there was a large change in the Earth field for which we have no direct measurements that could be used for compensation. Consequently, the noise level and threshold levels are higher than for **C22ns2**. Twenty anomalies were detected, most of them are along the north-south linear feature. Because of the higher noise level several compact targets seen in **C22ns2** and **B22ew** do not exceed threshold in this run (see targets 11 and 7 in the northeast corner of **C22ns2** which correspond to targets 5 and 2 in **B22ew**). Recall that the locations of targets in **C22ns3** are shifted relative to the other two missions.

The noise level for mission **E22ew** was the highest of any during the field test because of the large uncompensated drift in the Earth field which is evident as east-west banding in Figure 2-17. Twenty-three anomalies were detected, most along the western edge of the area covered. Most of the anomalies are isolated, however in the northwest corner there is a region of mixed positive and negative exceedences which confused the processor.

The next two missions had long north-south legs and the axes for the corresponding images (Figures 2-18 and 2-19) are highly distorted. Mission **B14ns** ended early due to equipment problems. The noise level was intermediate and moderate banding due to Earth field drift is seen. Twenty-eight anomalies are found, most are clustered near the gap in the center of the field and along the eastern edge. Most of the anomalies look like good dipoles, although several appear to be single pole exceedences due to environmental features (e.g., 4 and 5).

Equipment problems also caused mission **D14ns** to end early. In this file there was a large drift in the Earth field which was recorded with the reference magnetometer. Prior to compensation the noise level was just over 5 nT and the processor selected 10 anomalies. After compensation the data were reprocessed. With the reduced noise level of 2.7 nT, 45 anomalies were detected in the same data. It appears, as was the case with **C22ns2** the other low noise mission, that many of these reported anomalies are single pole threshold exceedences due to amplitude fluctuations on top of larger scale environmental features. It is likely that we will have to increase the threshold in the current version of *Magproc* for such low noise missions. A processor which uses a matched filter approach to detection would greatly reduce this type of problem.

2.7 COMPARISON OF OVERLAPPING TARGET REGIONS

We have only been supplied ground truth for one object buried at JPG, and this object was not seen in any of the magnetometer surveys. As a result it is difficult to check the accuracy of target localization and characterization in *Magproc*. Several of the missions (**C22ns2**, **B22ew** and **C22ns3**) covered areas which overlapped and we have used targets seen in these missions to check the consistency of results. Table 5 summarizes this analysis. In choosing anomalies to compare we picked isolated targets, avoiding the confused north-south linear feature seen in these missions. This was done to assure that the processor was working on the same anomaly. The number following the mission name in the second column of the table corresponds to the identification number in the color image (Figures 2-14 - 2-16) for that mission.

Anomaly Number			Fit Parameters					
			X(ft)	Y (ft)	Z (ft)	D (deg)	I (deg)	Rad (ft)
1	**B22ew**	4	-495.3	-2147.2	2.3	-125	12	0.56
	C22ns2	6	-491.2	-2144.5	2.5	-119	7	0.57
	C22ns3	2	-493.0	-2147.2	2.6	-128	6	0.58
2	**B22ew**	6	-455.7	-2100.5	3.2	62	93	0.28
	C22ns2	27	-453.3	-2099.0	8.3	0	137	0.56
	C22ns3	17	-449.7	-2098.7	6.8	283	150	0.65
3	**B22ew**	8	-529.3	-2090.6	2.1	-77	1	0.41
	C22ns2	17	-524.9	-2086.9	3.4	-79	-4	0.52
	C22ns3	10	-527.0	-2087.8	3.3	-92	3	0.53
4	**B22ew**	11	-432.6	-2081.3	2.0	82	94	0.25
	C22ns2	18	-430.4	-2078.9	1.0	83	35	0.19
	C22ns3	9	-429.9	-2081.5	2.4	-42	115	0.27
5	**B22ew**	12	-379.5	-2130.2	2.3	-3	102	0.19
	C22ns2	2	-377.5	-2130.0	1.8	10	44	0.21
	C22ns3	0	-379.5	-2130.8	0.0	29	-7	0.14
6	**B22ew**	14	-410.0	-2081.8	0.8	-175	5	0.23
	C22ns2	10	-409.2	-2078.3	0.0	17	10	0.17
	C22ns3	3	-410.5	-2078.7	1.4	172	0	0.29

Table 5. Comparison of Fits for the Same Objects from Different Missions

Position fits for all six objects in the table are consistent from mission to mission within a few feet (for this table the position error for missions **C22ns2** and **B22ew** has been estimated and removed). This is the random error that would be expected given the intrinsic accuracy of the SOCS GPS for repeat missions.

In *Magproc*, object depth is fit from the shape of the anomaly with amplitude information scaled out (see DeProspo, 1995, ref. (1)). Then the amplitude is used to estimate object size. As a result of this sequence, depth and size estimates from *Magproc* are highly correlated; if the estimated depth is too

great then the estimated size will be too large. Likewise, shallow depth estimates will lead to size estimates that are too small. This relationship is clearly seen in the data of table 5, in almost all cases the shallowest depth estimate is coupled with the smallest size estimate for a given object.

Of the items in table 5, two (anomalies 1 and 3) were fairly large dipole anomalies well isolated from other signal exceedences. For the first of these, results from the three runs are very similar. Depth estimates are with a few inches and size estimates are correspondingly close. The second large dipole, anomaly number three in the table, has a distinctly different result for mission **B22ew** than the other two missions. Looking at Figure 2-15 it is clear why the estimates are different for this mission. The anomaly, number 8 in the upper left corner, has a distortion in the positive peak. This distortion is not seen in the other two missions and probably results from an error in the absolute position between successive SOCS tracks. In the absence of this type of signal distortion we would expect *Magproc* to yield consistent estimates for large dipole anomalies.

Two items in the table (anomalies 4 and 6) are small shallow dipoles. For these objects the *Magproc* estimates consistently show shallow depths and small sizes, but the spread between estimates is larger. This larger spread is expected since *Magproc* has many fewer data points to work with for shallow objects than for deeper ones. Thus, the uncertainty of the fits are larger.

The final two items in the table are single pole anomalies (one pole dominates the other). It has been recognized for some time that the algorithms used in *Magproc* are not ideal for single pole fits. This is reflected in the large variation seen in the fits, even for object 2 which has many points to use in the fit. **The current SOCS schedule includes tests to obtain some data from single pole targets for which the ground truth is known, in order to upgrade the fitting algorithms for these anomalies.**

3.0 SUMMARY

In August and September of 1995 SOCS was tested at Jefferson Proving Grounds on the PRC 80-acre UXO test site. During this period seven missions were run and of these six had valid magnetometer data. In this report we describe these missions and analyses of the SOCS magnetometer data.

With SOCS running in automatic mode ground coverage by the magnetometer array is quite good. There is a problem with the mapping of the magnetometer positions during turns that is related to a problem in updating the vehicle heading. This problem is currently being worked on.

During the test period ferrous material near the magnetometers was removed. After this the directional offset for SOCS was smaller than could be measured with this type of data (smaller than a few nT). We recommend that all of the potentially ferrous bubble level bolts be removed from near the sensors, and that a series of tests be performed to determine the current level of directional offset for SOCS.

The noise levels estimated for whole missions were determined by the amount of temporal drift in the Earth field over the mission (this resulted because only one mission had concurrent reference magnetometer data). For missions with little temporal field drift, and for the one mission with the drift removed, the estimated noise was 2.5 to 3 nT. Some of this noise is due to spatial variation over the area covered by the mission. In an area with no apparent spatial features the estimated noise was 1 nT. We recommend a series of tests to determine the actual system noise level for SOCS and strongly recommend that reference magnetometer data collection be integrated into all future SOCS missions.

Magproc was run on all of the collected data without operational problems; output in the form of STD files are included on the diskette attached to this report. Analysis of the *Magproc* output indicates some areas that require further work. Parameter fits from anomalies with a single dominant pole are still erratic. This problem will be studied with data from upcoming tests with single pole targets for which the ground truth is known. When the estimated noise level for the whole mission is low (2-3 nT), the threshold calculated by *Magproc* is too low resulting in large numbers of targets which are probably fluctuations in the environmental noise. A minimum threshold for low noise runs will be implemented as a parameter in the next version of *Magproc*.

4.0 REFERENCES

(1) DeProspo, D. and R. DiMarco, Detection and Discrimination Techniques for Total Field Magnetometers and Multi-Axis Gradiometers, AETC, VA-064-064-95-TR, 1995.